

Review

Indole Compounds in Oncology: Therapeutic Potential and Mechanistic Insights

Sara M. Hassan ¹, Alyaa Farid ¹, Siva S. Panda ^{2,3,*}, Mohamed S. Bekheit ⁴, Holden Dinkins ², Walid Fayad ⁵ and Adel S. Girgis ^{4,*}

¹ Biotechnology Department, Faculty of Science, Cairo University, Giza 12613, Egypt

² Department of Chemistry and Biochemistry, Augusta University, Augusta, GA 30912, USA

³ Department of Biochemistry and Molecular Biology, Augusta University, Augusta, GA 30912, USA

⁴ Department of Pesticide Chemistry, National Research Centre, Dokki, Giza 12622, Egypt; m_bekheit@yahoo.com

⁵ Drug Bioassay-Cell Culture Laboratory, Pharmacognosy Department, National Research Centre, Dokki, Giza 12622, Egypt

* Correspondence: sipanda@augusta.edu or sspanda12@gmail.com (S.S.P.); girgisas10@yahoo.com or as.girgis@nrc.sci.eg (A.S.G.)

Abstract: Cancer remains a formidable global health challenge, with current treatment modalities such as chemotherapy, radiotherapy, surgery, and targeted therapy often hindered by low efficacy and adverse side effects. The indole scaffold, a prominent heterocyclic structure, has emerged as a promising candidate in the fight against cancer. This review consolidates recent advancements in developing natural and synthetic indolyl analogs, highlighting their antiproliferative activities against various cancer types over the past five years. These analogs are categorized based on their efficacy against common cancer types, supported by biochemical assays demonstrating their antiproliferative properties. In this review, emphasis is placed on elucidating the mechanisms of action of these compounds. Given the limitations of conventional cancer therapies, developing targeted therapeutics with enhanced selectivity and reduced side effects remains a critical focus in oncological research.

Keywords: indole; cancer; antiproliferation; synthesis; mode of action



Citation: Hassan, S.M.; Farid, A.; Panda, S.S.; Bekheit, M.S.; Dinkins, H.; Fayad, W.; Girgis, A.S. Indole Compounds in Oncology: Therapeutic Potential and Mechanistic Insights. *Pharmaceuticals* **2024**, *17*, 922. <https://doi.org/10.3390/ph17070922>

Academic Editors: Simone Lucarini and Florence McCarthy

Received: 18 June 2024

Revised: 28 June 2024

Accepted: 4 July 2024

Published: 10 July 2024



Copyright: © 2024 by the authors. Licensee MDPI, Basel, Switzerland. This article is an open access article distributed under the terms and conditions of the Creative Commons Attribution (CC BY) license (<https://creativecommons.org/licenses/by/4.0/>).

1. Introduction

Cancer is one of the biggest health challenges to mankind, considered the second most deadly disease, trailing cardiovascular disease [1–4]. Due to its invasive and aggressive proliferation, cancer may spread into other tissues, causing metastatic capability [5,6]. Despite several tools, therapeutics, and strategies currently developed and applied to manage the disease, many cancer patients are vulnerable to drug resistance, which reduces the efficacy of different therapies [7–9]. In this context, the search for safe anticancer agents with high potency, selectivity, and minimal off-target effects is an urgent demand. Paying attention to novel therapeutics such as gene [10], immune [11], and photodynamic [12] therapies is also a noticeable trend to attain effective approaches for combating diverse cancer types, especially in the advanced phases.

Indole analogs are widely distributed as natural compounds in animals, plants, and microorganisms [13–15]. Many indole analogs were reported with potential biological properties, among them anti-SARS-CoV-2 (severe acute respiratory syndrome coronavirus-2) [16–22], anti-malarial [23,24], antimicrobial [25,26], and anti-inflammatory [27–29], in addition to approved drugs for the treatment of several diseases [30–41] (Table 1).

Table 1. Cont.

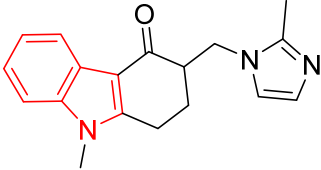
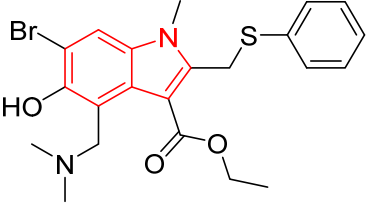
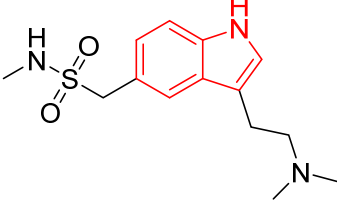
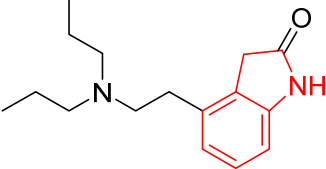
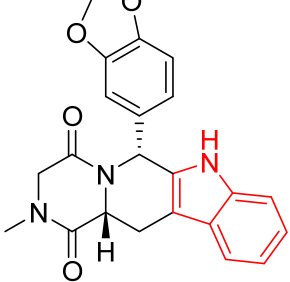
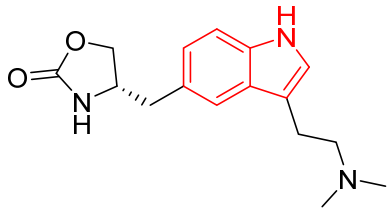
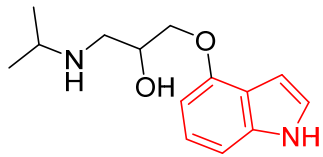
Drug	Bio-Properties	Reference
 <p>Ondansetron (6)</p>	Antiemetic	[35]
 <p>Arbidol/Umifenovir (7)</p>	Antiviral	[36]
 <p>Sumatriptan (8)</p>	For treatment of migraines and cluster headaches	[37]
 <p>Ropinirole (9)</p>	For treatment of symptoms of Parkinson's disease and restless legs syndrome	[38]
 <p>Tadalafil (10)</p>	For treatment of erectile dysfunction, benign prostatic hyperplasia, and pulmonary arterial hypertension	[39]

Table 1. Cont.

Drug	Bio-Properties	Reference
 <p>Zolmitriptan (11)</p>	For treatment of acute migraine with or without aura in adults	[40]
 <p>Pindolol (12)</p>	Antihypertensive (β -antagonist)	[41]

Cell death is crucial and fundamental for maintaining tissue balance and eliminating potentially harmful cells in multicellular organisms. Accidental cell death (ACD) is typically caused by unintentional injury, while regulated cell death (RCD) is programmed cell death controlled by signaling pathways necessary for an organism's development and/or tissue renewal [42]. Autophagy, necrosis, and apoptosis are significant types of RCD. They are potent approaches against cancer progression and metastasis and are important for developing potential anticancer agents [43,44].

Indole analogs have been recognized as potent anticancer agents targeting RCD and related signaling pathways [45,46]. So, they may control cancer cell progression via various biological targets, including tubulin polymerization, DNA topoisomerases, tumor vascularization, histone deacetylase (HDAC), and sirtuins [46–48]. Moreover, efficacy towards drug sensitivity and resistance in vitro and in vivo were also reported [49].

Sunitinib (Sutent[®]) 13 (Figure 1) is a famous clinically approved drug by the FDA against imatinib-resistant gastrointestinal, pancreatic, and high-risk renal cancer in adults. Sunitinib inhibits cellular signaling/multi-target tyrosine kinases related to tumor growth, angiogenesis, and metastatic progression. The antitumor activity of sunitinib is attributed to PDGFR and VEGFR (platelet-derived and vascular endothelial growth factor receptors, respectively) inhibition that reduces tumor vascularization and size [50,51]. Nintedanib (Ofev[®]) 14 is an indolinone-derived intracellular tyrosine kinase inhibitor drug awarded FDA approval against NSCLC (non-small cell lung cancer) with potential anti-angiogenesis properties and inhibitory activity against PDGFR- α , - β ; VEGFR-1, -2, -3; and FGFR-1, -2, -3 (fibroblast growth factor receptor) [52–57]. Alectinib (AlecNsa[®]) 15 is usable against NSCLC [58–61], panobinostat (FarydaK[®]) 16 against multiple myeloma [62], osimertinib (Tagrisso[®]) 17 against NSCLC [63], and anlotinib 18 against NSCLC as well as metastatic colon cancer [64]. They are also indolyl-containing drugs approved by the FDA (except anlotinib, which is approved by the National Medical Products Administration (NMPA) of China).

The current study summarizes the recently reported indolyl analogs, either naturally isolated or synthetically prepared, with potential antiproliferative activity against different cancer types within the last five years, utilizing different search engines (Scopus, ScienceDirect, and Pubmed) and specific keywords (indole; cancer; antiproliferation; synthesis; mode of action). The study adopts the classification of potential indole-containing compounds against the most common cancer types. The mode of action mentioned for the reported analogs is one of the main concerns of this study.

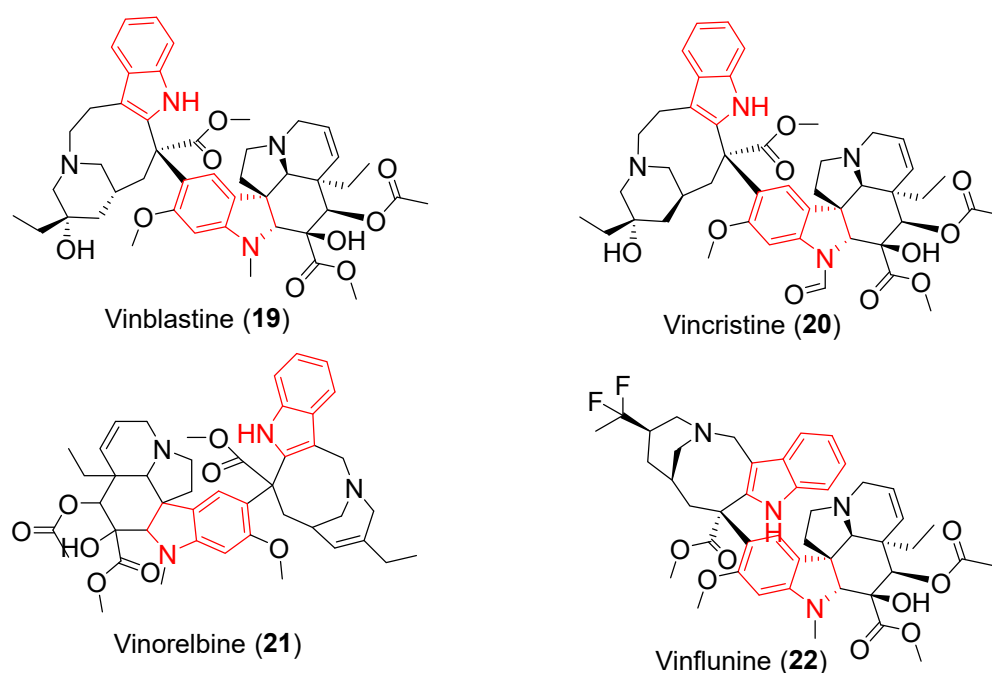


Figure 2. Chemical structure of vinca alkaloids (vinblastine 19, vincristine 20, vinorelbine 21, and vinflunine 22).

2.1. Breast Cancer

Breast cancer is one of the most common causes of death among women's cancer types globally. It is categorized into receptor-positive and triple-negative types [75]. Treatment options include surgery, radiotherapy, chemotherapy, hormone therapy, and immunotherapy [76,77]. Metastasis poses another challenge: the disease can spread to vital organs such as the lungs and bones or lead to lymphoma [77].

Harmine 23 (Figure 3) is an apoptosis-inducing indolyl analog isolated from the seeds of *Peganum harmala*. The antiproliferation and control of the migration of breast cancer cells (MDA-MB-231 "triple-negative" and MCF-7) by harmine were reported. Its capability for controlling/downregulating the overexpression of TAZ (PDZ binding motif) was also mentioned. Additionally, inhibition of proteins including p-Erk (phosphorylated extracellular signal-regulated kinase), p-Akt (protein kinase B), and Bcl-2 (B-cell lymphoma 2) was reported [78].

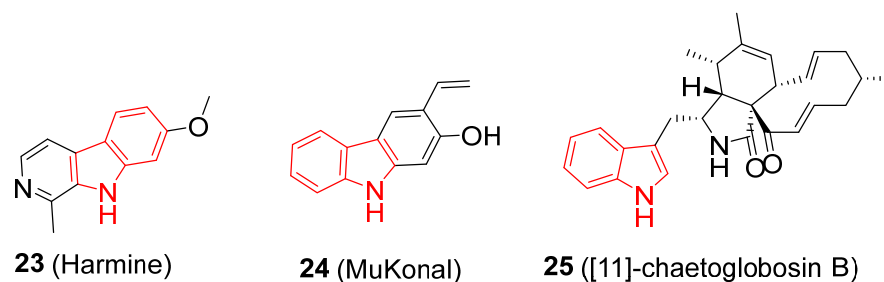


Figure 3. Chemical structure of indole alkaloids 23–25 with antiproliferation properties against breast cancer.

Mukonal 24 (obtained from *Murraya koenigii*) (Figure 3) exhibits potential antiproliferation properties against SK-BR-3 and MDA-MB-231 breast cancer cell lines with an IC_{50} value of 7.5 μ M (MTT "3-(4,5-dimethylthiazol-2-yl)-2,5-diphenyl-tetrazolium bromide" assay) and safety behavior against normal breast cells (MB-157). The antitumor effect was attributed to its apoptosis capability, which was supported by its role in the enhancement of the cleavage of PARP and caspase-3, as well as controlling the Bcl-2 level.

Enhancement of the expression of autophagy proteins (Beclin-1, LC3-I, and LC3-II) also emphasizes/justifies the anti-breast cancer properties. The *in vivo* study (xenografted mouse models) demonstrated that mukonal significantly decreased tumor weight and volume [79].

[11]-Chaetoglobosin B 25 (isolated from the fermentation of *Pseudeurotium bakeri* fungus) (Figure 3) exhibits promising cytotoxic activity against the MCF-7 cell line relative to that of doxorubicin hydrochloride ($IC_{50} = 6.2$ and $1.2 \mu\text{M}$, respectively). Arrest of the cell cycle at G2/M was achieved via flow cytometric assay. Moreover, the apoptotic activity was supported due to the increment of the Bax and CyT-c levels, the cleavage of caspase-3 and PARP, and the decrease in Bcl-2 expression (Western blotting technique) [80].

2.2. Lung Cancer

Lung cancer is a leading cause of worldwide mortality. Many environmental risk factors, along with smoking, are associated with lung cancer [81–83]. NSCLC is an aggressive type [81]. Surgery and chemotherapy are preferred options for early-stage patients, but detecting the disease early is challenging. Prevention through dietary changes and avoiding tobacco smoking is important [84].

Indole-3-carbinol 26 (Figure 4) (found at high levels in *Cruciferous* vegetables) displays anticancer activity against H1299 lung (NSCLC) cancer cell with $IC_{50} = 449.5 \mu\text{M}$ (MTT assay) and safe behavior against CCD-18Co, a normal cell. It also increases the expression of ROS (reactive oxygen species) and activates apoptosis-related signals. Furthermore, it enhances pro-apoptosis expression and blocks anti-apoptosis proteins (FOXO3/Bim/Bax and Bcl-2/Bcl-xL, respectively) [84].

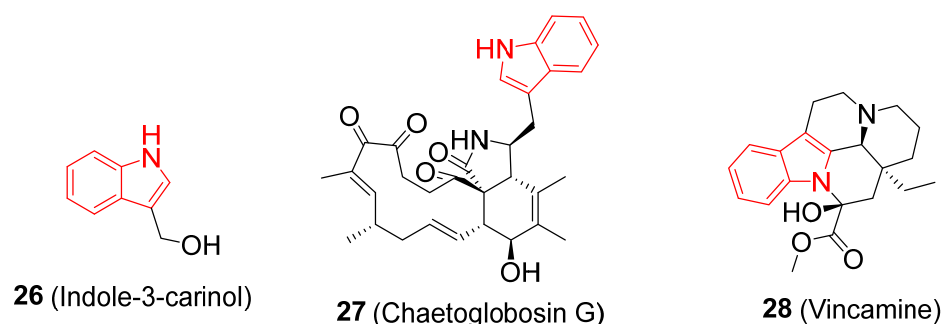


Figure 4. Chemical structure of indole alkaloids 26–28 with antiproliferation properties against lung cancer.

Chaetoglobosin G 27 (Figure 4) is a secondary metabolite in the *Chaetomium globosum* fungus. It possesses antiproliferation activity against lung (NSCLC) cancer A549 cells (MTT assay). The mechanistic study revealed that it enhances the autophagic effect via inhibition of p-EGFR, p-MEK, and p-ERK proteins and incrementally increases the LC3-II protein level. Flow cytometry supports its ability for apoptosis induction and cell cycle arrest at the G2/M phase. Controlling/downregulating cyclin B1 protein and enhancing p21 protein are also reported [85].

Vincamine 28 (Figure 4), isolated from the *Vinca minor* leaves and used as a diet for aging combat, was reported as an apoptosis inducer. Its antiproliferation properties against the A549 cell line ($IC_{50} = 309.7 \mu\text{M}$) were mentioned (MTT assay). In addition to the potential change in mitochondrial membrane potential, the potential activity towards ROS and caspase-3 was the mode of action mentioned that supported the anticancer activity revealed [86].

2.3. Gastric Cancer

The fifth most common cancer in the world is gastric cancer, which is also known as stomach cancer [87]. Usually, surgery and chemotherapy are the options considered for diagnosed patients with stomach cancer [88].

Bufothionine **29** (Figure 5) isolated from the toad *Bufo bufogargarizans* reveals inhibition of the gastric cancer cell lines MKN28 and AGS (CCK-8 assay) with apoptosis induction (supported by flow cytometric analysis). It facilitates caspase-3/8/9 apoptosis in both cell lines in addition to upregulating Bcl-2 and downregulating Bax proteins. In vivo, a gastric cancer xenograft mouse model supported its ability to suppress tumor growth and weight [89].

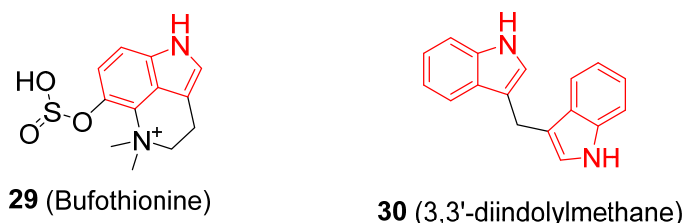


Figure 5. Chemical structure of indole alkaloids **29** and **30** with antiproliferation properties against gastric cancer.

3,3'-Diindolylmethane **30** (Figure 5) obtained from *Cruciferous* plants has been demonstrated to induce ferroptosis in BGC-823 gastric cancer cells through the upregulation of lipid-ROS levels and a decrease in GSH generation [90].

2.4. Colorectal Cancer

The second most frequent cancer-related cause of death in the US and the third one globally is colorectal cancer [91,92]. Recurrence and metastasis reduce the survival rate for this disease [92]. It has been reported that colon polyps are the main cause of the disease, in addition to heredity/family history and colitis [93]. Surgery is the first option for the disease; meanwhile, chemotherapy is appropriate for metastasis [94].

Brucine **31** and strychnine **32** (Figure 6) were obtained from the seeds of *Strychnos nux-vomica* L., used as a traditional medication for tumor treatment. Brucine and strychnine exhibit inhibitory effects on the growth of human colorectal cancer cells DLD1, SW480, and Lovo (MTT assay). The Wnt/ β -catenin signaling pathway is involved in the activity since both induce an apoptosis effect through DKK1 and APC expression and downregulate the β -catenin, c-Myc, and p-LRP6 levels. In vivo studies (nude mice) support their effect/suppression of DLD1 tumors [95].

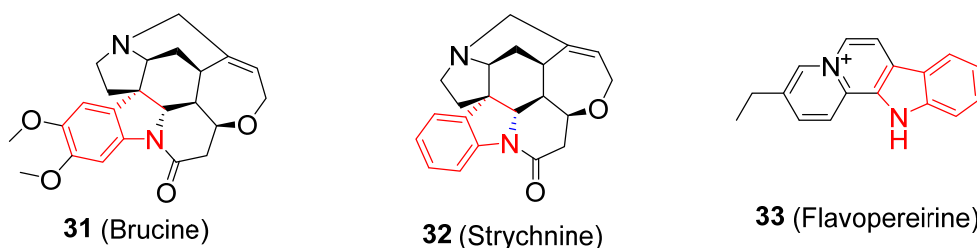


Figure 6. Chemical structure of indole alkaloids **31–33** with antiproliferation properties against colorectal cancer.

Flavopereirine **33** (Figure 6) is a β -carboline alkaloid extracted from *Geissospermum vellosii*. It affects the viability of different malignant stages of colorectal cell lines (SW480, SW620, DLD1, HCT116, and HT29, with IC_{50} = 15.33, 10.52, 10.76, 8.15, and 9.58 μ M, respectively). Its activation of p53 and p21 protein expression justifies the growth suppression and apoptotic cell death of colorectal cancer [96].

2.5. Pancreatic Cancer

Worldwide, pancreatic cancer ranks as the 12th most common male cancer and the 11th most common female cancer [97]. Pancreatic cancer is classified into two categories based on its origin: exocrine or neuroendocrine; the latter is less common but more accessible in prognosis [98].

Staurosporine **34** (Figure 7), an alkaloid obtained from *Streptomyces staurosporeus*, can induce apoptosis in pancreatic cancer cells (PaTu 8988t and Panc-1). Activation of caspase-9 in both cells was reported (Western blotting analysis). Additionally, both Bcl-2 and Bad expression were mentioned in PaTu 8988T cells [99].

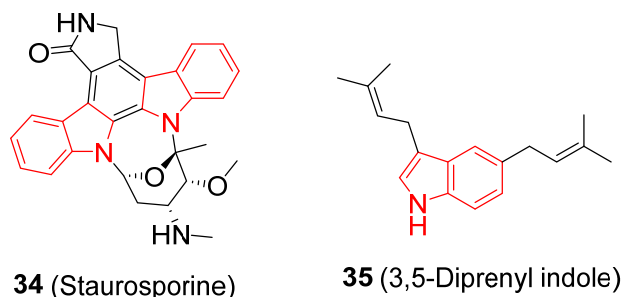


Figure 7. Chemical structure of indole alkaloids **34** and **35** with antiproliferation properties against pancreatic cancer.

Indole-based alkaloids were obtained from *Ravenia spectabilis* Engl. (leaf extract), revealing noticeable antiproliferation properties against various cancer cell lines, including HeLa, A549, and MIA PaCa-2, with a safety index against the normal cell line WI-38. 3,5-Diprenyl indole **35** (Figure 7) is the most promising cytotoxic agent observed against MIA PaCa-2 (a human pancreatic adenocarcinoma cancer cell line) with an $IC_{50} = 9.5 \pm 2.2 \mu M$, comparable to the positive drug/control gemcitabine $0.6 \pm 0.4 \mu M$ (MTT assay) [100].

2.6. Liver Cancer

It is the third-most deadly cause of mortality among many cancer types. The chance of its diagnosis is almost three times higher for men than for women [101]. Although surgical resection is an appropriate option for liver cancer patients, its accessibility is limited due to many serious factors, including easy recurrence and metastasis. Chemotherapy is also an important clinical pathway with or without surgery against this disease [102].

Dehydrocrenatidine **36** (Figure 8) is a β -carboline alkaloid isolated from the stem of *Picrasma quassioides*. It exhibits promising growth inhibitory effects against hepatocellular carcinoma in vitro and in vivo, with potent antiproliferation properties (MTT assay) against HepG2 and Hep3B cell lines ($IC_{50} = 3.5$ and $5.87 \mu M$, respectively). Effects on apoptosis-related proteins such as Bax and Bcl-xl, mitochondrial dysfunction, and a decrease in the mitochondrial membrane were reported to cause apoptosis induction in hepatocellular cancer cells [103].

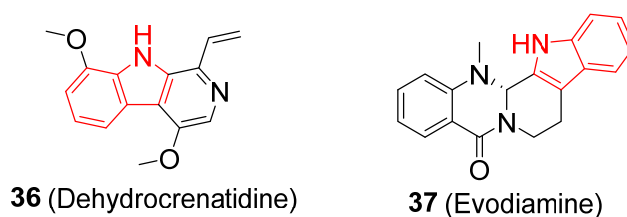


Figure 8. Chemical structure of indole alkaloids **36** and **37** with antiproliferation properties against liver cancer.

Evodiamine **37** (Figure 8), obtained from fructus Evodiae, exhibits antiproliferation activity against liver cancer cell lines HepG2 and SMMC-7721 ($IC_{50} \approx 1 \mu M$ for both cell lines). Evodiae arrests the cell cycle at G2/M (flow cytometric analysis) and induces

apoptosis via upregulation of p53 and Bax, decreasing the Bcl-2, CyclinB1, and cdc2 protein levels. Furthermore, it enhances apoptosis through NOD1 signaling suppression [104].

2.7. Cervical Cancer

It is one of the most severe cancer diseases in women. It is usually caused by the infection of a specific type(s) of human papillomavirus (HPV) [105,106]. Two types of cervical cancer were identified: ectocervix and endocervix, which are the outer and inner parts of the cervix, respectively [107].

Sclerotiamides C (Figure 9) is a notoamide-type alkaloid obtained from the marine fungus *Aspergillus sclerotiorum*. It has been demonstrated to stop cell division and trigger cell death in HeLa cells via elevation of the phosphorylation of JNK, ERK, and p38. Sclerotiamides C can potentially stimulate the activation of apoptosis-associated proteins, including Cyt-c, Bax, and p53. Demonstrating the MAPK pathway is also mentioned as influencing cell growth and death in HeLa cells [108,109].

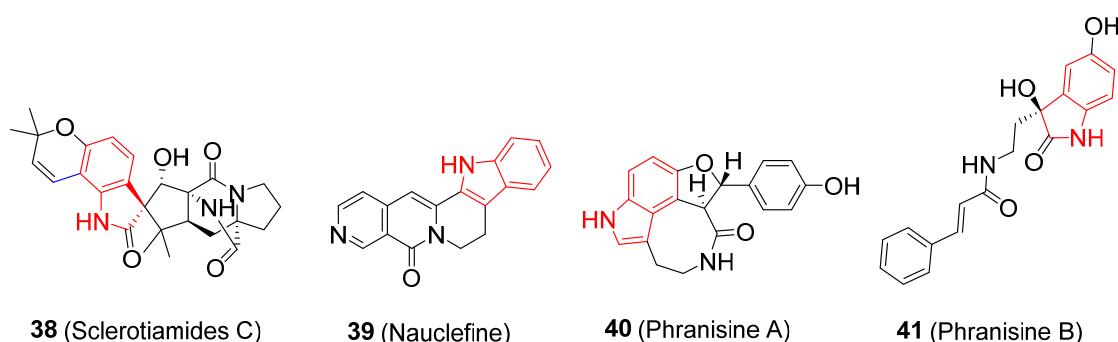


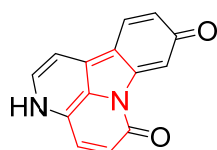
Figure 9. Chemical structure of indole alkaloids 38–41 with antiproliferation properties against cervical cancer.

Nauclefine 39 (Figure 9) is an indolyl alkaloid analog obtained from the bark of *Nauclea subdita* with potent cytotoxicity against HeLa cells ($IC_{50} < 10$ nM). Additionally, in HeLa cells, nauclefine triggers the PDE3A-SLFN12-dependent (phosphodiesterase family member) pathway, inducing apoptosis [110].

Phranisine A 40 and phranisine B 41 (Figure 9) are natural indolyl alkaloids isolated from the roots of *Phragmites australis*. Both exhibit moderate cytotoxicity against HeLa cancer cells, with phranisine A having lower efficacy ($IC_{50} = 54$ μ M) than that of phranisine B ($IC_{50} = 19$ μ M) [111].

2.8. Ovarian Cancer

The eighth most frequent cancer type in women and the 18th most frequent cancer overall is ovarian cancer [112]. 9-Hydroxycanthin-6-one 42 (Figure 10) is a natural β -carboline alkaloid (isolated from the stem bark of *Ailanthus altissima*), revealing promising antiproliferation properties (MTT assay) against three ovarian cancer cells, including A2780, SKOV3, and OVCAR-3 ($IC_{50} = 17.4 \pm 1.1$, 13.8 ± 0.6 , and 18.8 ± 0.7 μ M, respectively). It triggers apoptosis by activating caspase-3, -8, and -9, increasing the intercellular ROS-dependent level [113].



42 (9-hydroxycanthin-6-one)

Figure 10. Chemical structure of 9-hydroxycanthin-6-one 42 with antiproliferation properties against ovarian cancer.

2.9. Leukemia

Leukemia is one of the most prevalent diseases in children (less than 15 years old) and usually affects elderly individuals [114,115]. Based on the affected white blood cell type, leukemia is divided into two categories/classes: lymphocytic/lymphoid and myeloid, which may be either acute or chronic [116,117].

The marine alkaloid 3,10-dibromofascaplysin **43** (Figure 11) (obtained from *Fascaplysinopsis reticulata*) exerts anticancer activity on several myeloid leukemia cells (K562, THP-1, MV4-11, and U937; IC_{50} = 318.2, 329.6, 233.8, and 318.1 nM, respectively). It induces apoptosis by upregulating the expression of genes encoding the leukemia cell survival proteins, such as E2F1, and by downregulating the expression of FLT3 genes. It can arrest the S and G2 cell cycle phases (9-hydroxycanthin-6-one flow cytometry study) [118].

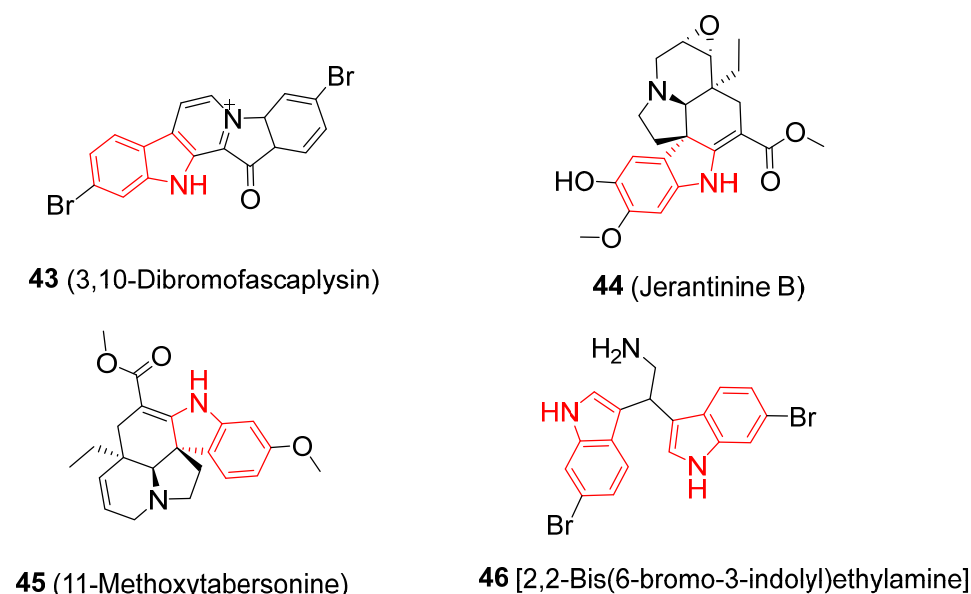


Figure 11. Chemical structure of indole alkaloids **43–46** with antiproliferation properties against leukemia.

Jerantinine B **44** (Figure 11) extracted from the *Tabernaemontana corymbosa* leaf reveals potential antiproliferation properties (IC_{50} = 0.3, 0.4, and 0.8 μ M against MV4-11, HL-60, and KG1a cells, respectively) and apoptosis in acute myelocytic leukemia cells with activation of the c-Jun/JNK pathway [119].

11-Methoxytabersonine **45** (Figure 11), extracted from *Melodinus cochinchinensis*, displays promising antiproliferation properties against acute lymphoblastic leukemia (MOLT-4) and pro-myeloid leukemia (HL-60) cells (IC_{50} = 0.71 and 1.10 μ M, respectively). Its antiproliferation properties were attributed to cell death via ROS accumulation and calcium level increases by inhibiting the PI3K/Akt/mTOR pathway in MOLT-4 cells [120].

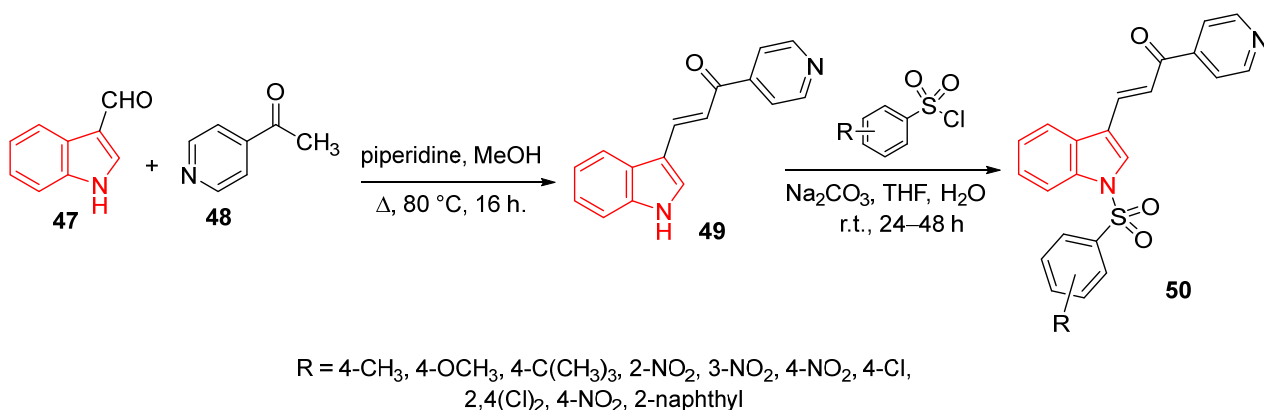
2,2-Bis(6-bromo-3-indolyl) ethylamine **46** (Figure 11) is found in both *Didemnum candidum* and the New Caledonian sponge *Orina*. It induces apoptosis in U937 (human myelomonocytic lymphoma cells) by inhibiting Bcl-2 and Bcl-xL and elevating Bax protein levels [121].

3. Synthesized Indoles with Potential Antiproliferation Properties

Synthesized compounds/heterocycles are uniquely positioned in drug discovery programs, providing potent agents and clinically accessible drugs. Many of the synthesized analogs developed are inspired by natural compounds due to the considerable bio-observations revealed. Different medicinal chemical techniques are accessible for designing the targeted hits/leads in addition to the various computational methods, including QSAR, pharmacophoric analysis, docking, and molecular dynamic simulation [122–128].

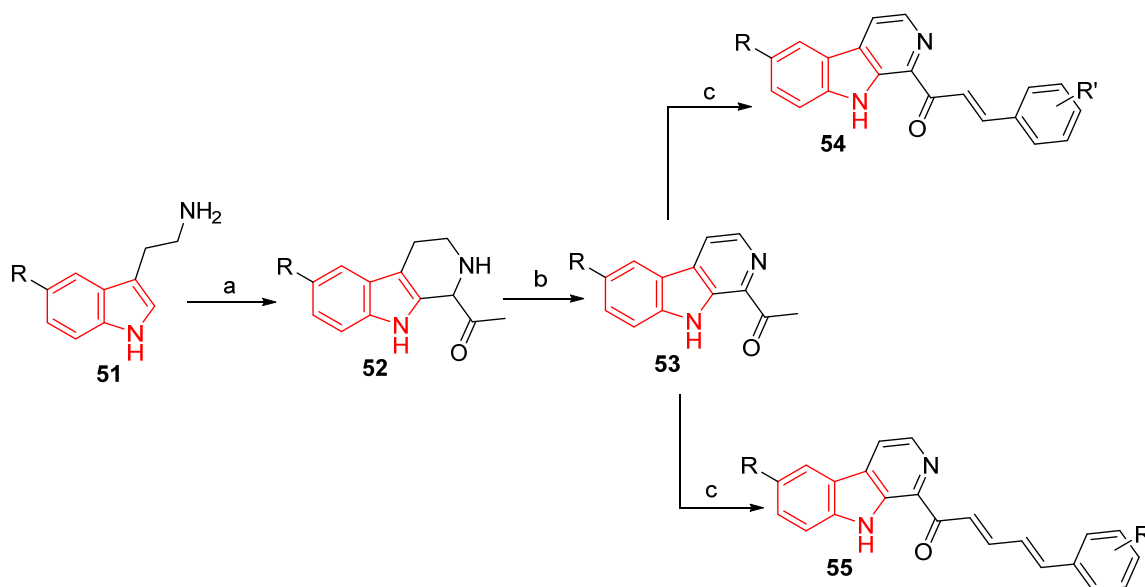
3.1. Breast Cancer

A series of pyridyl-indolyl-based chalcones incorporating the sulfonamide group were synthesized through Knoevenagel condensation of indol-3-carboxaldehyde **47** with 4-acetylpyridine **48** in the presence of piperidine (refluxing MeOH), giving the corresponding chalcone **49**. Treatment of chalcone **49** with sulfonyl chlorides in THF/H₂O (50%) containing Na₂CO₃ (stirring at room temperature) produced the corresponding sulfonamide analogues **50** (Scheme 1). The antiproliferation properties of chalcones **50** were determined against MCF-7 (breast), HepG-2 (hepatoma), and HEK293 (embryonic kidney) cancer cell lines (MTT assay). Among the synthesized agents, two conjugates with R = 2,4-Cl₂ and 4-NO₂ possess effective properties against the MCF-7 cancer cell line (IC₅₀ = 12.2 and 14.5 μM, respectively), which is more potent than that of the reference drug doxorubicin (IC₅₀ = 20.2 μM). These analogs revealed promising antiproliferation properties (IC₅₀ = 14.8 and 18.3 μM, respectively) against HepG2 relative to the standard drug, doxorubicin (IC₅₀ = 18.7 μM). Significant induced apoptosis in the MCF-7 cancer cell line was reported during the apoptosis assay study. No considerable antiproliferation properties against the HEK293 cell line were noticed by the synthesized agents (IC₅₀ > 150 μM). Inhibitory properties against human carbonic anhydrases (hCA IX, hCA II) were experimentally supported as the mode of action of the constructed agents (Supplementary Figure S1). Molecular modeling (Autodock 4.2 software) utilizing PDB ID: 3IAI was considered for explaining the observed enzymatic inhibitory properties [129].



Scheme 1. Synthetic route towards pyridyl-indole-based chalcones incorporated in sulfonamide group **50**.

Harmine is a natural compound called “9H-pyrido[3,4-*b*] indole analog” with potential antitumor properties; however, its clinical accessibility is hindered due to the associated toxicological effects. Conjugation of harmine with chalcone scaffolds was considered for enhancement of antitumor properties and toxicity reduction. The targeted agents **54** and **55** were obtained via condensation of the appropriate aldehyde with the corresponding harmine-based analog **53** in the presence of ethanolic NaOH at room temperature (Scheme 2). Considerable antiproliferation properties of the targeted agents **54** and **55** were investigated against MCF-7, MDA-MB-231 (breast), HepG2 (liver), HT29 (colorectal), A549 (lung), and PC-3 (pancreatic) cancer cell lines and compared with L02 (normal cell line) utilizing the MTT assay (Supplementary Figure S2). The most potent agent observed was **54** (R = H, R' = 3-NO₂-4-Cl; IC₅₀ = 0.34, 0.98, 1.61, 0.57, 2.02, 1.17, and 9.61 μM, respectively). Induction of apoptosis against MCF7 (breast cancer) was attributed to its ability to decrease Bcl-2 and increase Bax, PARP, and phosphorylated Bim proteins. Additionally, suppression and migration of the breast cancer cell (MCF7) due to downregulation of the MMP-2 protein were mentioned. Inhibition of topoisomerase I was supported and justified as the mode of action against cancer. Molecular docking was used to explain the estimated mode of action relative to that of camptothecin (a co-crystallized ligand of PDB ID: 1T8I, Discovery Studio 2016 software) [130].

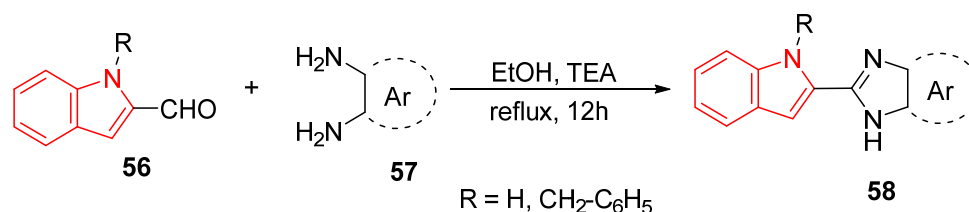


(a) pyruvicaldehyde, 1% H₂SO₄, r.t., 12 h; (b) KMnO₄, DMF, 0 °C–r.t., 10–12 h;
(c) aldehyde, EtOH, NaOH, r.t., 12 h

R = H, OMe; R' = 4-Br, 4-NO₂, 3-Br, 3-I, 2-Cl, 4-OMe, 4-Et, 3-OMe-4-F, 2,3-dihydrobenzo[*b*][1,4]dioxin-6-yl, 3,6-diCl, 3-NO₂-4-Cl, 2,6-diOMe, 2,3,4-triOMe, 2-Br,4,5-diOMe, 3,4,5-triF, 3-Me,4-Cl, 2,6-diMe, H

Scheme 2. Synthetic route towards harmine–chalcone conjugates **54** and **55**.

A set of indole–benzimidazole conjugates **58** was synthesized as selective estrogen receptor modulators. The targeted compounds were obtained by the cyclocondensation reaction of 1*H*-indole-2-carbaldehyde **56** with different ortho-diamines **57** (EtOH/TEA) [131] (Scheme 3).



Scheme 3. Synthetic route towards indole–benzimidazole derivatives **58**.

Amongst all the synthesized agents, two bromo-substituted analogs possess promising antiproliferation properties against the estrogen-sensitive breast cancer (T47D) cell line (Figure 12, Supplementary Figure S3). Both conjugates were found to decrease mRNA and ER- α (estrogen receptor- α) activity. The binding activity of both conjugates towards ER- α (PDB ID: 4XI3) was reported to be in the same way as bazedoxifene (an FDA-approved drug to treat osteoporosis and breast cancer, Maestro 9.6 software) [131].

Indole-2-carbohydrazones **60** were obtained through a reaction of indole-2-carbohydrazides **59** with the appropriate aromatic aldehyde. The reaction **60** with thioglycolic acid in refluxing benzene afforded the corresponding thiazolidines **61** (Scheme 4). Some of the synthesized hydrazones **60** (X = Cl, R¹ = CF₃, R² = H) and (X = Cl, R¹ = CN, R² = H) showed good antiproliferation properties against the MCF-7 cell line (IC₅₀ = 0.42 ± 0.06 and 0.17 ± 0.02 μ M, respectively; SRB “sulforhodamine B” assay), relative to the reference standard, combretastatin A-4 (IC₅₀ = 0.016 ± 0.003 μ M). The tubulin polymerization inhibition revealed by the promising agents discovered (IC₅₀ = 1.7 ± 0.6 and

$1.4 \pm 0.02 \mu\text{M}$, respectively) is close to that of the reference standard, combretastatin A-4 ($\text{IC}_{50} = 1.2 \pm 0.08 \mu\text{M}$) [132].

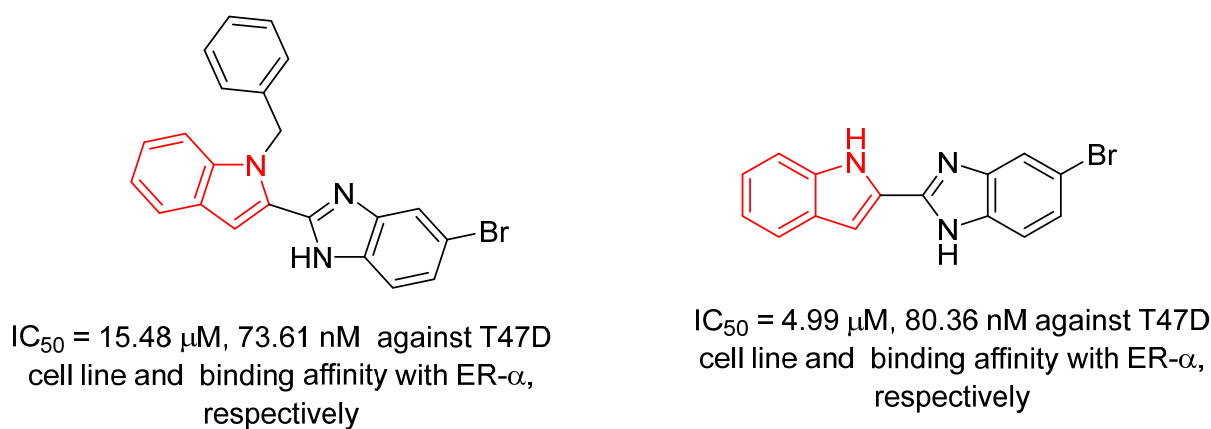
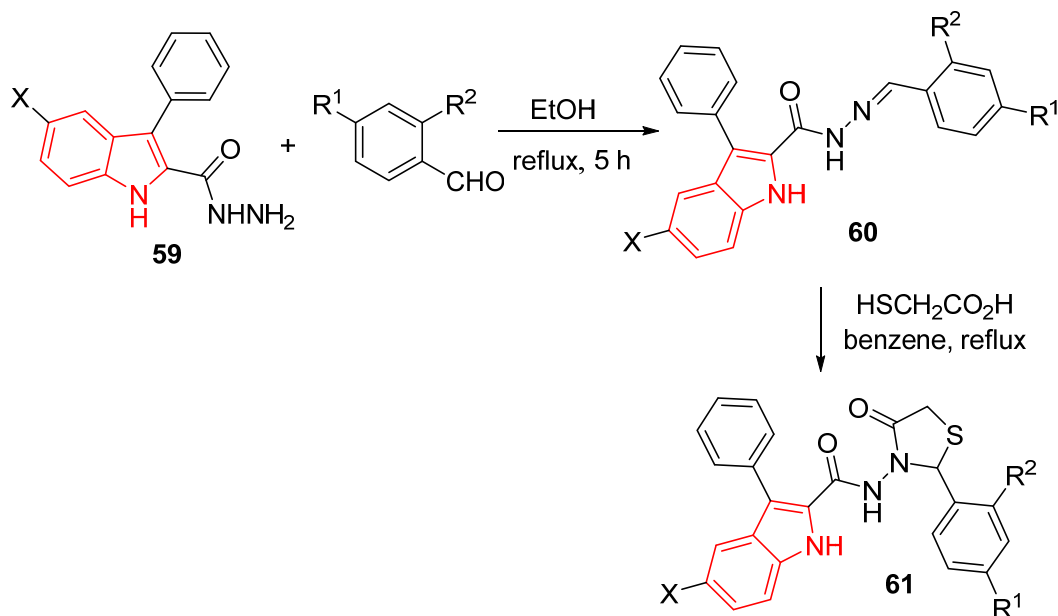
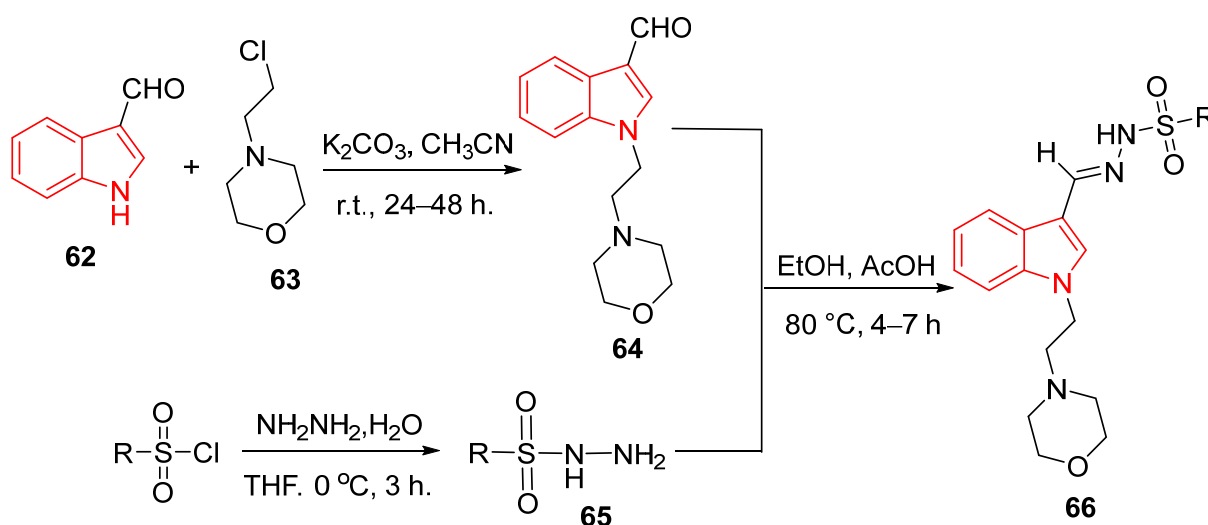


Figure 12. Promising antiproliferative indole–benzimidazole conjugates 58.



Scheme 4. Synthetic route towards indole-2-carbohydrazides 60 and thiazolidines 61.

Indolyl sulfonylhydrazones 66 bearing morpholinyl scaffold were synthesized through a condensation reaction (EtOH/ AcOH, 80 °C) of sulfonyl hydrazides 65 with 3-indolecarboxaldehyde 64 (obtained from the reaction of 62 with chloroethyl morpholine 63 in the presence of $\text{K}_2\text{CO}_3/\text{CH}_3\text{CN}$ at room temperature) (Scheme 5). Antiproliferative properties were investigated (MTT assay) against MCF7 (estrogen receptor-positive) and MDA-MB-468 (triple-negative) breast cancer cell lines. Some of the synthesized agents revealed considerable anti-breast cancer properties, of which the p-chlorophenyl-containing analog ($\text{R} = 4\text{-ClC}_6\text{H}_4$) showed promising properties ($\text{IC}_{50} = 13.2$ and $8.2 \mu\text{M}$ against MCF-7 and MDA-MB-468, respectively) compared with doxorubicin (positive drug control, $\text{IC}_{50} = 0.06$ and $0.08 \mu\text{M}$, respectively). All the tested compounds behaved safely toward HEK 293, a non-cancer cell, in concentrations up to $100 \mu\text{M}$ [133] (Supplementary Figure S4).



R = 4-H₃COC₆H₄, 4-H₃CC₆H₄, Ph, 4-FC₆H₄, 4-NO₂C₆H₄, 4-ClC₆H₄, 4-Me₃CC₆H₄, C₆H₄CH₂, 2-naphthyl, 1,1'-biphenyl, 5-quinoliny

Scheme 5. Synthetic route towards indolyl sulfonohydrazone 66.

Various thiazolyl hydrazones linked to indolyl scaffold 71 were synthesized by reacting the appropriate 3-indolecarboxaldehyde 68 with thiosemicarbazide (EtOH, room temperature). The reaction of the resulting thiosemicarbazones 69 with the appropriate phenacyl bromide 70 produced the targeted hydrazones 71 (Scheme 6). The antiproliferation and tubulin polymerization inhibitory properties of the synthesized agents were studied (Supplementary Figure S5). The most promising agent observed is that of R¹ = H, R² = OMe, and R³ = 3-Br (IC₅₀ = 0.46, 0.21, and 0.32 μM against MCF-7 (breast), A549 (lung), and Hela (cervical) cell lines, respectively; with tubulin polymerization inhibitory properties IC₅₀ = 1.68 μM) relative to colchicine and combretastatin A-4 “CA-4” (IC₅₀ = 0.75, 0.68, and 0.72; 0.52, 0.24, and 0.48 μM against MCF-7, A549, and Hela cell lines; with tubulin polymerization inhibitory properties IC₅₀ = 3.28 and 2.12 μM, respectively). Its ability to induce apoptosis and arrest the cell cycle at the G2/M phase was supported by flow cytometric analysis/study. Docking studies (PDB ID: 1SA0, Discovery Studio 3.5 software) were utilized to explain the mode of action considered [134].

Indole-triazole conjugates 74 and 75 were obtained through the reaction of indolyl-triazolethione 73 with allyl bromide and 1-bromopropan-2-ol (stirring in dry Me₂CO containing K₂CO₃ at room temperature overnight), respectively (Scheme 7). Conjugate 75 reveals better activity/inhibitory properties than that of 74 against PARP-1 “poly(ADP-ribose) polymerase-1” (IC₅₀ = 0.35 ± 0.05 and 0.33 ± 0.10 μM ± SD, respectively) relative to olaparib (standard reference/drug IC₅₀ = 1.8 × 10⁻³ ± 0.0001 μM) (Figure 13). PARP-1 is a key enzyme in DNA repair. It represents an important target in combating oncology in breast cancer cells and is safe against normal cells with lethal mode selectivity [135].

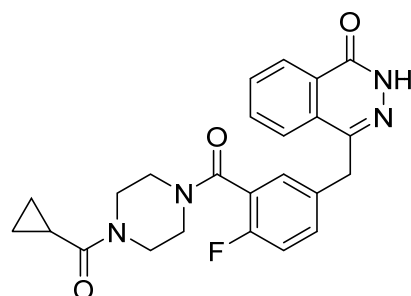
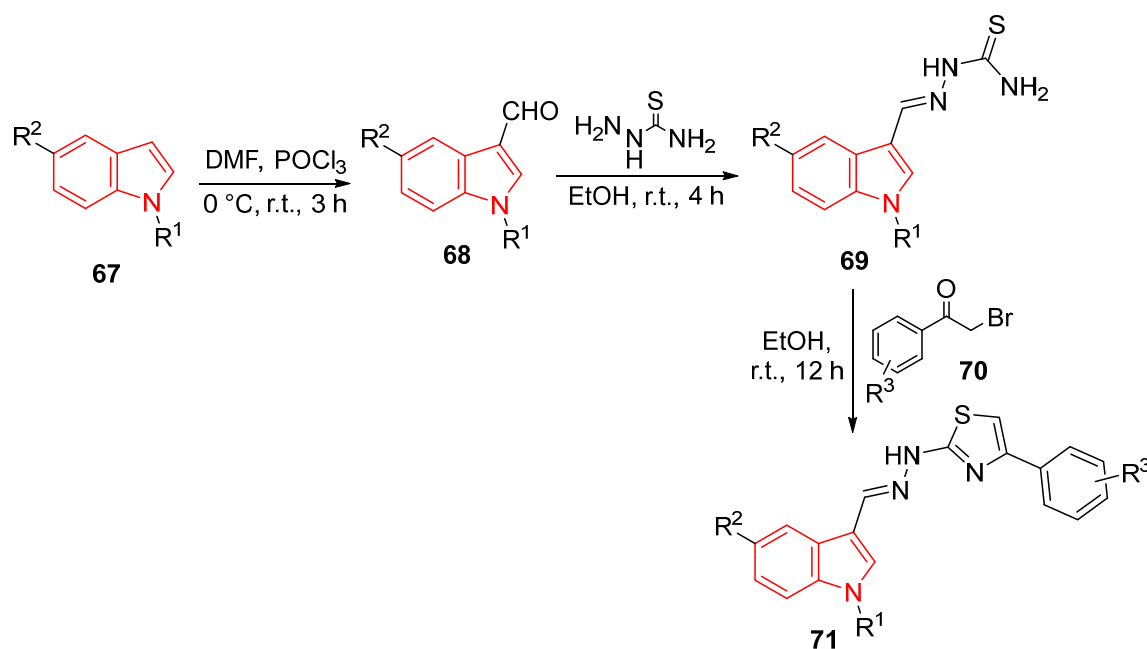
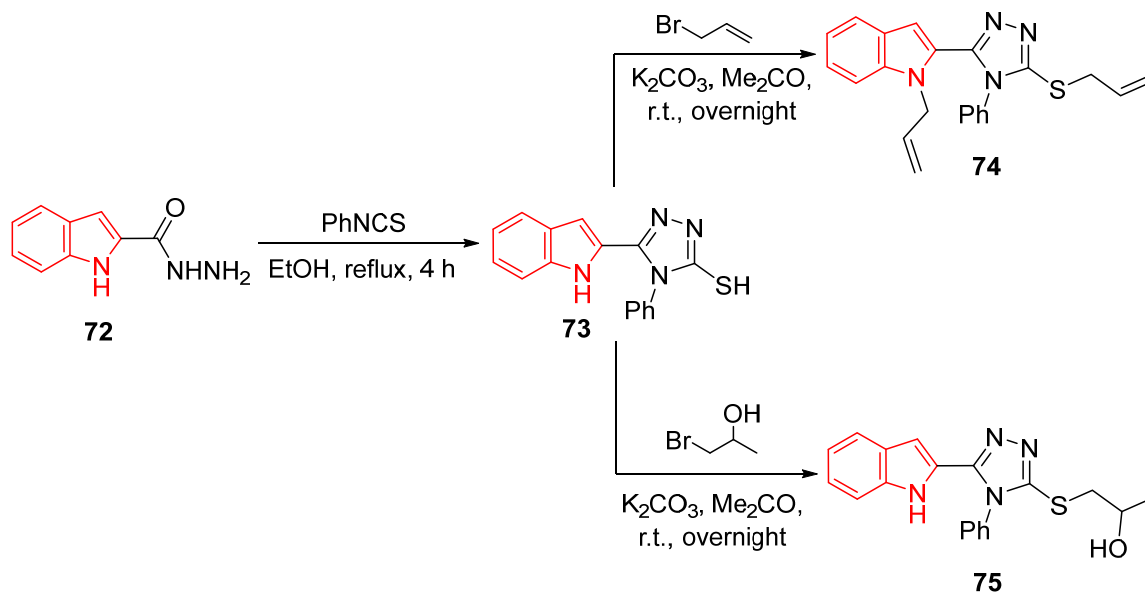


Figure 13. Chemical structure of olaparib (standard drug against PARP-1).



$\text{R}^1 = \text{H, Me}; \text{R}^2 = \text{H, OMe, Br}; \text{R}^3 = \text{H, 2-OMe, 4-OMe, 3-Br, 4-Br, 4-CF}_3, \text{4-phenyl}$

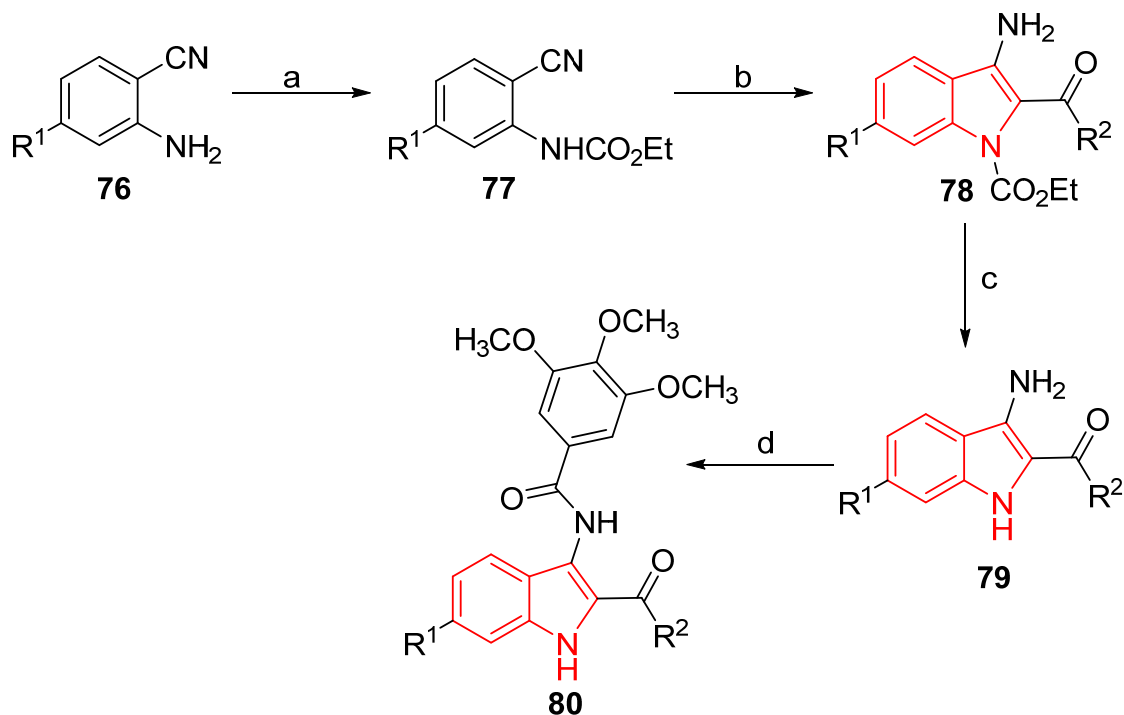
Scheme 6. Synthetic route towards thiazolyl hydrazones linked to indolyl scaffold 71.



Scheme 7. Synthetic route towards indole-triazol congenates 74 and 75.

A short library of 3-amido indoles **80** was synthesized via hydrolysis (NaOH in refluxing aqueous EtOH) of the corresponding 1-ethyl carbonyl indoles **78**, giving the *N*-unsubstituted indoles **79**, followed by acylation with 3,4,5-trimethoxybenzoyl chloride in anhydrous THF containing TEA (triethylamine) at room temperature (Scheme 8). Some of the synthesized agents revealed considerable antiproliferation properties (MTT assay) against breast cancer cell lines MCF-7, MDA-MB-231, BT549, T47D, MDA-MB-468, and HS578T. The most promising is that with $\text{R}^1 = \text{Cl}$, $\text{R}^2 = 4\text{-ClC}_6\text{H}_4$ displays considerable activity with tubulin polymerization inhibitory properties ($\text{IC}_{50} = 10.87, 6.43, 3.17, 0.04,$ and $7.92 \mu\text{M}$ against MCF-7, MDA-MB-231, BT549, T47D, and MDA-MB-468, respectively; $\text{IC}_{50} = 9.5 \mu\text{M}$ against tubulin polymerization) relative to combretastatin A-4 (CA-4, reference agent, $\text{IC}_{50} = 3.00, 3.17, 1.71, 1.89,$ and 1.55 nM against MCF-7, MDA-MB-231, BT549,

T47D, and MDA-MB-468, respectively; $IC_{50} = 4.22 \mu\text{M}$ against tubulin polymerization) (Supplementary Figure S6). Its flow cytometric studies evidenced the cell cycle arrest at the G2/M phase. Molecular docking studies (PDB ID: 5lyj; SURFLEX module of SYBYL 7.3) revealed its interaction in the colchicine binding active site [136].



$R^1 = \text{H, Me, Cl, MeO}$; $R^2 = \text{C}_6\text{H}_5, 4\text{-BrC}_6\text{H}_4, 4\text{-ClC}_6\text{H}_4, 4\text{-FC}_6\text{H}_4, 4\text{-MeC}_6\text{H}_4, 3,4\text{-F}_2\text{C}_6\text{H}_3, 4\text{-MeOC}_6\text{H}_4, 3\text{-MeOC}_6\text{H}_4, 3\text{-OH-4-MeOC}_6\text{H}_3, 2\text{-furyl, thiophen-2-yl, biphenyl, naphthyl}$

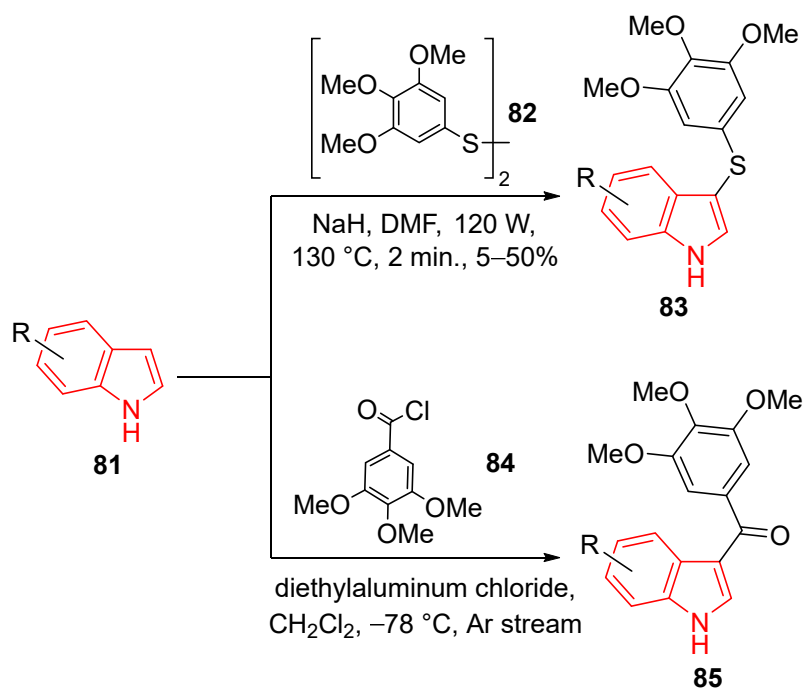
(a) ClCO_2Et , reflux; (b) K_2CO_3 , α -bromoketones, DMF, r.t.; (c) aqueous EtOH, 2M NaOH, reflux; (d) 3,4,5-trimethoxybenzoyl chloride, Et_3N , THF, r.t.

Scheme 8. Synthetic route towards 3-amidoindoles **80**.

3-Arylthio-1*H*-indoles **83** bearing heterocyclic rings at positions 5, 6, or 7 of the indolyl nucleus were synthesized through the reaction of the appropriate indole **81** with bis(3,4,5-trimethoxyphenyl)disulfide **82** in anhydrous DMF containing NaH (microwave “MW” radiation, 120 W, 130 °C) (Scheme 9). Potent antiproliferative properties against MCF-7 (a non-metastatic breast cancer cell line, MTT assay) were exhibited (IC_{50} in nanomolar value). Compounds **83**, where R = 6-thiophen-3-yl and 7-thiophen-2-yl, are the most potent agents revealed ($IC_{50} = 4.5$ and 29 nM, respectively) relative to the reference drug CA-4 ($IC_{50} = 13$ nM). Additionally, tubulin polymerization inhibition is promising ($IC_{50} = 0.58$ and 0.57 μM , respectively) compared to CA-4 ($IC_{50} = 1.0 \mu\text{M}$).

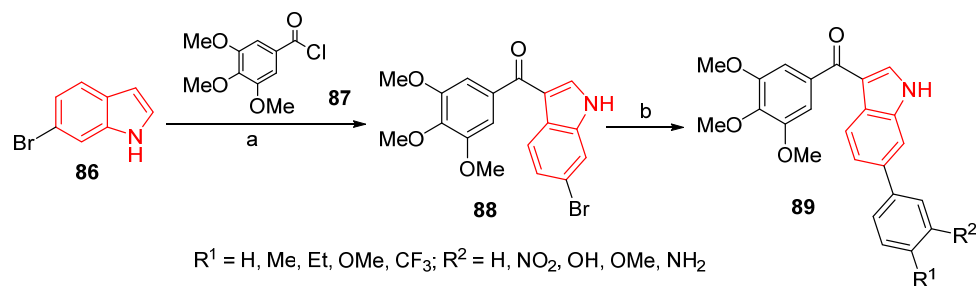
The role of the sulfur bridging atom was studied by constructing an **85**-containing carbonyl function. The 3-aryl-1*H*-indoles **85** were obtained through a reaction of the appropriate indole **81** with 3,4,5-trimethoxybenzoyl chloride **84** in the presence of diethylaluminum chloride in CH_2Cl_2 (inert atmosphere at $-78 \text{ }^\circ\text{C}$). Although promising antiproliferation properties were observed by some of the synthesized agents against the MCF-7 cell line, a dramatic drop was exhibited due to the analogs with sulfur bridging mentioned upon utilizing carbonyl function ($IC_{50} = 18$ and 550 nM for R = 6-thiophen-3-yl and 7-thiophen-2-yl, respectively) (Supplementary Figure S7). Molecular docking stud-

ies (PDB ID: 1SA0) were considered for compounds with potent tubulin polymerization inhibition for understanding and explaining the mode of action shown [137].



Scheme 9. Synthetic route towards 3-arylthio- **83** and 3-aryl-1H-indoles **85**.

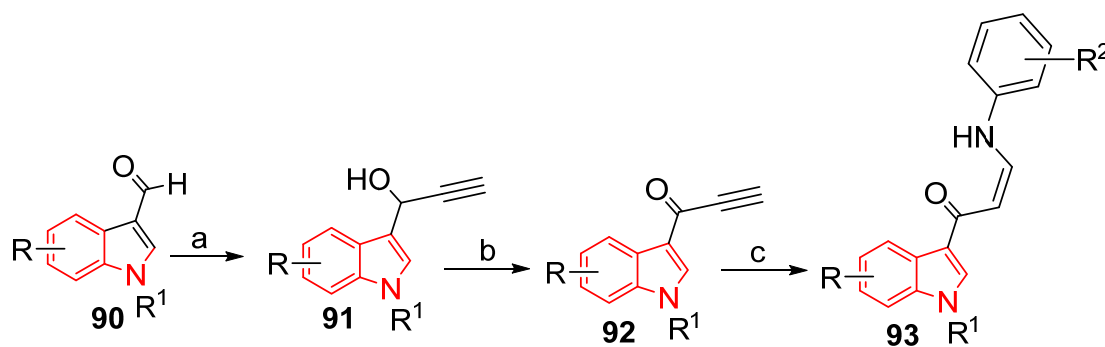
Friedel-Craft acylation of 6-bromoindole **86** using 3,4,5-trimethoxybenzoyl chloride **87** afforded the corresponding 3-aroil indole **88** (HFIP (hexafluoroisopropanol) at room temperature is an adequate condition for inter- and intramolecular Friedel-Craft acylation) [138,139]. The Suzuki coupling reaction of **88** with various aryl boronic acids produced the targeted 6-aryl indoles **89** in DME (dimethoxyethane)/H₂O under microwave irradiation conditions [138] (Scheme 10). Antiproliferation properties (SRB assay) and inhibitory tubulin polymerization against breast cancer cell lines (MCF-7 and MDA-MB-231) were observed for the targeted agents **89** relative to those of CA-4 (Supplementary Figure S8). The most promising analog ($\text{R}^1 = \text{H}$, $\text{R}^2 = \text{OH}$) discovered can arrest the cell cycle at the G2/M phase in the MDA-MB-231 cell (flow cytometry), disrupt the microtubule structure, and inhibit cell migration. Molecular docking studies revealed valuable insights regarding key interactions towards the colchicine site (PDB ID: 1SA0, Discovery Studio 4.5 software) [138].



(a) HFIP, r.t., 12 h; (b) aryl boronic acid, DME/H₂O (2:1), MW, 15 min.

Scheme 10. Synthetic route towards 6-aryl-3-aroil-indoles **89**.

Molecular conjugation is an important and famous approach intensively used in medicinal chemistry for designing/optimizing highly promising hits/leads against different diseases. This usually takes place by connecting biologically active functional group(s) and/or scaffold(s) to each other with or without a linker [140–144]. Indolyl-arylaminopropenone conjugates **93** were prepared by reacting indole-3-carboxaldehydes **90** with ethynyl magnesium bromide, producing the corresponding arylprop-2-yn-1-ols **91**. Oxidation of the latter alcohols using 2-iodoxybenzoic acid (IBX) in DMSO yielded the corresponding alkynes **92**, which were subjected to reaction with various anilines (EtOH, r.t.), giving the targeted conjugates indolyl-arylaminopropenones **93** (Scheme 11). The antiproliferation properties (MTT assay) of **93** were determined against MCF-7, HeLa, A549, and DU145 (breast, cervical, lung, and prostate cell lines, respectively). Among them, synthesized conjugates [R = H, R¹ = 4-chlorobenzyl, R² = 3,4,5-(OMe)₃] and [R = H, R¹ = benzyl, R² = 3,4,5-(OMe)₃] exhibited considerable properties against the MCF-7 cell line (IC₅₀ = 2.3 and 1.9 μM, respectively) relative to doxorubicin (IC₅₀ = 0.8 μM) (Supplementary Figure S9). Both compounds showed cell cycle arrest at G₀/G₁ (flow cytometry) and induction of cell death apoptosis. Molecular docking (PDB ID: 4AQ3, Schrodinger suite 2014–3) observations of the most promising agents discovered support the Bcl-2 protein (anti-apoptotic protein) interactions and bio-properties revealed [145].



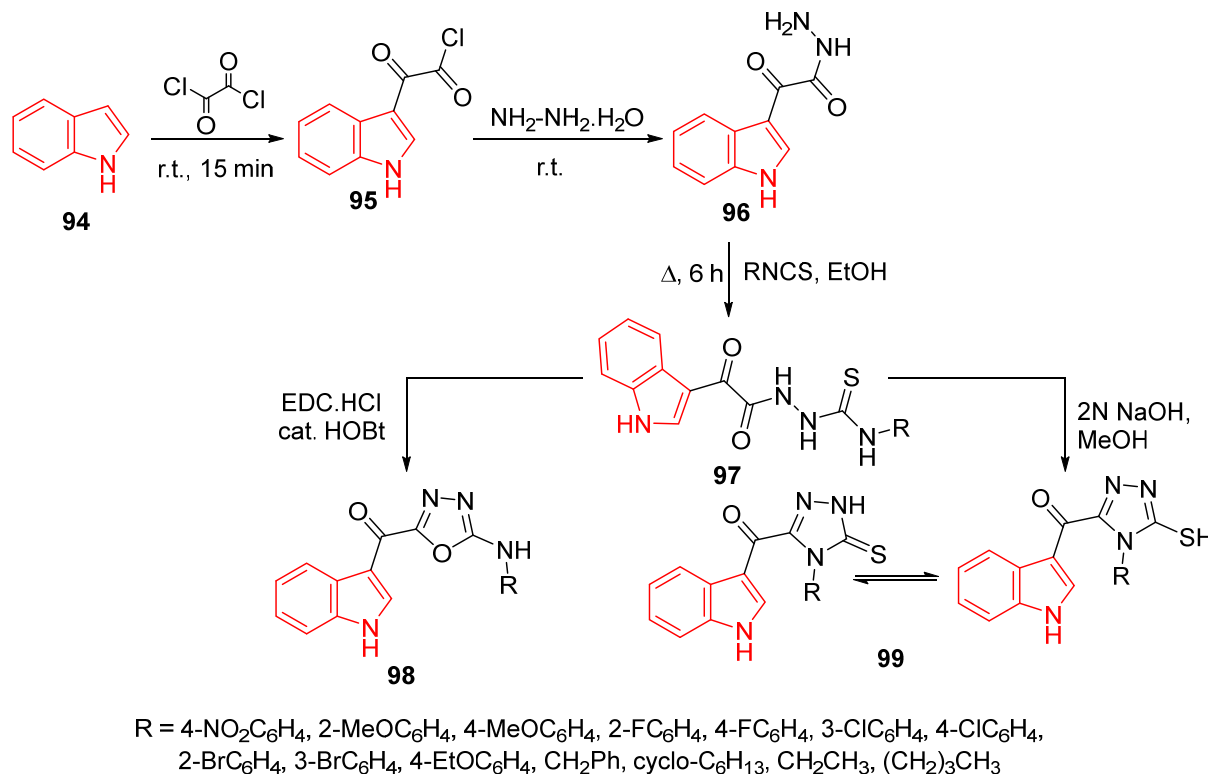
(a) Ethynyl magnesium bromide, dry THF, 0 °C–r.t., 4h; (b) IBX, DMSO, 0 °C–r.t. 2h;
(c) substituted anilines, EtOH, r.t., 3–4h

R = H, 6-Br; R¹ = 4-Cl-benzyl, benzyl, methyl; R² = H, 4-Cl, 4-F, 4-OCH₃,
3,4,5-(OCH₃)₃, 3,4-F₂

Scheme 11. Synthetic route towards indolyl-arylaminopropenone conjugates **93**.

1,3,4-Oxadiazole-indole **98** and 1,3,4-triazole-indole conjugates **99** were synthesized in a multi-step reaction sequence. 3-Indolyl-2-oxoacetyl chloride **95** was obtained from the reaction of indole **94** and oxalyl chloride, which was further subjected to the reaction with hydrazine hydrate, yielding the corresponding oxoacetohydrazide **96**. Refluxing the hydrazide **96** with isothiocyanates produced the corresponding thiosemicarbazides **97**. Cyclization of the latter with either EDC.HCl (*N*-ethyl-*N'*-(3-dimethylaminopropyl)carbodiimide hydrochloride) or HOBt (hydroxybenzotriazole) produced the 1,3,4-oxadiazole-indole conjugates **98**. However, cyclization of **97** with 2N NaOH afforded the corresponding 1,3,4-triazole-indole conjugates **99** (Scheme 12). Antiproliferation properties (MTT assay) revealed the promising anti-MCF-7 activity of some synthesized oxadiazole **98** (R = 4-NO₂C₆H₄, 2-FC₆H₄, and 3-ClC₆H₄; IC₅₀ = 5.98, 2.42, and 8.11 μM, respectively) and triazole conjugates **99** (R = 4-FC₆H₄ and 3-BrC₆H₄; IC₅₀ = 3.06 and 3.30 μM, respectively) relative to doxorubicin and CA-4 (IC₅₀ = 6.31 and 2.16 μM, respectively). Furthermore, the potent synthesized oxadiazole hybrid **98** (R = 2-FC₆H₄) shows cell cycle arrest in the G₀/G₁ phase (flow cytometry), disruption of the mitochondrial membrane, and reduction in cell migration.

Additionally, tubulin polymerization inhibitory properties ($IC_{50} = 3.89 \mu\text{M}$) relative to those of nocodazole ($IC_{50} = 2.49 \mu\text{M}$) (Figure 14) were supported by *in vitro* studies. Molecular modeling studies (PDB ID: 1SA0) were utilized to explain the β -tubulin and antiproliferation properties [146].



Scheme 12. Synthetic route towards 1,3,4-oxadiazole-indole **98** and 1,3,4-triazole-indole conjugates **99**.

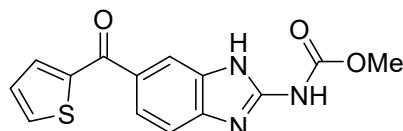
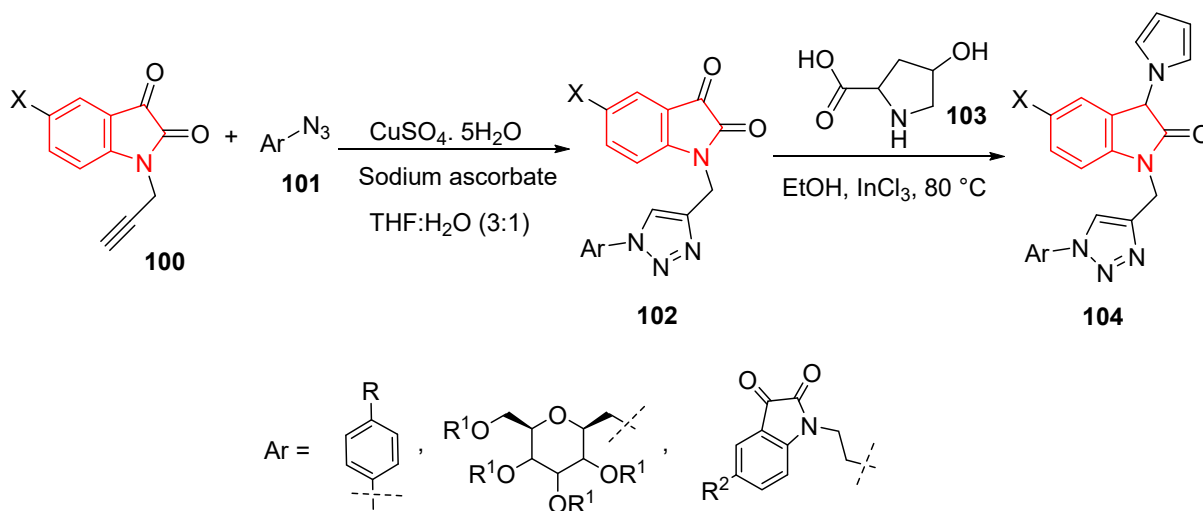


Figure 14. Chemical structure of nocodazole, an antineoplastic agent that exerts its activity by interfering with the polymerization of microtubules.

A set of 3-pyrrolylisatin-triazole conjugates **104** was obtained through the reaction of 4-hydroxyproline **103** with 1,2,3-triazole-isatin analogs **102** (obtained from the click reaction of *N*-indole alkynes **100** with substituted azides **101**) in EtOH (80 °C) containing InCl₃ (indium (III) chloride) as a Lewis acid catalyst (Scheme 13). Antiproliferative properties (MTT assay) of the targeted agents **104** against breast cancer (MCF-7 and MDA-MB-231) cell lines demonstrated that some of them have more potent activity than that of tamoxifen (an approved drug for breast cancer treatment, Figure 15), with similar behavior against the normal cell line HEK-293 (human embryonic) (Supplementary Figure S10). Molecular docking studies have evidenced the potential binding interaction of the potent agents synthesized and tamoxifen with topoisomerase II (PDB ID: 1ZXM) [147].

Spirochromenocarbazols linked to 1,2,3-triazole **106** were obtained through a multi-component click reaction of *N*-propargyl isatin **100**, malononitrile, 4-hydroxycarbazole **105**, sodium azide, and alkyl bromides using Cell-CuI NPs (cellulose-supported CuI nanoparticles) catalysis in DMF-H₂O (1:2 *v/v*) at 70 °C (Scheme 14). The antiproliferation properties (MTT assay) were determined against MCF7, MDA-MB-231 (breast), HeLa (cervical), A549 (lung), PANC-1 (pancreatic), and THP-1 (leukemia) cell lines (Supplementary Figure S11). Some synthesized spiro-analogs showed promising antiproliferative properties against MCF-7, MDA-MB-231, and HeLa cancer cells. The most effective agents are those with

R = H and R¹ = 4-NO₂C₆H₅ (IC₅₀ = 2.13 μM), revealing more enhanced properties than those of doxorubicin (IC₅₀ = 4.63 μM) against MCF7, with a satisfied safety profile towards HUVEC (umbilical vein endothelial/non-cancerous cell). Apoptotic cell death was suggested to be the leading cause of the reduced proliferation of breast cancer cells, which was supported by AO (acridine orange)/EtBrz (ethidium bromide) stains and fluorescence microscopy [148].



X = H, Cl; R = H, F, Cl, Br, NO₂, CH₃, OCH₃; R¹ = H, Ac; R² = H, Cl

Scheme 13. Synthetic route towards 3-pyrrolylisatin-triazole conjugates **104**.

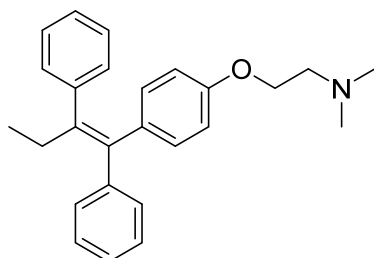
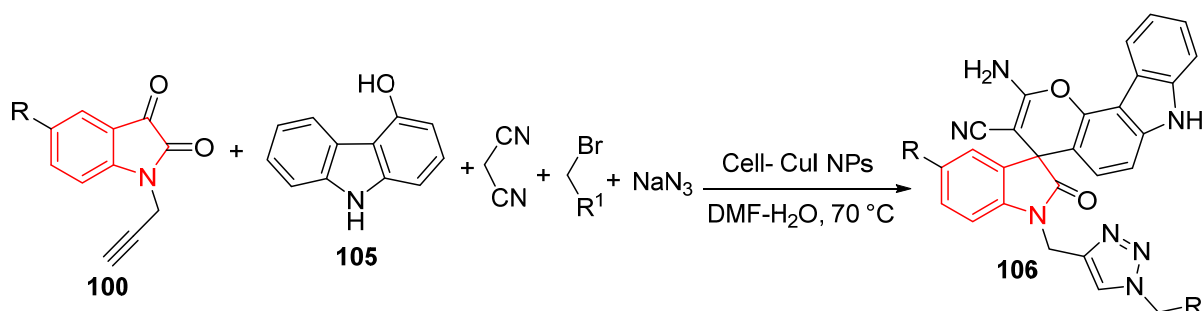


Figure 15. Tamoxifen (an approved drug for breast cancer).

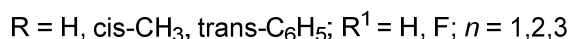
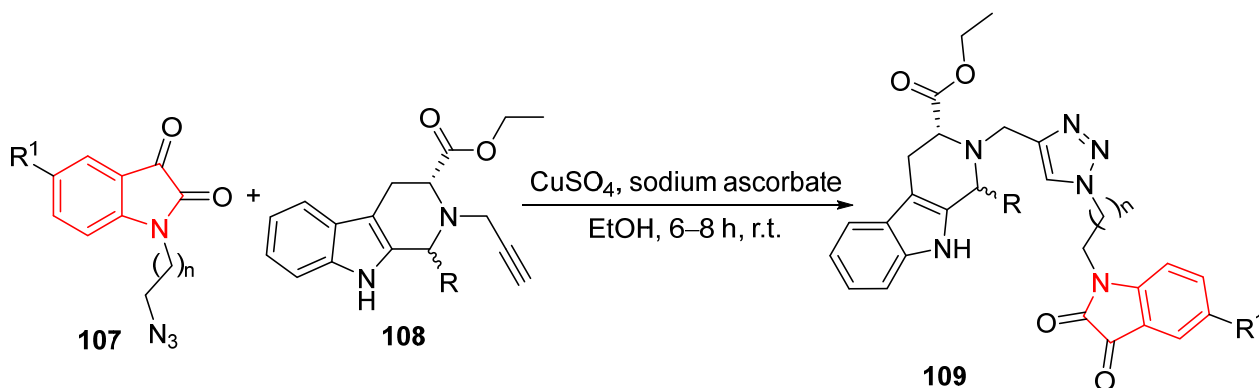


R = H, F, Cl, Br, Me; R¹ = C₆H₅, 4-FC₆H₄, 4-ClC₆H₄, 4-MeC₆H₄, 4-NCC₆H₄, 4-NO₂C₆H₄, 4-F₃CC₆H₄, 3,4,5-(OMe)₃C₆H₂, CO₂Et, (CH₂)₃-CH₃, CH₂CH(Br)CH₃

Scheme 14. Synthetic route towards spirochromenocarbazols linked to 1,2,3-triazole **106**.

A series comprising tetrahydro-β-carboline and isatin scaffolds connected by 1*H*-1,2,3-triazolyl heterocycle **109** was synthesized through click cycloaddition of the azide-alkyne isatins **107** and the corresponding carboline **108** in the presence of CuSO₄/sodium ascorbate in EtOH at room temperature (Scheme 15). The antiproliferation properties (MTT) of **109**

were studied against MCF-7 and MDA-MB-231 cell lines (Supplementary Figure S12). Few of the synthesized agents revealed promising antitumor properties against MCF7. The most promising is that with $R = R^1 = H$, $n = 2$ ($IC_{50} = 37.42 \mu M$) relative to peganumine A (β -carboline analog, obtained from *Peganum harmala*) and tamoxifen ($IC_{50} = 38.5$ and $50 \mu M$, respectively). The docking study (PDB ID: 3ERT, Autodock Vina software, V 1.5.6) explained the bio-properties exhibited [149].



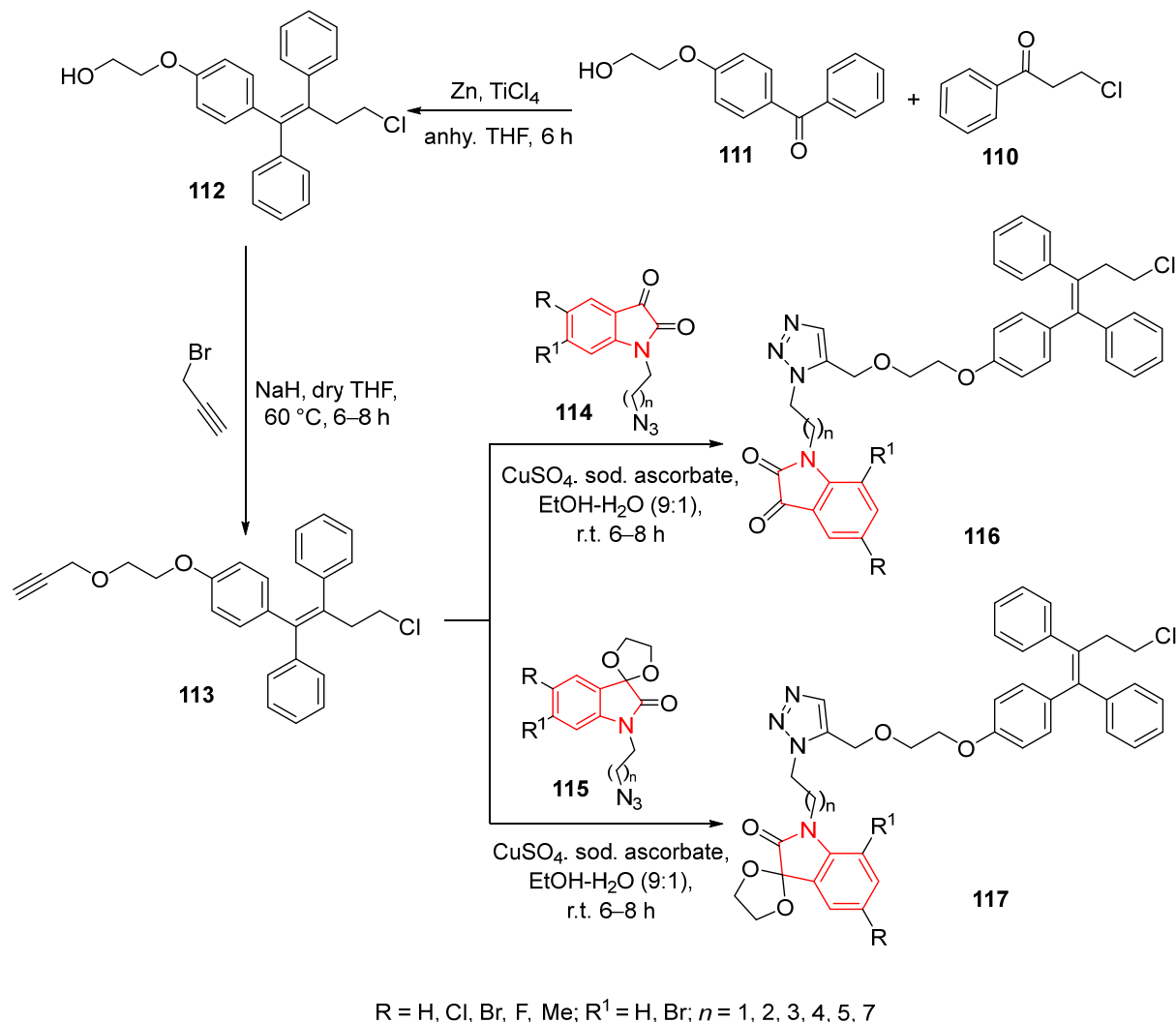
Scheme 15. Synthetic route towards 1H-1,2,3-triazole connecting tetrahydro- β -carboline and isatin scaffolds 109.

A group of ospemifene-isatins **116** and ospemifene-spiroisatins **117** conjugates linked through a 1H-1,2,3-triazolyl heterocycle was synthesized via click cycloaddition ($CuSO_4$, sodium ascorbate in EtOH/ H_2O) of the appropriate azide-containing indoles **114/115** with alkynes containing ospemifene **113** (Scheme 16). Antiproliferation properties (MTT assay) were studied against breast cancer (MCF-7 and MDA-MB-231) cell lines. Some of the synthesized conjugates revealed considerable anti-MCF7 properties. The most promising is the conjugate **116** ($R = R^1 = Br$, $n = 1$; $IC_{50} = 1.56 \mu M$) relative to that of the standard references ($IC_{50} = 55$ and $50 \mu M$ of ospemifene and tamoxifen, respectively). It has been noticed that when a more extended spacer/alkyl group was considered ($n = 2$ or 3), the anti-MCF-7 properties were drastically reduced ($IC_{50} = 16.54$ and $10.99 \mu M$, respectively) (Supplementary Figure S13). Molecular docking studies (PDB ID: 3ERT, ER α active site, Autodock Vina software V 1.5.6) explained the biological properties exhibited [150].

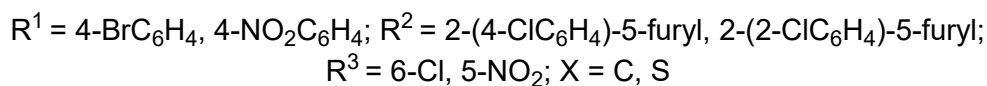
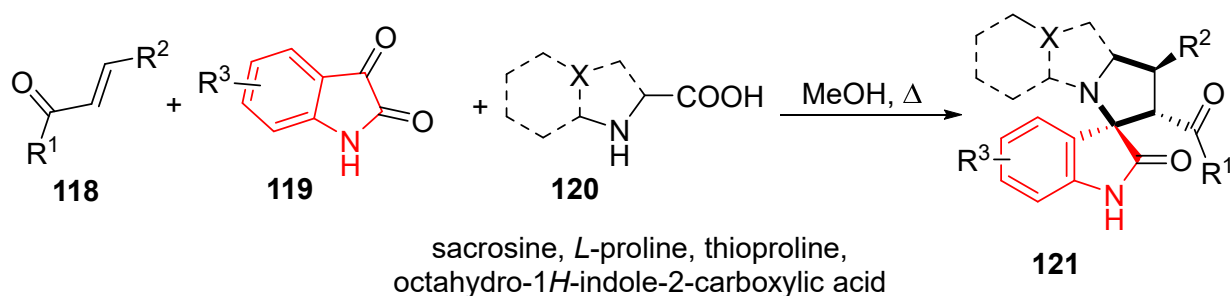
A series of spiroxindoles bearing 2-furanyl heterocycle **121**, prepared from the azomethine ylide reaction (obtained from isatins **119** and amino acids **120**) with furanyl-containing chalcones **118** in refluxing MeOH (Scheme 17), showed promising results. The antiproliferation properties (MTT technique) of **121** were assessed against the MCF7 cell line. Amongst all, the analog derived from chalcone with $R^1 = 4-BrC_6H_4$, $R^2 = 2-(4-ClC_6H_4)-5-furyl$, 6-chloroisatin, and octahydro-1H-indole-2-carboxylic acid (Figure 16) exhibited potent activity ($IC_{50} = 4.3 \mu M/mL$) compared with the standard staurosporine ($IC_{50} = 17.8 \mu M/mL$) (Supplementary Figure S14). The molecular modeling of the potent agent suggested a dual mode of action against EGFR and CDK-2 (PDB ID: 1M17 and 2A4L, respectively; AutoDock Vina software V 1.5.6) [151], indicating the potential for further development.

Spiroxindoles **124** were obtained through a multi-component condensation reaction of isatins **119**, aroylacetonitriles **122**, and 5-aminopyrazole **123** (Scheme 18). Some targeted agents **124** exhibited mild antiproliferation properties (MTT assay) against the MDA-MB-231 cell line (Supplementary Figure S15). The most promising are those with $R/R' = H/Ph$, Cl/Ph , and Br/Ph ($IC_{50} = 6.70$, 6.40 , and $6.70 \mu M$, respectively) relative to doxorubicin (adriamycin, $IC_{50} = 0.12 \mu M$). Safety behavior against WI-38 (lung normal cell) was evidenced for the effective agents discovered ($IC_{50} = 78.1$, 43.2 , and $39.3 \mu M$ for compounds **124** with $R/R' = H/Ph$, Cl/Ph , and Br/Ph , respectively). Upregulation of Bax and downregulation of Bcl-2 proteins in addition to elevation of caspase-3 levels evidenced the induction of

apoptosis of the effective agents discovered (effect = 405.5, 353.7, and 0.80; 0.3958, 0.7449, and 2.692; 0.3501, 0.4058, and 0.0111 pg/mL for compounds **124** with R/R' = H/Ph and Cl/Ph against Bax, Bcl-2, and caspase-3, respectively). Inhibition of EGFR was reported as the mode of action for the promising agents discovered relative to erlotinib [152].



Scheme 16. Synthetic route towards ospemifene-isatin/ospemifene-spiroisatin **116/117**, linked through 1*H*-1,2,3-triazole, respectively.



Scheme 17. Synthetic route towards spirooxindoles **121**.

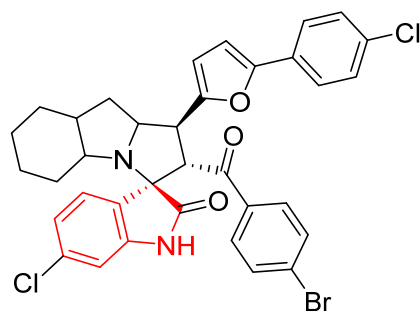
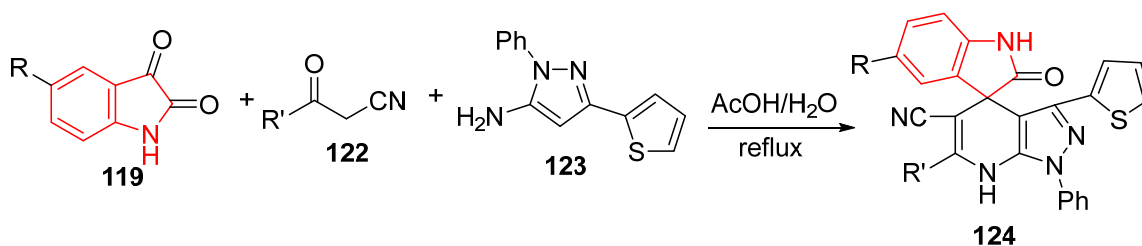


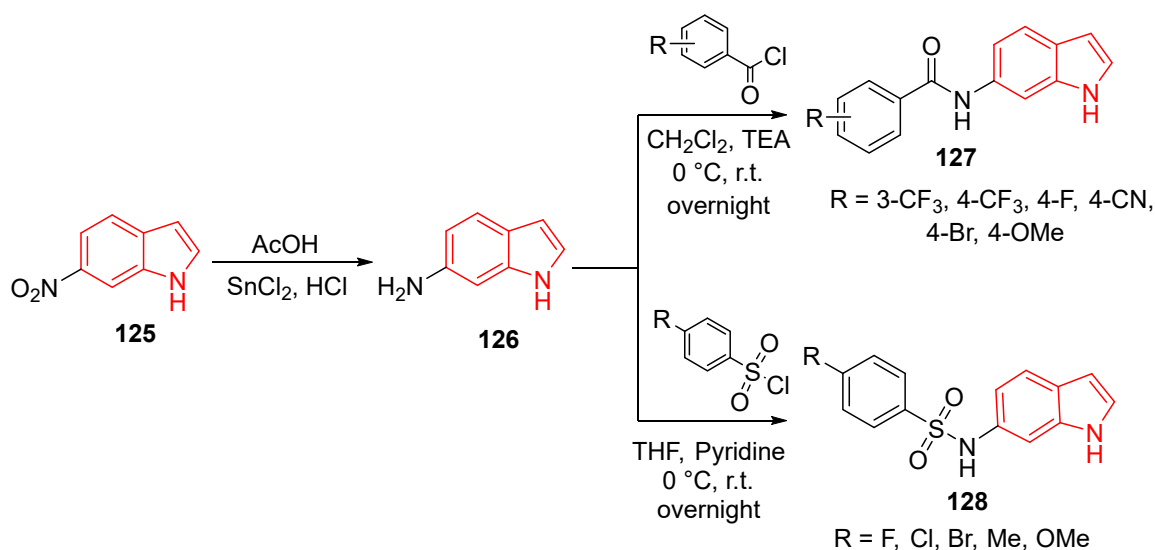
Figure 16. Most potent spiroindole **121** against the MCF7 cell line.



R = H, Cl, Br, OMe; R' = Ph, 4-MeC₆H₄, 4-MeOC₆H₄, 4-ClC₆H₄

Scheme 18. Synthetic route towards spiroindoles **124**.

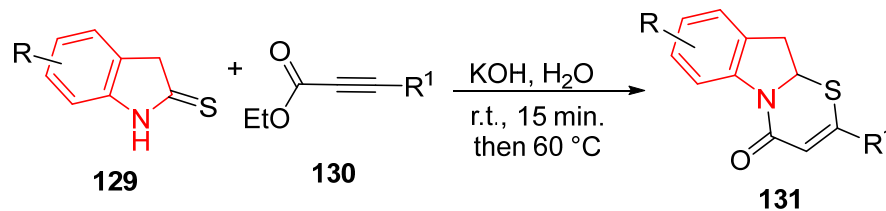
N-(1*H*-indole-6-yl) benzamides **127** and their benzene sulfonamide analogs **128** were obtained through acylation/sulfonylation of 6-aminoindole **126**. The latter was synthesized via reduction (SnCl₂/HCl/AcOH) of the corresponding 6-nitroindole **125** (Scheme 19). Cell viability assays of the synthesized compounds against breast cancer cell lines (MCF7 and T47D) were studied (Supplementary Figure S16). The most promising was **127**, where R = 3-CF₃ (IC₅₀ = 28.23 and 30.63 μM) relative to tamoxifen (IC₅₀ = 34.42 and 42.40 μM) against the T47D and MCF7 cell lines, respectively. A reduction in tumor size in Ehrlich ascites carcinoma (EAC)-bearing mice was observed by compounds **127** (R = 3-CF₃) and **128** (R = F), supporting their potential necrosis effect and decrease in ER-α expression in tumor sections [153].



Scheme 19. Synthetic route towards *N*-(1*H*-indole-6-yl)benzamides/benzene sulfonamides **127** and **128**.

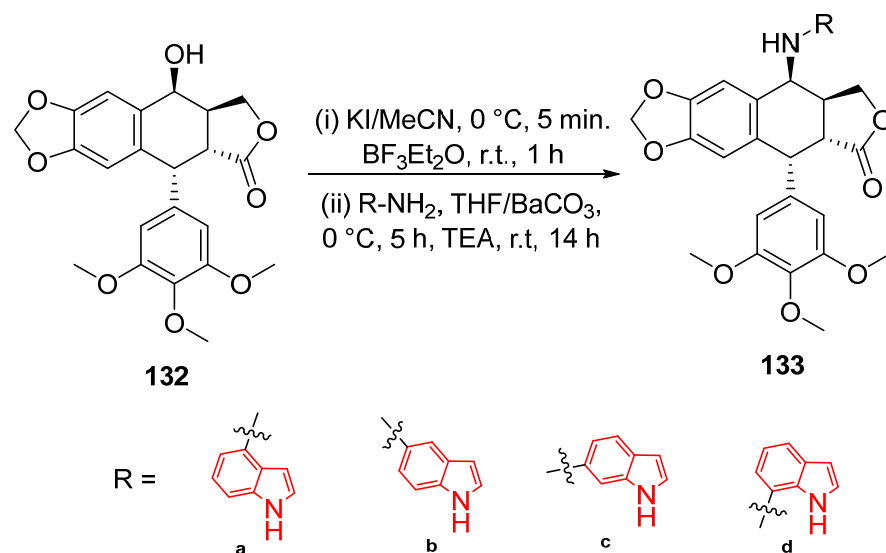
[1,3]Thiazino[3,2-*a*]indol-4-ones **131** were obtained from the reaction of indoline-2-thiones **129** and propionic acid esters **130** in aqueous medium by KOH/H₂O (Scheme 20). The antiproliferative properties (MTT assay) against the MDA 231 and MDA 468 cell lines

were studied (Supplementary Figure S17). Two of the synthesized agents ($R/R^1 = H/CH_3$ and $5-CH_3/n-C_3H_7$, $IC_{50} = 302$ and $116; 330$ and $97 \mu M$ against MDA-231 and MDA-468, respectively) displayed considerable antiproliferation properties [154].



Scheme 20. Synthetic route towards 4H-[1,3]thiazino[3,2-a]indol-4-ones 131.

Podophyllotoxin **132** is an important agent with antiproliferation properties against diverse cancer cell lines, exhibiting affinity at the colchicine binding site and identifying tubulin polymerization inhibitory properties. A series of indole-podophyllotoxin conjugates **133** was developed via the halogenation reaction of **132** using KI and BF_3OEt_2 in MeCN, affording the 4 β -iodopodophyllotoxin, which was subjected to nucleophilic attack of the indolyl derivative using $BaCO_3$ and triethylamine (TEA) in tetrahydrofuran (THF), affording the targeted conjugates **133** (Scheme 21). Potent tubulin polymerization inhibition was revealed by **133c** ($GI_{50} < 0.1 \mu M$). Moreover, **133c** displayed outstanding antiproliferation properties (MTT method) against HepG-2, HeLa, A549, and MCF-7 cell lines ($IC_{50} = 0.07$ – $0.1 \mu M$) relative to nocodazole ($IC_{50} = 0.2$ – $0.4 \mu M$) (Supplementary Figure S18). In vivo studies demonstrated that **133c** reduced tumor volume in the nude mouse xenograft MCF-7 cell model, supporting the idea that it can be considered a promising viable anticancer agent with tubulin polymerization inhibitory properties. Molecular docking studies (PDB ID: 5JCB, Discovery Studio software) were considered to explain the observed mode of action [155].

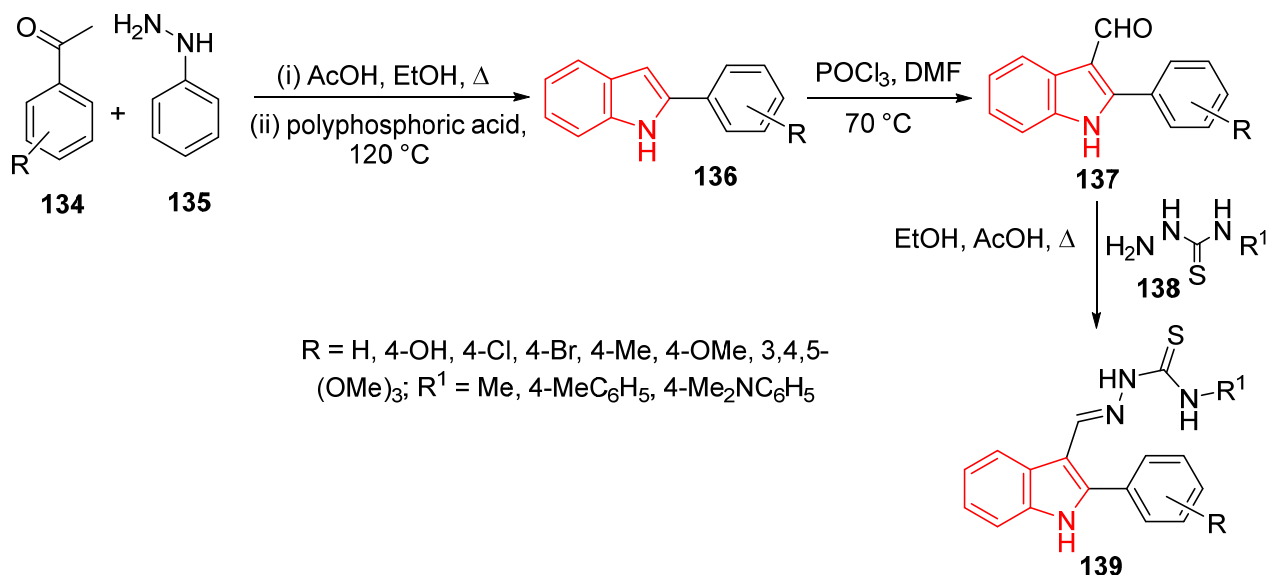


Scheme 21. Synthetic route towards indole-podophyllotoxin conjugates 133.

3.2. Lung Cancer

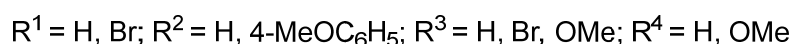
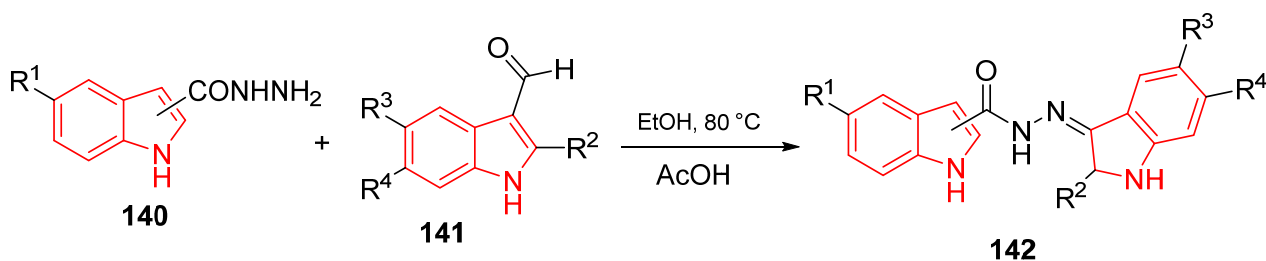
Indolylthiosemicarbazones **139** were obtained through condensation of indole-3-carboxaldehydes **137** (obtained from the Fischer reaction of acetophenones **134** with phenyl hydrazine **135** followed by the Vilsmeier formylation reaction) with the appropriate thiosemicarbazides **138** (Scheme 22). One of the synthesized agents **139** ($R = 4-OMe$, $R^1 = Me$) revealed potent antiproliferation properties (MTT method) against the lung

A549 cell line ($IC_{50} = 12.50 \mu\text{M}$), i.e., about three-fold more potency than the reference drug etoposide ($IC_{50} = 34.25 \mu\text{M}$) (Supplementary Figure S19). Apoptosis induction was reported for the potent agent discovered based on morphological and flow cytometric studies. Molecular modeling studies (PDB ID: 1S0 and 1ZXN, Discovery Studio 4.1 software) were considered for assigning the tubulin polymerization and topoisomerase II inhibitory properties, respectively [156].



Scheme 22. Synthetic route towards indolylthiosemicarbazones 139.

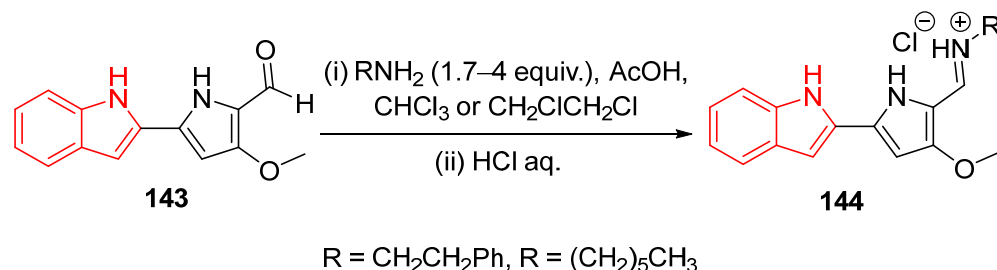
Microtubule assembly plays a crucial role in cellular division. For this reason, anti-tubulin/microtubule polymerization inhibition is one of the most effective approaches for combating many cancer types. Bis(indolyl)hydrazide-hydrazones 142 as tubulin polymerization inhibitors were designed. The targeted agents were obtained by refluxing a mixture of indolylcarboxylic acid hydrazides 140 with indole-3-carboxaldehydes 141 in EtOH containing a catalytic amount of AcOH (Scheme 23). The antiproliferation properties (MTT method) of 142 were evaluated against the lung cancer (A549) cell line, revealing that the compound with $\text{R}^1 = \text{R}^2 = \text{R}^4 = \text{H}$ and $\text{R}^3 = \text{OMe}$ was the most effective analog relative to colchicine ($IC_{50} = 2$ and $0.02 \mu\text{M}$, respectively) in arresting the cell cycle at the G2/M phase (flow cytometry) and tubulin polymerization inhibition ($IC_{50} \sim 7.5 \mu\text{M}$) [157] (Supplementary Figure S20).



Scheme 23. Synthetic route towards bis(indolyl)hydrazide-hydrazones 142.

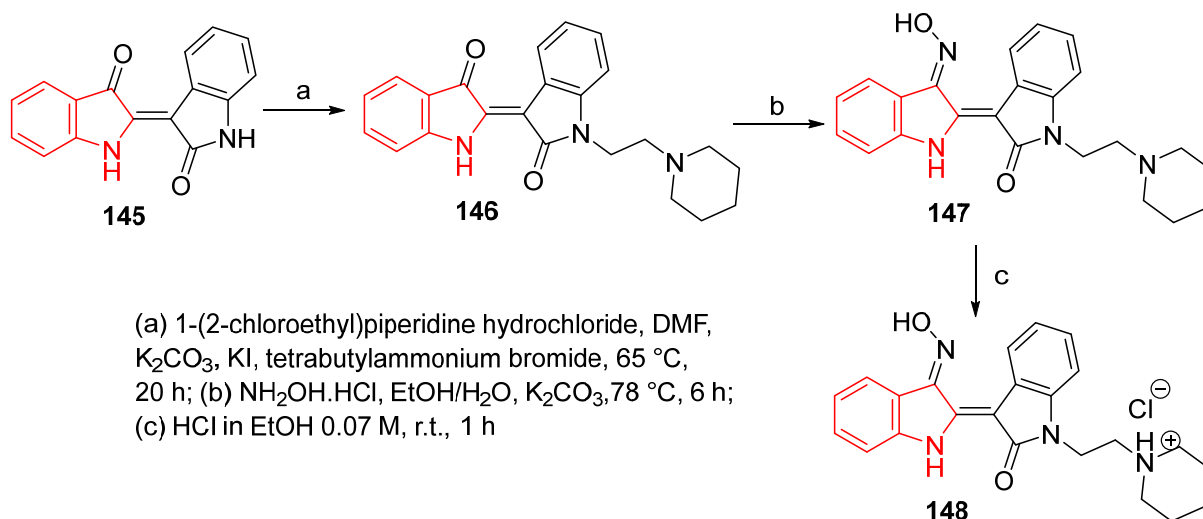
Tambjamine is a natural compound obtained from marine invertebrates with the ability to compromise cell survival. Indole-based tambjamine analogs 144 were synthesized as natural-based antitumor active agents by condensing the aldehydic analog 143 with the appropriate amine (Scheme 24). A potent inhibitory effect of the synthesized

analogs against lung cancer cell lines relative to cisplatin was observed (Supplementary Figure S21). The synthesized compounds introduced several gene expressions demonstrating induced cell death/apoptosis in addition to ROS (reactive oxygen species)-induced cellular stress [158]. It has also been mentioned that **144** with R = (CH₂)₅CH₃ can block Janus kinase/signal transducers, supported by a reduction in survivin protein levels and confirming the potential anti-lung efficacy through STAT3 inhibition [159].



Scheme 24. Synthetic route towards indole-based tambjamine analogs **144**.

Indirubin **145** is a natural compound with potential anti-leukemia activity in many plants and some protein kinase (CDK and GSK-3 β) inhibitory properties. Indirubin-piperidine conjugate **147** was synthesized via alkylation of **145** with 1-(2-chloroethyl)piperidine HCl, followed by condensation with NH₂OH-HCl. The HCl salt **148** was formed by the effect of EtOH/HCl on **147** (Scheme 25). Promising antiproliferation properties were revealed by the synthesized conjugate **147** and its HCl salt **148** against SW480, A549, HepG2, and B16F10 (colorectal, lung, liver, and melanoma cell lines, respectively; MTT technique) relative to bortezomib (Supplementary Figure S22). A better or more enhanced tumor reduction was exhibited through the in vivo testing (mouse model with skin cancer) of **148** compared to the standard (bortezomib) [160].



Scheme 25. Synthetic route towards indirubin-piperidine conjugate **146** and its HCl salt **147**.

Piperlongumine **149** is a natural alkaloid found in *Piper longum* L. with various biological properties (Figure 17). Conjugation of indolyl scaffold with the pharmacophoric unit of piperlongumine was considered for assigning promising antitumor active agents. The reaction of acyl chlorides **150** (obtained from the action of oxalyl chloride on the corresponding carboxylic acids) with lactams **151** (dry THF, TEA, 0 °C) produced the targeted conjugates **152** (Scheme 26) [161]. In vitro, cytotoxicity against A54, HCT116, ZR-75-30, and MDAMB-231 (lung, colon, breast ductal, and breast carcinoma, respectively) in addition to MRC-5 (normal) cell lines was studied (Supplementary Figure S23). Enhanced antiproliferation properties (MTT method) were noticed by the synthesized analogs **152** relative to the precursor piperlongumine **149**, with safe behavior against the normal lung cell line

(MRC-5). The most promising agents synthesized are $R = \text{Me}$ and $R^1 = \text{Cl}$, which exhibit induced apoptosis against the lung (A549) cancer cell line (flow cytometry), arresting the cell cycle at the G2/M phase. Furthermore, in vivo studies (BALB/C mice with lung cancer, A549 cells) of the promising agent (2 mg/kg/day, i.p., 14 days) revealed inhibition of tumor growth/volume (54.6%) compared with the parent piperlongumine **149** and doxorubicin (38.3 and 53.3%, utilizing 2 and 10 mg/kg/day for **149** and doxorubicin, respectively) [161].

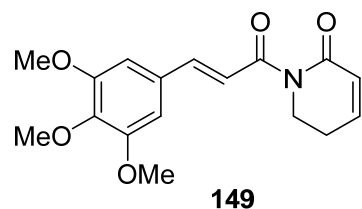
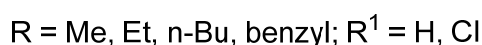
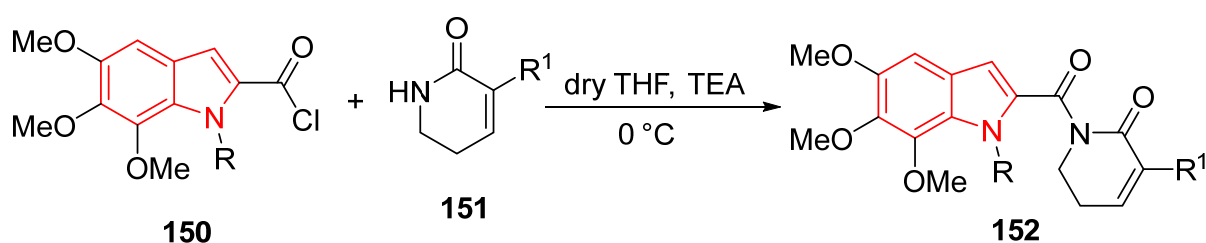


Figure 17. Chemical structure of piperlongumine **149**.

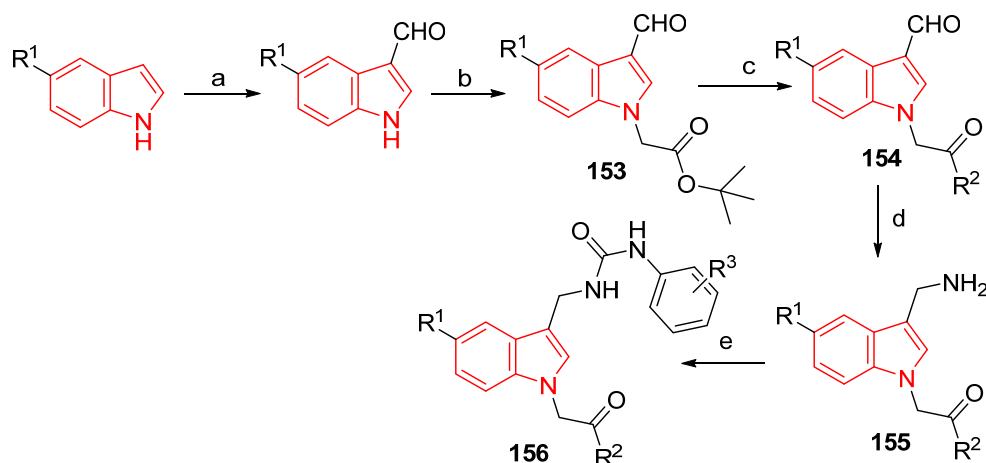


Scheme 26. Synthetic route towards indole-piperlongimine conjugates **152**.

Discoidin domain receptors (DDR), like many tyrosine kinases (TKs), have a unique place in cancer chemotherapy due to their role in cellular proliferation/differentiation. Inhibition of DDRs is an effective pathway for controlling many diseases, including cancer. A group of indole-containing compounds linked to urea function **156** was designed as inhibitors of DDRs employing virtual screening (molecular docking, PDB ID: 4CKR). The targeted agents **156** were prepared in a multi-step reaction sequence. The 3-formyl-1-indole acetate **153** was allowed to react with the appropriate amine in the presence of EDC [*N*-ethyl-*N*-(3-dimethylaminopropyl)carbodiimide] and HOBT (hydroxybenzotriazole), affording the corresponding 3-formyl-1-(2-amino-2-oxo-ethyl)-1*H*-indoles **154**. The reaction of the latter with NH_2OH (EtOH/ H_2O) then $\text{NiCl}_2 \cdot 6\text{H}_2\text{O}$ was added, followed by NaBH_4 producing the 2-[3-(aminomethyl)-1*H*-indol-1-yl]ethan-1-ones **155**, which were subjected to the reaction with the appropriate phenyl isocyanate (CHCl_3 , TEA, room temperature), affording the targeted **156** (Scheme 27). Some of the synthesized conjugates revealed considerable DDR1/2 and TK-A/-B/-C inhibitory properties (Supplementary Figure S24). The most promising agent observed was that with $R^1 = \text{F}$, $R^2 = 1\text{-methyl-4-piperazinyl}$, and $R^3 = 2,4\text{-F}_2$, which was subjected to an antiproliferation properties investigation against lung (A549, SPC-A-1, and H1975) cancer cell lines relative to that of dasatinib ($\text{IC}_{50} = 1.84, 3.51, \text{ and } 1.87; 2.55, 2.46, \text{ and } 1.26 \mu\text{M}$, respectively). Additionally, the in vivo testing (30 mg/kg dose, mouse model) evidenced its capability for inhibition of bleomycin-induced lung injury [162].

EGFR (epidermal growth factor receptor) is an important category of tyrosine kinases, occupying a unique place in cancer chemotherapy. Overexpression of the EGFR is associated with cellular proliferation and many other activities. Many agents have been identified as EGFR inhibitors, and some of them have been chemotherapeutically approved against various cancer types. Several quinazoline-containing compounds were developed with EGFR inhibitory properties and approved against different types of cancers (Figure 18). Conjugation of quinazoline with indole scaffolds was considered for attaining potential EGFR inhibitors. The reaction of 4-chloroquinazolines **158** (obtained through chlorination “thionyl chloride, $90 \text{ }^\circ\text{C}$ ” of the corresponding quinazolinones **157**) with the appropriate indoles using HFIP (hexafluoroisopropanol) and Tf_2NH [bis(trifluoromethane sulfonimide)]

in a sealed tube at 100 °C produced the corresponding conjugates **159–161** (Scheme 28). Enzymatic inhibitory properties of the synthesized conjugates were assayed against the EGFR [L858R] (Supplementary Figure S25). The most promising was **161** with $R^3 = \text{Et}$, $R^4 = \text{Ph}$, and $R^5 = \text{H}$, revealing potent EGFR inhibitory activity [$\text{IC}_{50} = 5.2, 9.6,$ and 1.9 nM , against EGFR(WT), EGFR(d746-750), and EGFR(L858R), respectively], antiproliferation properties ($\text{IC}_{50} = 4.1, 0.5,$ and $2.1 \mu\text{M}$ against A549, PC-9, and A431, respectively), arresting the cell cycle at the G₀/G₁ phases (flow cytometry), and apoptosis induction, in addition to tumor growth suppression evidenced by in vivo testing (BALB/c nude mouse model, oral administration) [163].



$R^1 = \text{OMe}, \text{F}; R^2 = 1\text{-pyrrolidinyl}, 1\text{-piperidinyl}, 4\text{-morpholinyl}, 1\text{-methyl-4-piperazinyl};$
 $R^3 = 2\text{-Cl}, 4\text{-Me}, 4\text{-OMe}, 2,4\text{-F}_2, 4\text{-CF}_3,$

(a) $\text{POCl}_3, \text{DMF}, -20 \text{ }^\circ\text{C}$ to r.t., 1 h; (b) tert-butyl bromoacetate, $\text{K}_2\text{CO}_3, \text{DMF}, \text{r.t.}, 2 \text{ h};$
 (c) $\text{CF}_3\text{COOH}, \text{CH}_2\text{Cl}_2, \text{r.t.},$ overnight, and then amines, EDC, HOBT, $\text{CH}_2\text{Cl}_2, \text{r.t.},$
 overnight; (d) $\text{NH}_2\text{OH}, \text{EtOH}, \text{r.t.}, 1 \text{ h},$ then $\text{NiCl}_2 \cdot 6\text{H}_2\text{O}, \text{NaBH}_4, 0 \text{ }^\circ\text{C};$
 (e) Phenyl isocyanates, $\text{CHCl}_3, \text{Et}_3\text{N}, \text{r.t.}, 2 \text{ h}.$

Scheme 27. Synthetic route towards indoleyl analogs linked to urea function **156**.

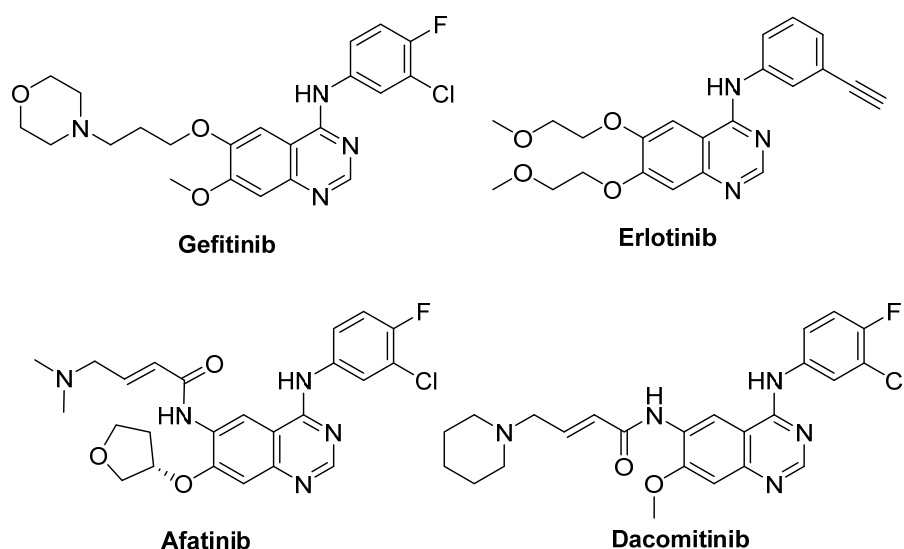
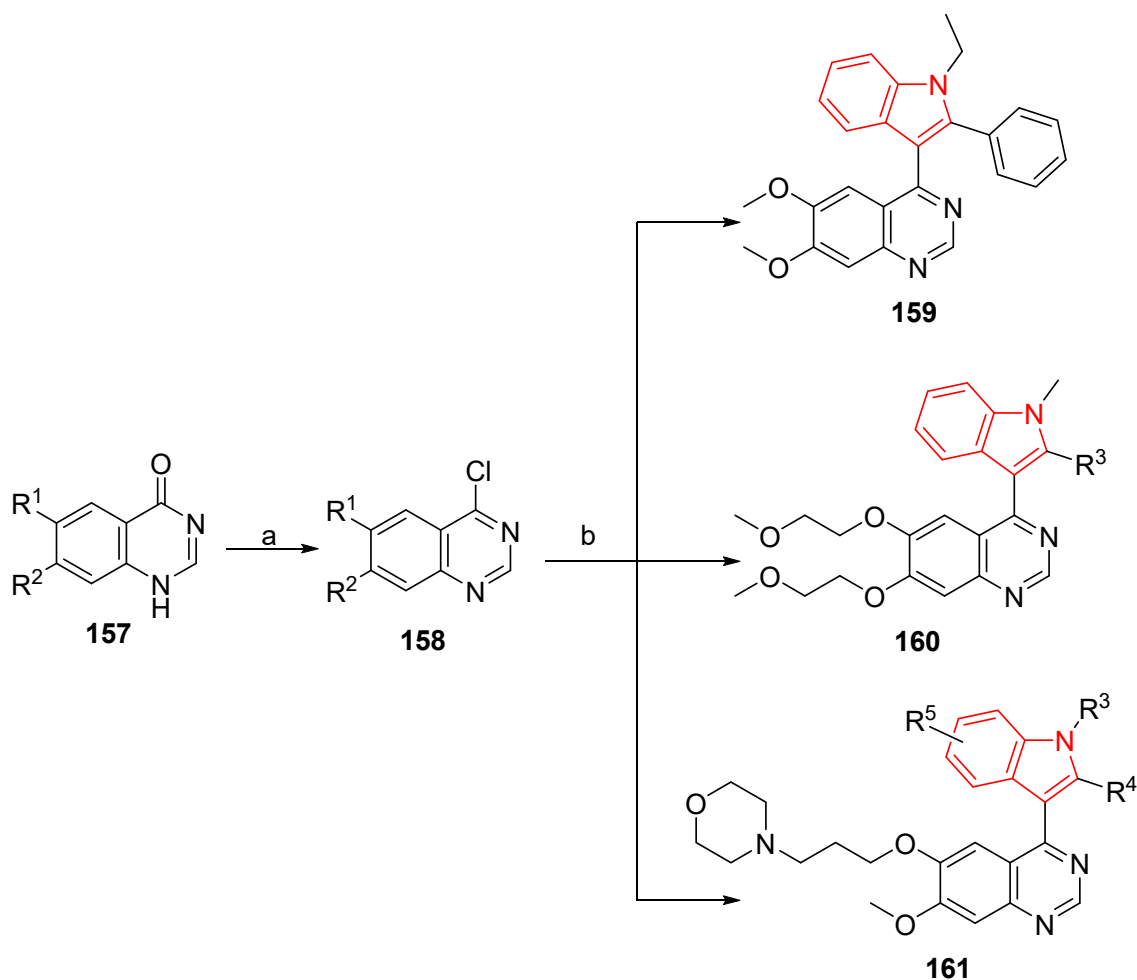


Figure 18. Clinically approved quinazoline-containing compounds with EGFR inhibitory properties.

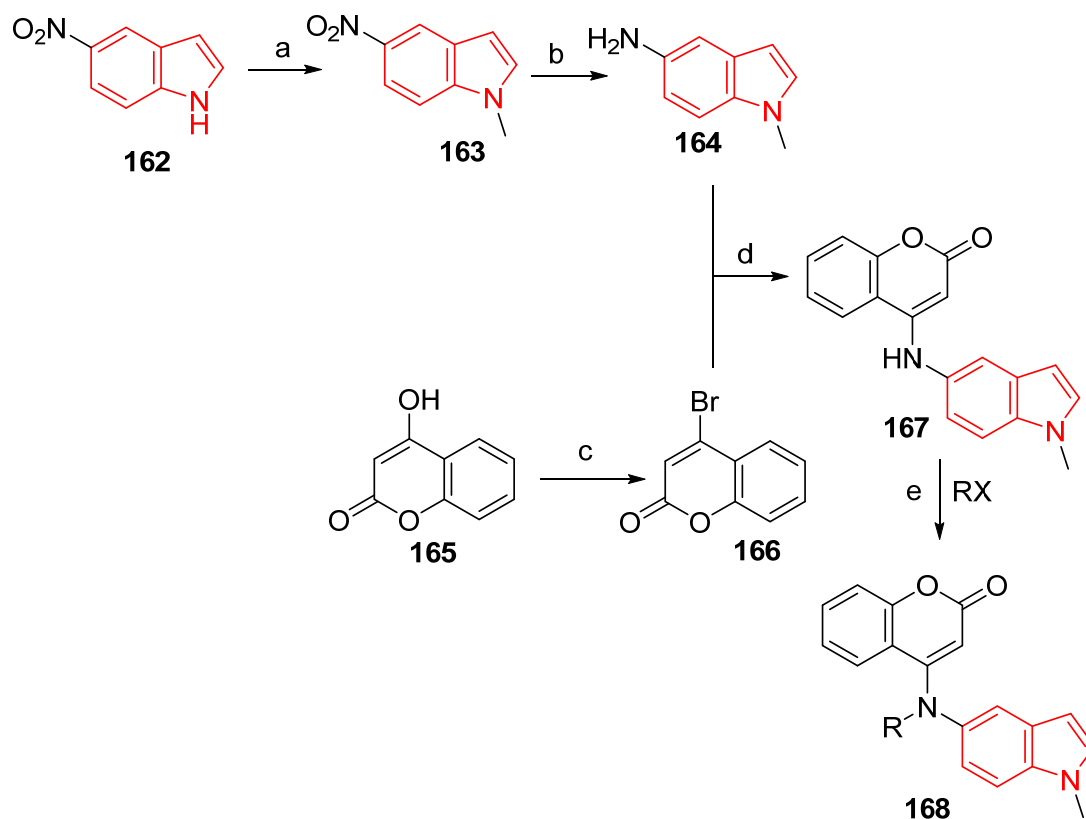


R^1 = OMe, $O(CH_2)_2OMe$, NO_2 ; R^2 = H, OMe, $O(CH_2)_2OMe$. R^3 = H, Me, Et, n-butyl, benzyl, 2- ClC_6H_4 , 3- ClC_6H_4 , 4- ClC_6H_4 , 3,4- $Cl_2C_6H_3$, 2- BrC_6H_4 , 3- BrC_6H_4 , 3- MeC_6H_4 , 4-cyanobenzyl, 3-trifluoromethylbenzyl; R^4 = H, Ph, 3- MeC_6H_4 , 4- MeC_6H_4 , 4-(*i*- C_3H_7) C_6H_4 , 4-(*n*- C_4H_9) C_6H_4 , 4- $MeOC_6H_4$, 3- FC_6H_4 , 3- ClC_6H_4 , 4- ClC_6H_4 , 4- BrC_6H_4 , 3- $NO_2C_6H_4$, 4- $F_3CC_6H_4$, 4-biphenyl, β -naphthyl, benzyl, phenylethyl; R^5 = H, 4-OMe, 5-OMe, 6-OMe

(a) $SOCl_2$, 90 °C, 8 h; (b) electron-rich arene, Tf_2NH , HFIP, 100 °C, 6 h

Scheme 28. Synthetic route towards quinazoline-indole conjugates **159–161**.

A series of coumarin-indole conjugates **168** was synthesized through dehydrohalogenation (DMF containing DIPEA “*N,N*-diisopropylethylamine”, 110 °C) of 5-amino-1-methylindole **164** (obtained from alkylation of 5-nitroindole **162**, followed by a reduction in the nitro group) with 4-bromocoumarin **166** (formed from bromination of coumarin **165**), followed by alkylation (Scheme 29). The antiproliferation properties of **168** were studied against A549, HepG2, and MCF7 cell lines. The most promising agent discovered was that with $R = Me$ against lung cancer cell line A549 ($IC_{50} = 1.79 \times 10^{-3} \mu M$) relative to that of cisplatin and colchicine ($IC_{50} = 5.62$ and $0.01 \mu M$, respectively) (Supplementary Figure S26). The most promising agent discovered revealed cell cycle arrest of A549 at the G2/M phase with induction of apoptosis and presumed tubulin polymerization inhibition, as evidenced by molecular docking studies (PDB ID: 1SA0, Autodock Vina software) [164].



R = Me, CH₂C₆H₄-OMe-3, CH₂C₆H₄-F-2, CH₂C₆H₄-Br-2, CH₂C₆H₄-Cl-3, CH₂C₆H₄-CN-4, CH₂C₆H₄-F-4, CH₂C₆H₄-CO₂Me-2, CH₂C₆H₄-Cl-4, CH₂C₆H₄-Me-4, n-Pr

(a) Me₂SO₄, NaOH, DMF, r.t.; (b) Fe, NH₄Cl, EtOH, H₂O, 80 °C; (c) POBr₃, 130–160 °C; (d) DIPEA, DMF, 110 °C; (e) Cs₂CO₃, CH₃CN, RX, 60 °C

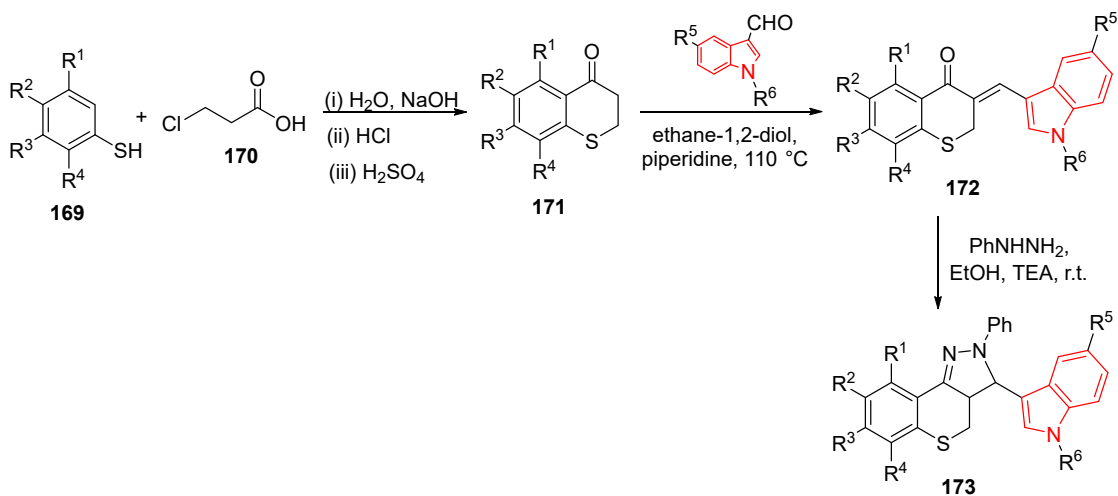
Scheme 29. Synthetic route towards coumarin-indole conjugates **168**.

3.3. Gastric Cancer

A series of thiochromeno[4,3-*c*]pyrazole-indole conjugates **173** were obtained through Aldol condensation of thiochroman-4-ones **171** with indole-3-carbaldehydes (ethane-1,2-diol, piperidine, 110 °C), followed by cyclocondensation with phenyl hydrazine (EtOH, TEA, room temperature) (Scheme 30). Antiproliferation properties (MTT methodology) against MGC-803, Hela, MCF-7, Bel-7404 (gastric, cervical, breast, and liver cancer), and L929 (normal) cell lines were studied (Supplementary Figure S27). Some synthesized hybrids revealed considerable bio-properties relative to etoposide and cisplatin (standard references). The most promising against MGC-803 were those exhibited in Figure 19, which were subjected to a topoisomerase I/II inhibitory assay, revealing selective inhibition against topoisomerase II and no efficacy against topoisomerase I until 100 μM. This behavior was supported by docking studies (PDB ID: 5GWK, Glide XP of Maestro software). They also showed cell cycle arrest (MGC-803 cell) at the G2/M phase [165].

A series of *N*-arylsulfonylindoles **175** was obtained through condensation of the appropriate 3-aldehydic/ketonic indoles **174** with aminoguanidine, semicarbazide, or thiosemicarbazide (Scheme 31). Some of the synthesized indolyldiazine-1-carboximidamides **175** (X = NH) displayed considerable antiproliferation properties against SGC7901 and A590 (gastric and lung) cancer cell lines (Supplementary Figure S28). The most promising was that with R = 5-Br, R¹ = 4-Me, and R² = Me, with safe behavior against the normal

HEK 293T cell line ($IC_{50} = 1.51, 4.44, \text{ and } 56.39 \mu\text{M}$, against SGC7901, A590, and HEK 293T, respectively) [166].



$R^1 = \text{H, Me}; R^2 = \text{H, Cl, F, Me, OMe}; R^3 = \text{H, Cl, Me}; R^4 = \text{H, Cl, F, Me}; R^5 = \text{H, Br}; R^6 = \text{H, Me}$

Scheme 30. Synthetic route towards thiochromeno[4,3-c]pyrazole-indole conjugates **173**.

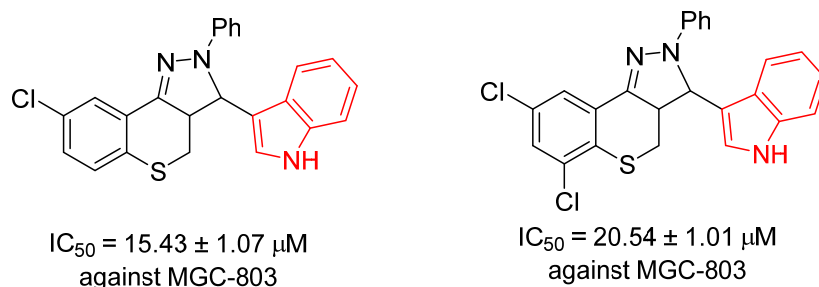
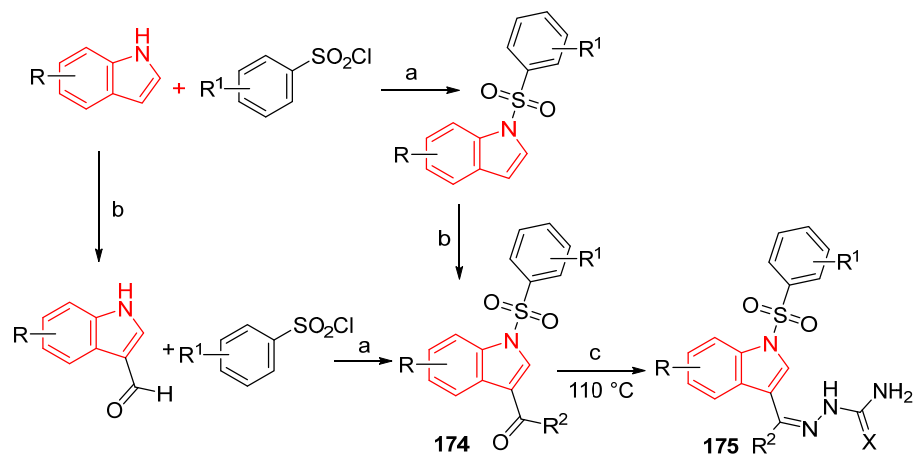


Figure 19. The promising agents of **173** observed against the MGC-803 (gasteric) cancer cell line.



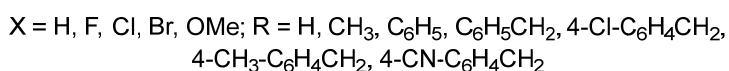
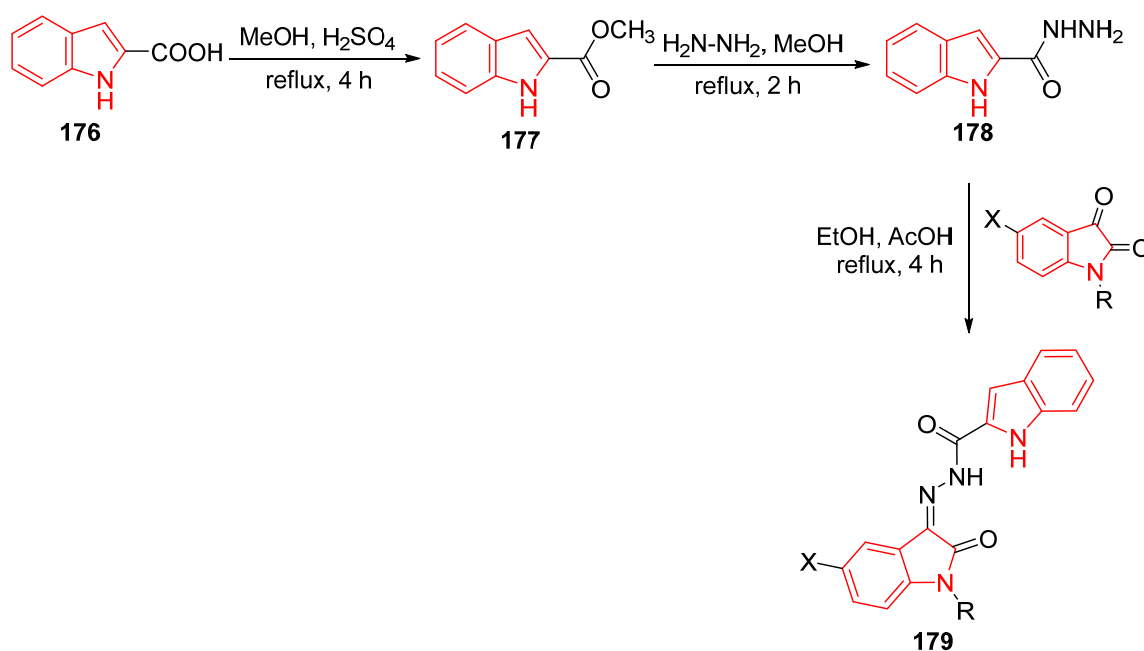
$R = \text{H, 5-Br}; R^1 = \text{H, 4-Me}; R^2 = \text{H, Me, Et}; X = \text{O, S, NH}$

(a) NaOH, TEBA "benzyltriethylammonium chloride"; (b) POCl_3/DMF ;
(c) conc. HCl in MeOH in case of aminoguanidine hydrochloride,
 $\text{CH}_3\text{CO}_2\text{Na}/\text{EtOH}$ in case of semicarbazide hydrochloride,
KOH/EtOH in case of thiosemicarbazide

Scheme 31. Synthetic route towards *N*-arylsulfonylindoles **175**.

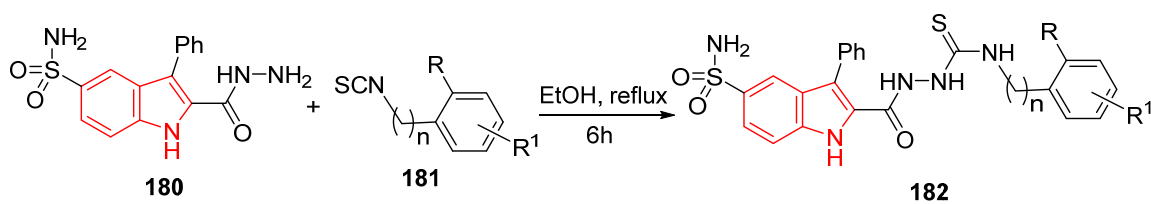
3.4. Colorectal Cancer

A variety of 2-oxo-3-indolylidene-2-indolecarbohydrazones **179** was prepared through condensation (refluxing EtOH containing AcOH in a catalytic amount) of the appropriate isatin with 3-indolecarbazones **178** (Scheme 32). The antiproliferative properties of the prepared hydrazones **179** against HT-29, ZR-75, and A-549 (colon, breast, and lung) cancer cell lines were studied (Supplementary Figure S29). The most promising agent is X = Cl and R = CH₂C₆H₅, comparable to sunitinib (IC₅₀ = 2.02, 0.74, and 0.76; 10.14, 8.31, and 5.87 μM, respectively). It was also noted that the most promising agent discovered arrested cell cycle at the G1 and G2 phases of the A549 testing cell. Western blot studies revealed the enhancement of BTG1, cdc-2, BAX (B cell translocation gene 1, cyclin-dependent kinase 1, and Bcl-2-associated X protein, respectively), and caspase-3 proteins [167].



Scheme 32. Synthetic route towards isatin–indole conjugates **179**.

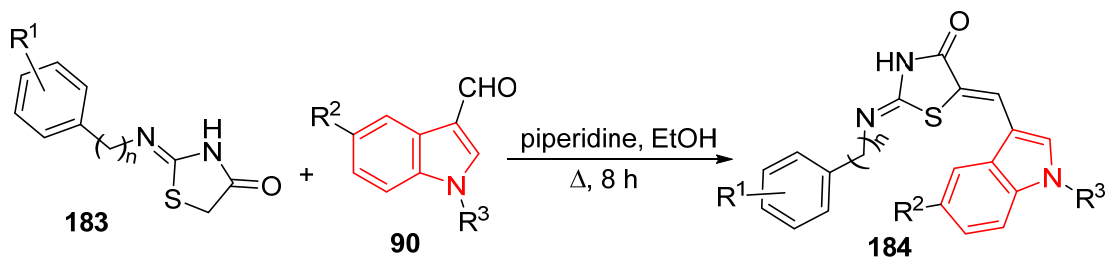
A series of 1-(indole-2-carbonyl)thiosemicarbazides collaborating with a sulfonamide group **182** was obtained via a reaction of the 2-indolocarbazole **180** with the appropriate isothiocyanate **181** in refluxing ethanol (Scheme 33). A few of the synthesized agents showed mild to considerable antiproliferation properties against HT-29 (colorectal) and skin normal (CCD-86Sk) cell lines (MTT method). The most promising is that with R = H, R¹ = 4-F, and n = 0 (IC₅₀ = 53.32 and 74.64 μM, respectively) relative to doxorubicin (IC₅₀ = 17.20 and 0.17, respectively). Carbonic anhydrase inhibitory properties against hCA I, hCA II, hCA IX, and hCA XII exhibited the high potency of some of the synthesized agents. The most effective agents are R = H/H, R¹ = 3-SO₂NH₂/4-SO₂NH₂, and n = 0 (k_i = 78.7/75.9, 38.0/19.5, 2.1/1.4, and 0.69/0.87 nM, respectively) relative to acetazolamide (reference standard, k_i = 250.0, 12.5, 25.0, and 5.7, respectively) (Supplementary Figure S30). Molecular docking (Maestro software v2022-3, PDB ID: 3B4F) and molecular dynamic studies were considered to explain the inhibitory behavior against carbonic anhydrases of the promising agents observed [168].



R = H, F; R¹ = H, 3-F, 4-F, 3-Cl, 4-Cl, 3-Br, 4-Br, 3-Me, 4-Me, 4-OMe, 4-CF₃, 4-NO₂, 3-CN, 4-CN, 3-SO₂NH₂, 4-SO₂NH₂; n = 0, 1, 2

Scheme 33. Synthetic route towards 1-(indole-2-carbonyl)thiosemicarbazides **182**.

Thiazolidinone-indoles **184** were synthesized through a base-catalyzed condition (refluxing EtOH in the presence of piperidine) of thiazolidinediones **183** with indole-3-carboxaldehyde **90** (Scheme 34). Some synthesized hybrids revealed considerable antiproliferation properties (MTT method, A549, NCI-H460, lung; HCT-29, HCT-15, colon; and MDA-MB-231, breast cancer cell lines). The most promising is that with $n = 2$, R¹ = 4-OMe, R² = Br, and R³ = H relative to podophyllotoxin with safe behavior against normal lung cell L132 (IC₅₀ = 0.92 and 0.029; 10.84 and 0.021 μ M, against HCT-15 and L132, respectively) (Supplementary Figure S31). Tubulin polymerization inhibition was the molecular target for the most promising agent discovered (IC₅₀ = 2.92 μ M), with cell cycle arrest at the sub-G1 and G2/M phases. Furthermore, a decrease in mitochondrial membrane potential was observed with an increased intracellular ROS level [169].

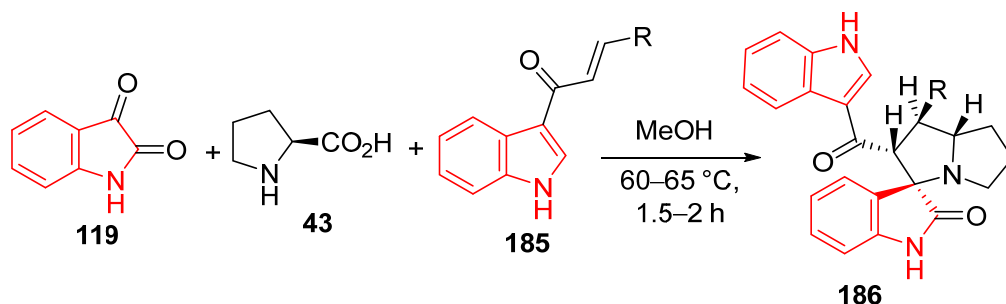


$n = 1, 2$; R¹ = H, 4-OMe, 4-F, 2-Cl, 3-Cl, 3,4-Cl₂, 3,4-(OMe)₂, 3,5-(F₃C)₂, *t*-butyl, 3,4,5-(OMe)₃, 4-OH; R² = H, I, Br, OMe; R³ = H, Me, 4-chlorobenzyl, phenacyl, 4-methoxyphenacyl, 4-bromophenacyl

Scheme 34. Synthetic route towards thiazolidinone-indole hybrids **184**.

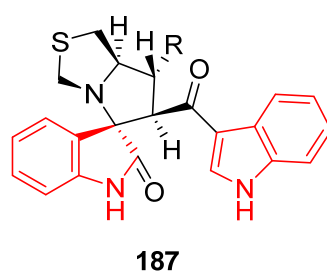
Spiro[indoline-3,3'-pyrrolizin]-2-ones **186** were obtained in diastereoselectivity through a catalyst-free cycloaddition reaction of isatin **119**, *L*-proline **43**, and indolyl-bearing chalcones **185** in boiling MeOH (Scheme 35). Some analogs synthesized displayed promising activity (MTT method) against the HCT116 (colon) cancer cell line, of which R = 3-MeC₆H₄, 3-BrC₆H₄, 4-CF₃C₆H₄, and 2,4-Cl₂C₆H₃ relative to cisplatin (IC₅₀ = 7.0, 9.0, 9.0, 9.0, and 12.5 μ M, respectively) (Supplementary Figure S32). Phosphodiesterase 1 (PD-1) inhibitory properties were observed by one of the promising agents observed (R = 2,4-Cl₂C₆H₃), revealing activity at 2 μ M with 74.2%, which is explained by molecular docking (PDB ID:1NOP, OpenEye software version 4.1.2) studies [170].

Spiroindoles **187** were similarly obtained upon utilizing *L*-thioproline instead of *L*-proline (Figure 20). A few synthesized compounds showed considerable antiproliferation properties. The most promising is that with R = 4-F₃CC₆H₄ compared to cisplatin (IC₅₀ = 7.0, 5.5, and 6.0; 12.6, 5.5, and 5.0 μ M against HCT116, HepG2, and PC-3, respectively) (Supplementary Figure S33). Inhibition of the MDM2-P53 interaction was mentioned as the mode of action of the synthesized agents based on theoretical/computational studies (molecular docking, PDB ID: 5law, OpenEye software version 2.2.5) [171].



R = Ph, 3-MeC₆H₄, 4-MeC₆H₄, 4-MeOC₆H₄, 3,4,5-(Me)₃C₆H₂, 3-FC₆H₄, 4-FC₆H₄, 4-ClC₆H₄, 2,4-Cl₂C₆H₃, 3-BrC₆H₄, 4-BrC₆H₄, 4-CF₃C₆H₄, 2-thienyl, 2-furanyl

Scheme 35. Synthetic route towards spiro[indoline-3,3'-pyrrolizin]-2-ones **186**.



R = Ph, 4-MeC₆H₄, 4-ClC₆H₄, 2,4-Cl₂C₆H₃, 4-MeOC₆H₄, 4-BrC₆H₄, 4-FC₆H₄, 3-FC₆H₄, 3-MeC₆H₄, 3-BrC₆H₄, 4-F₃CC₆H₄, 2-thienyl, 2-furanyl, 3,4,5-(Me)₃C₆H₂

Figure 20. Chemical structure of the synthesized spiroindoles **187**.

3.5. Pancreatic Cancer

Qin et al. reported the efficacy of 2-methylindole **188** against pancreatic cancer, revealing apoptosis and exhibiting antiproliferation properties (Figure 21). Suppression of capan-1, aspc-1, and MIApaCa-2 was mentioned as the apoptotic mode of action. Down-regulation of ZFX led to the deactivation of P13K, and AKT phosphorylation was also mentioned [172].

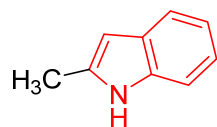
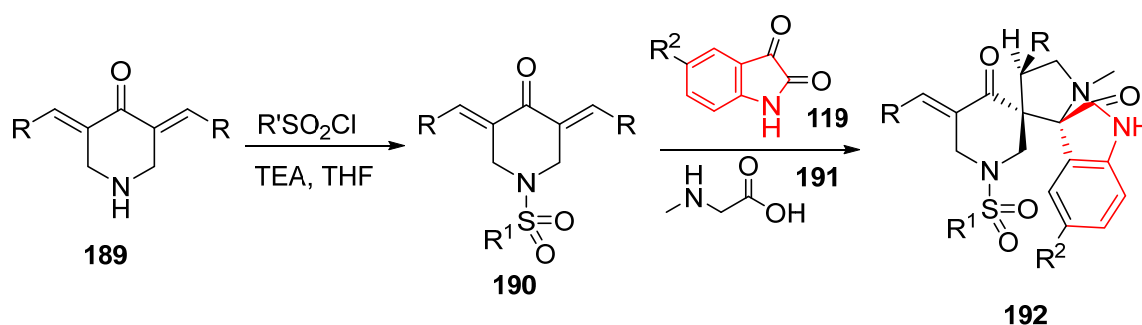


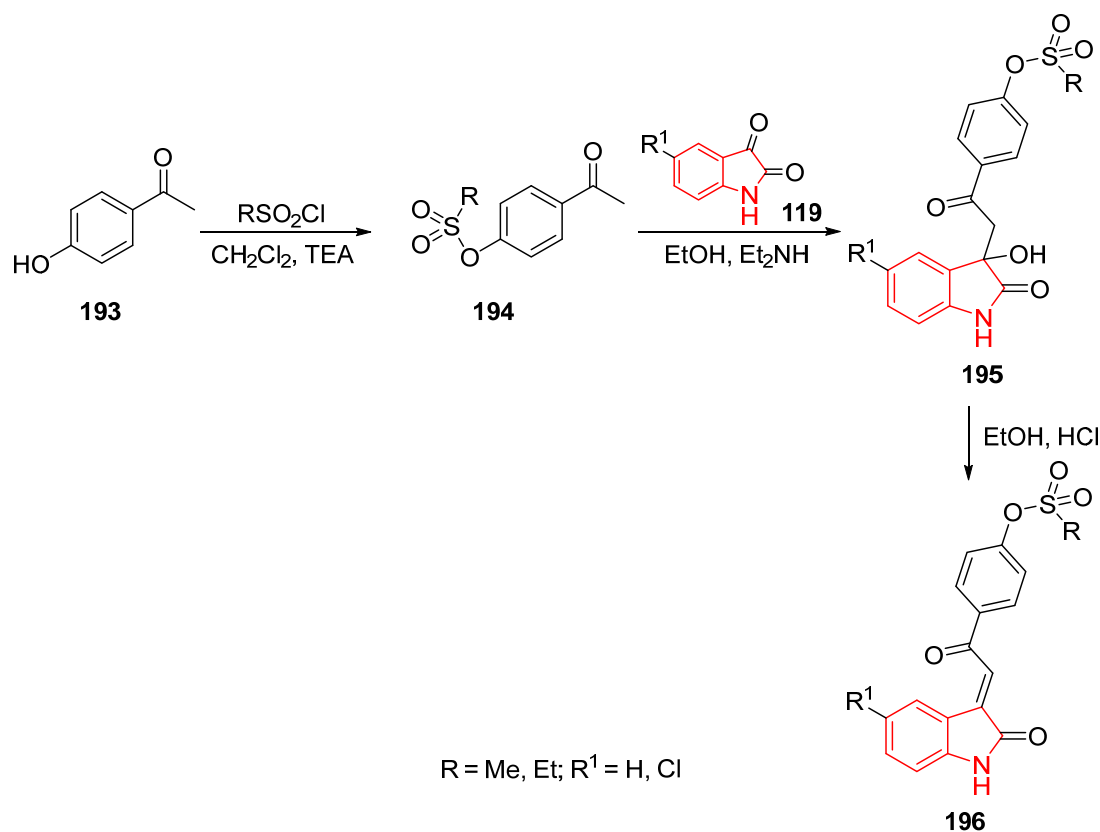
Figure 21. Chemical structure of 2-methylindole **188**.

Spiroindoles **192** were synthesized through a one-pot reaction of 3,5-diyldene-4-piperidones attached to sulfonyl function **190** with isatins **119** and sarcosine **191** (azomethine cycloaddition) (Scheme 36). The antiproliferation properties (MTT method) of **192** were assessed against PaCa2, MCF7, HCT116, and A431 (pancreatic, breast, colon, and skin) cancer cell lines. Promising properties, relative to the standard drugs (sunitinib and 5-fluorouracil) with inhibitory properties (western blotting study), were observed against VEGFR-2 and the EGFR (Supplementary Figure S34). The most promising against PaCa2 is that with R = 4-BrC₆H₄, R¹ = Me, and R² = H (IC₅₀ = 12.500 μM), which is more potent than sunitinib (an FDA-approved drug against pancreatic cancer) (IC₅₀ = 16.91 μM). The safety index of **192** was assigned by studying the cytotoxicity against the normal RPE1 cell line [20].

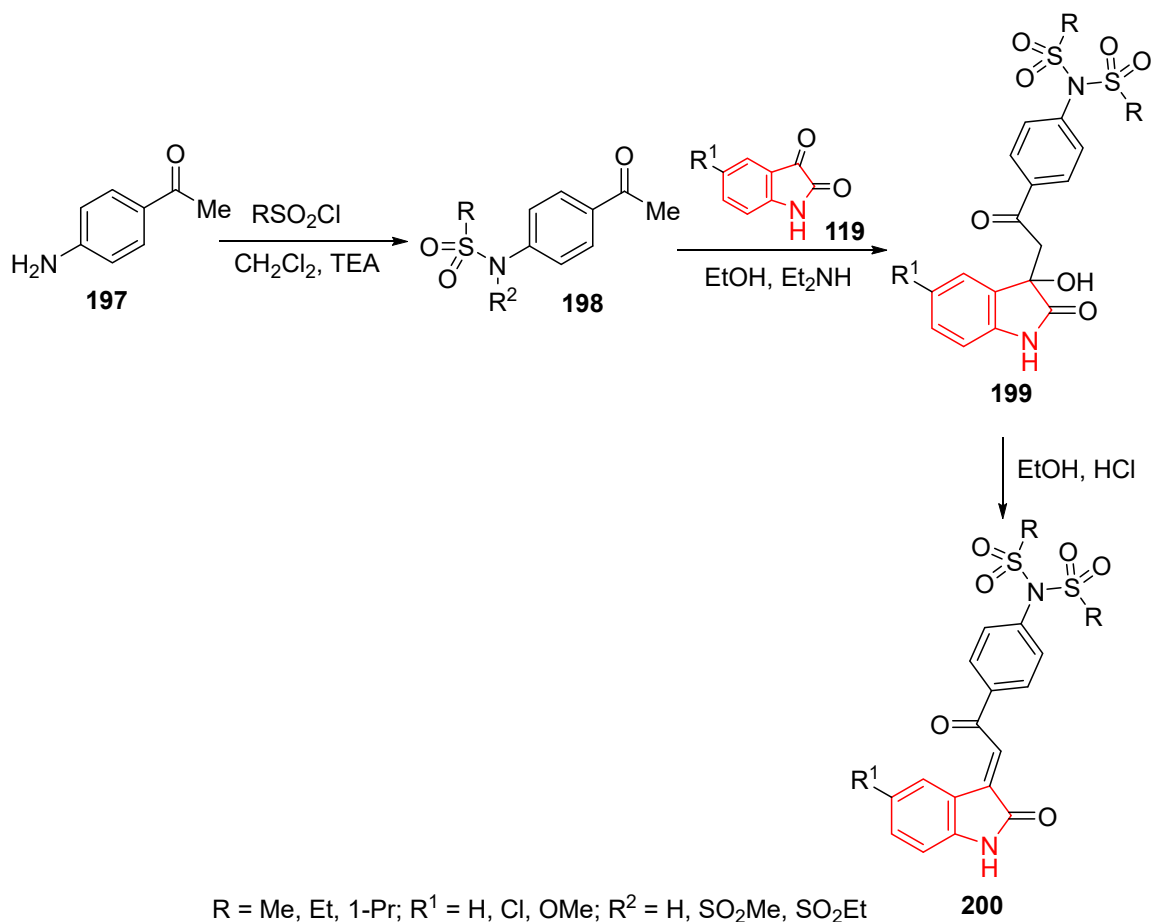


Scheme 36. Synthetic routes towards spiroindoles **192**.

The reaction of sulfonated acetophenones **194** with isatins **119** (EtOH/Et₂NH) produced the corresponding 3-hydroxy-2-oxindolines **195**. Acid dehydration (EtOH/HCl, room temperature) of **195** afforded the targeted 3-alkenyl-2-oxindoles bearing the sulfonate group **196** (Scheme 37). Applying similar reaction sequences/conditions, 3-alkenyl-2-oxindoles bearing the sulfonamide group **200** were obtained (Scheme 38). 3-Alkenyl-2-oxindoles **196** (R = Et, R¹ = Cl) and **200** (R = Et, R¹ = H) are the most promising antiproliferative agents, displaying efficiency against PaCa2 of about 3.4 and 3.3 folds to that of sunitinib (IC₅₀ = 4.99, 5.08, and 16.91 μM, respectively). Anti-angiogenic capabilities close to those of sunitinib were supported by CAM (chick chorioallantoic membrane) experiments revealing qualitative and quantitative reductions in blood vessels. Considerable properties were also noticed against MCF7 and HCT116. Inhibitory properties of kinases (VEGFR-2 and c-kit) were noticed by the targeted agents, supporting their mode of action as multi-targeted inhibitors [21] (Supplementary Figure S35).

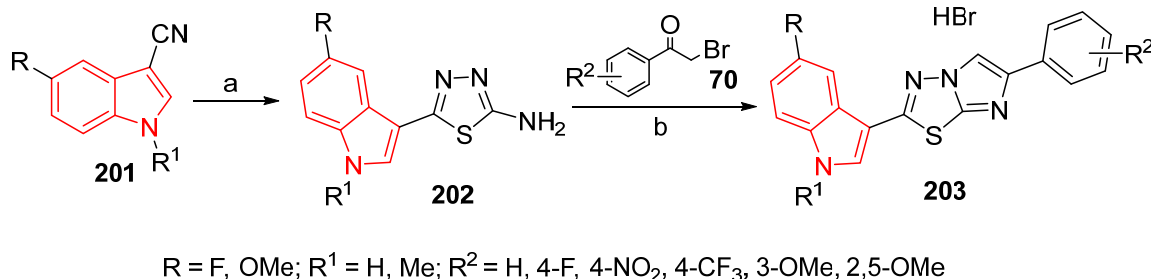


Scheme 37. Synthetic route towards 3-alkenyl-2-oxindoles **196**.



Scheme 38. Synthetic route towards 3-alkenyl-2-oxindoles **200**.

Indole linked to imidazo[2,1-*b*][1,3,4]thiadiazoles **203** was obtained through the reaction of indole-3-carbonitriles **201** with thiosemicarbazide in CF₃CO₂H at 60 °C, producing the corresponding 2-aminothiadiazols **202**. The reaction of phenacyl bromides **70** with **202** (refluxing EtOH) yielded the targeted agents **203** as hydrobromide salts (Scheme 39). A few of the synthesized **203** exhibited cytotoxic properties against pancreatic cancer cell lines (SUIT-2, Capan-1, and Panc-1; SRB method) (Supplementary Figure S36). A decrease in the tested cell migration in the scratch wound-healing assay was also observed [173].

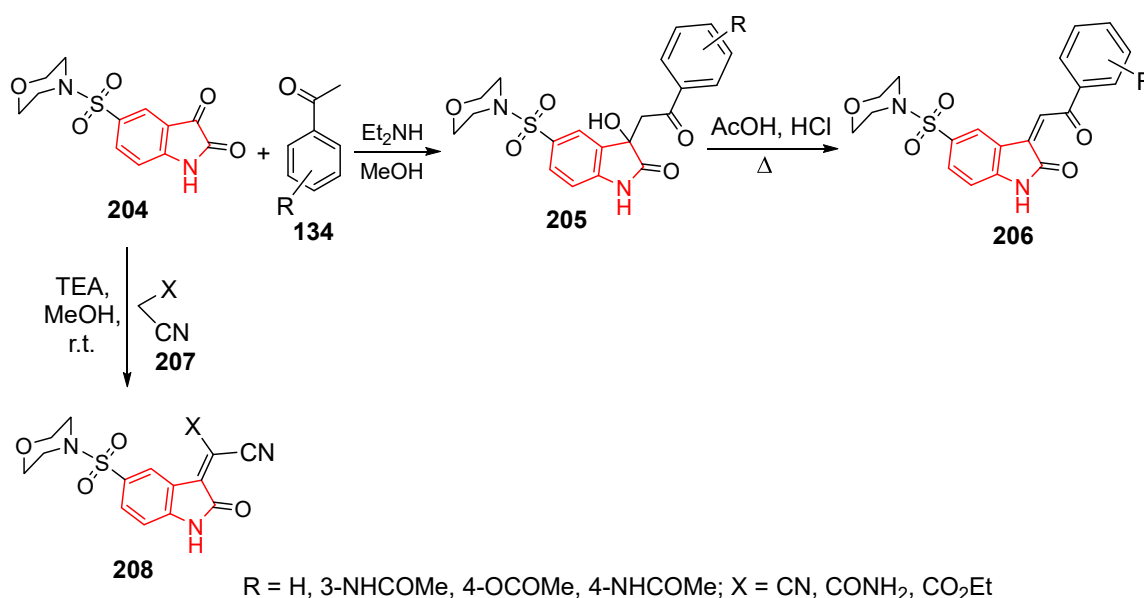


(a) CF₃CO₂H, thiosemicarbazide, 60 °C, 3.5 h; (b) EtOH, reflux, 24 h

Scheme 39. Synthetic route towards indole linked to imidazo[2,1-*b*][1,3,4]thiadiazoles **203**.

3.6. Liver Cancer

The reaction of 5-morpholinosulfonylisatin **204** with the appropriate acetophenone **134** under basic conditions (MeOH, Et₂NH) followed by acidic dehydration (AcOH, HCl, reflux) produced the corresponding 5-(morpholinosulfonyl)-2-indoline **206** (Scheme 40). Two of the synthesized **206** (R = 3-NHCOCH₃ and 4-OCOCH₃) exhibited promising antiproliferation properties against MCF-7, HepG-2, and HCT-116 cell lines (SRB method) relative to doxorubicin. Considerable EGFR inhibitory properties of **206** (R = 3-NHCOCH₃) were noticed relative to lapatinib (IC₅₀ = 0.0191 and 0.0283 μM, respectively). Additionally, condensation of the isatin analog **204** with active methylenes **207** (MeOH, TEA, r.t.) produced the corresponding ylidenes **208**, which also revealed considerable antiproliferation and EGFR inhibitory properties (Supplementary Figure S37). Molecular docking (PDB ID: 1M17, MOE software 10.2008) was considered for explaining the EGFR inhibitory observations [174].

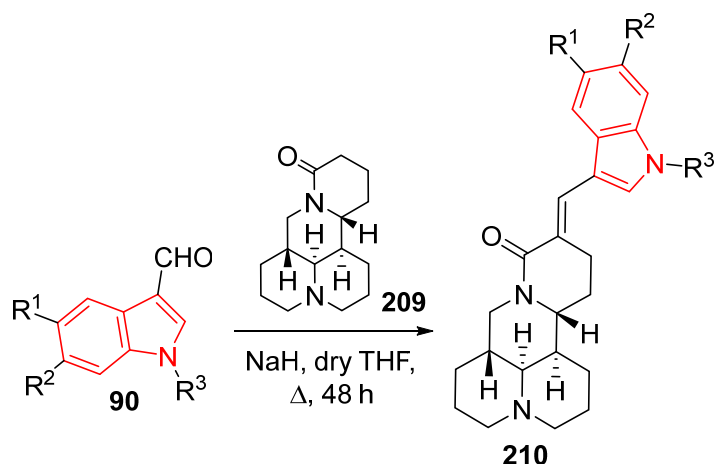


Scheme 40. Synthetic route towards 5-(morpholinosulfonyl)-2-indolinones **206** and ylidenes **208**.

Sophoridine **209** is a traditional Chinese medication useful for combating a few cancer types (lung, liver, and gastric) in combination with other chemotherapeutics. Sophoridine-indole conjugates **210** were obtained by the Aldol condensation reaction of **209** with the appropriate indole-3-carboxyaldehyde **90** (NaH, dry THF, reflux, 48 h) (Scheme 41). Noticeable antiproliferation properties (MTT method) against HepG2 were observed by **210** relative to sophoridine and camptothecin. The most promising anti-HepG2 agent discovered was R¹ = OMe, R² = H, and R³ = 4-BnOBn (IC₅₀ = 1.96, 4670, and 6.08 μM for the potent agents discovered, sophoridine **209** and camptothecin “CPT, natural origin topoisomerase inhibitor”, respectively). Moreover, promising properties were also noticed by this analog against hepatocellular (SMMC-7721), cervical (Hela, CNE1, CNE2), and breast (MCF7) carcinoma cell lines (Supplementary Figure S38). Apoptosis induction of the promising agent discovered was supported by the biochemical observations due to activation of caspase-3, increment/upregulation of the cleaved caspase-3 and Bax, and downregulation/decreasing of Bcl (i.e., reduction in the Bcl-2/Bax ratio). Molecular docking revealed its ability to inhibit topoisomerase I (PDB ID: 1k4t, MOE software version 2008). In vivo (mouse model) studies showed the suppression of the HepG-2 xenograph with no side effects observed [175].

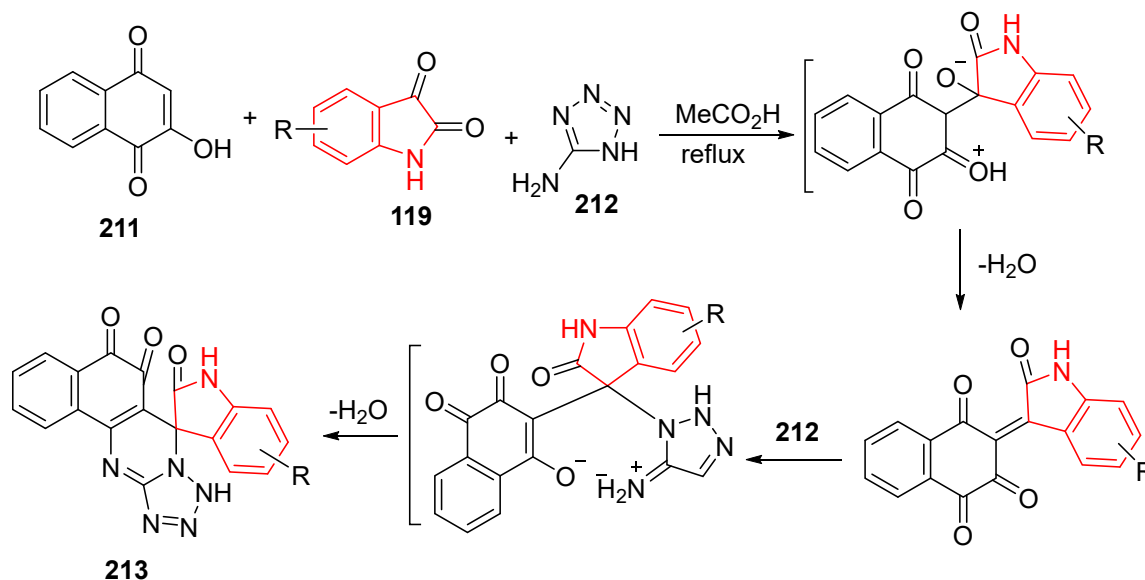
A variety of spirooxindoles **213** was obtained through a reaction of 2-hydroxy-1,4-naphthoquinone **211**, isatins **119**, and 5-amino tetrazole **212** in refluxing acetic acid (Scheme 42). Some of the synthesized analogs displayed noticeable antiproliferative properties (MTT methodology) against HepG-2 and safe behavior against normal LO2 cancer cell lines (Supplementary Figure S39). The most promising agents are those with R = 5-F, 7-Cl, and

7-CF₃ (IC₅₀ = 2.86, 3.03, and 7.9 μM, respectively) relative to the positive control tanshinon IIA (TSA “natural cytotoxic agent isolated from *Salvia miltiorrhiza*”, IC₅₀ = 23.85 μM) [176].



R¹ = H, Me, OMe, Br; R² = H, Cl; R³ = Bn, 2-MeBn, 3-MeBn, 4-MeBn, 3,5-di-MeBn, 4-^tBuBn, 2-ClBn, 4-ClBn, 2,6-di-ClBn, 2-BrBn, 3-BrBn, 4-BrBn, 3-MeOBn, 4-MeOBn, 3,5-di-MeOBn, 2-Br-5-MoBn, 2-naphthyl, 4-BnOBn, 4-F₃COBn, 4-BnOBnMe-4, 4-BnOBnBu^t-4, 4-BnOBnF-4, 4-BnOBnCl-4, 4-BnOBnBr-4, 4-BnOBnOMe-4,

Scheme 41. Synthetic route towards sophoridine-indole conjugates **210**.



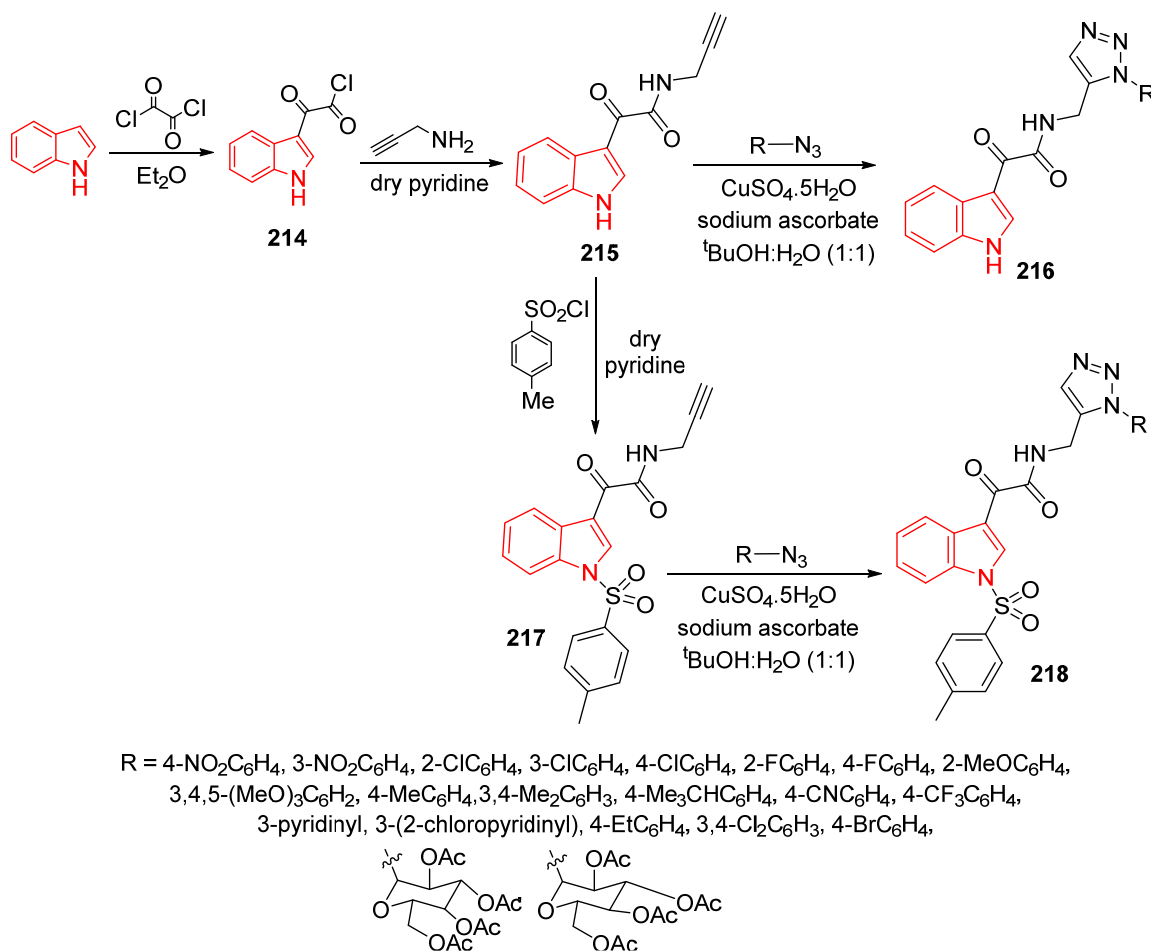
R = H, 5-Br, 5-Cl, 6-Br, 1-Me-7-F, 7-Cl, 5-F, 7-Br, 1-C₆H₅, 5-Me, 6-Cl, 6-OMe, 5-OCF₃, 7-CF₃

Scheme 42. Synthesis of spirooxindoles **213**.

3.7. Prostate Cancer

In an attempt to determine the role of COX (cyclooxygenase) and 5-LOX (5-lipoxygenase) as hypothesized biochemical pathways potentially correlated in cancer inhibition/antiproliferation, a set of 1,2,3-triazole-indole-3-glyoxamides **216** and **218** was designed and explored for their potential properties against the targeted anti-inflammatory and antitumor enzymes. The reaction of indole-3-glyoxalyl chloride **214** with propargyl amine produced the cor-

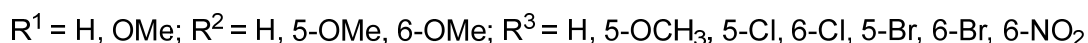
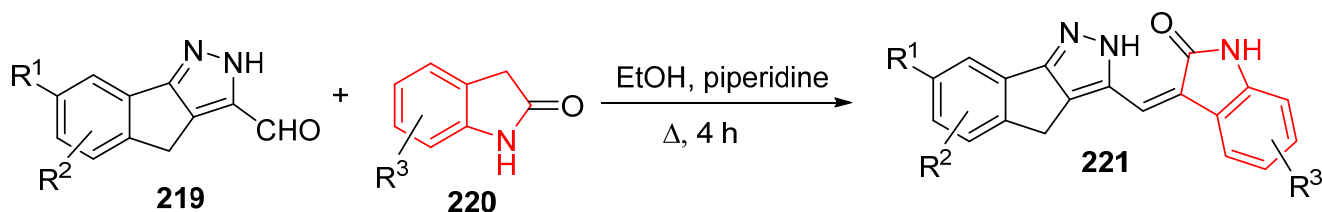
responding propargylated agent **215**. The click reaction of **215** with azide analogs (in tert-BuOH—H₂O “1:1 v/v” using CuSO₄·5H₂O, sodium ascorbate) yielded the corresponding indole-triazole conjugates **216**. Similarly, the indole-triazole conjugates bearing the sulfonyl group **218** were also synthesized (Scheme 43). The antiproliferation properties of the synthesized agents were assessed against SKOV3, DU145, and HELA (ovarian, prostate, and cervical, respectively) cell lines (MTT assay). A few of the synthesized agents **216** (R = 4-C₂H₅C₆H₅ and R = 4-FC₆H₅) showed promising antiproliferation properties relative to etoposide (VP16) against the DU145 cell line (IC₅₀ = 8.17, 8.69, and 9.80 μM, respectively). Tubulin polymerization inhibition was evidenced for the promising agent discovered **216** (R = 4-C₂H₅C₆H₅). Promising COX-2 and 5-LOS inhibitory properties were revealed for the synthesized agent discovered **216** (R = 4-C₂H₅C₆H₅, IC₅₀ = 0.12 and 7.73, respectively), relative to the anti-inflammatory drugs indomethacin and celecoxib (IC₅₀ against COX-2 = 0.049 and 0.041 μM, respectively), and norhiydroguaiaretic acid (NDGA, IC₅₀ against 5-LOX = 7.31 μM) (Supplementary Figures S40 and S41). Molecular docking studies (PDB ID: 4RRX, 3V99, Maestro version 9.6 implemented from Schrodinger software suite) evidenced the observations against COX and 5-LOX bio-properties. Additionally, in silico studies (PDB ID: 4O2B) supported the ability of the promising agent(s) discovered for mapping in the colchicine binding site. Anti-inflammatory properties were supported for the promising agents discovered through in-vivo testing in rats (carrageenan paw edema method) with no gastric ulceration [177].



Scheme 43. Synthetic route towards 1,2,3-triazole-indole-3-glyoxamides **216** and **218**.

3.8. Cervical Cancer

A set of 3-[(indeno[1,2-*c*]pyrazole-3-yl)methylene]indolin-2-ones **221** was assessed as tubulin polymerization inhibitors. The targeted agents **221** were synthesized through Knoevenagel condensation of indolin-2-ones **220** with indeno[1,2-*c*]pyrazole-3-carbaldehydes **219** in refluxing EtOH using piperidine as a basic catalyst (Scheme 44). The antiproliferation properties (SRB assay) of the targeted compounds against HeLa, A549, and MDA-MB-231 (cervical, lung, and breast) cancer cell lines and compared to non-cancer HEK-293 cell lines were studied relative to combretastatin A-4 (CA-4) (Supplementary Figure S42). Amongst all, analog **221** with R¹ = OMe, R² = 5-OCH₃, and R³ = 6-Cl exhibited promising properties relative to CA-4 (IC₅₀ = 1.33 and 1.43 μM, respectively). It also increased the checkpoint protein levels (cyclin B1 and CDK1), exhibiting cell cycle arrest in HeLa at the G₂/M phase (leading to apoptosis, flow cytometry). Upregulation of tumor suppressor proteins (p53, p21, and pro-apoptotic Bax) was also observed. Tubulin polymerization inhibition was evidenced via the occupation of the colchicine binding pocket in molecular docking studies (PDB ID: 1SA0, Autodock 4 software) [178].

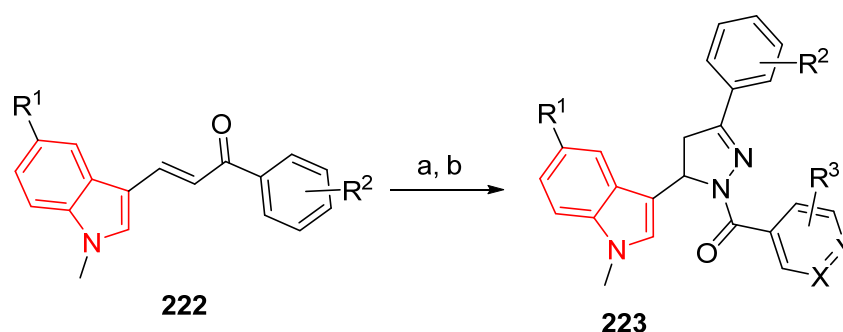


Scheme 44. Synthetic route towards 3-[(indeno[1,2-*c*]pyrazole-3-yl)methylene]indolin-2-ones **221**.

Sets of nicotinoyl/isonicotinyl pyrazolines featuring indolyl heterocycle **223** were designed as tubulin polymerization inhibitors. The targeted compounds were obtained through the reaction of indolyl chalcones **222** with hydrazine hydrate in refluxing EtOH. Then, the pyrazolinyl intermediates were allowed to react with nicotinic or isonicotinic acid in an inert atmosphere immediately, without any purification (Scheme 45). The antiproliferative properties of the targeted agents were assessed against four cancer cell lines (MTT technique). Promising antiproliferative properties were noticed by some of the synthesized agents. The most promising is that with R¹ = OMe, R² = 3-OMe, R³ = 6-Me, X = N, and Y = C against the tested cell lines MCF-7, A549, HepG2, and HeLa relative to CA-4 (GI₅₀ = 0.09, 0.59, 0.029, and 0.034; 0.14, 0.31, 0.17, and 0.092 μM, respectively) with safe observations against the non-cancer 293T cell line (CC₅₀ = > 300 μM for both). Remarkable tubulin polymerization inhibition was noticed by the promising agent discovered relative to that of CA-4 (IC₅₀ = 1.6 and 2.1 μM, respectively) (Supplementary Figure S43). In vivo testing (HeLa-xenograft mouse model) of the promising agent revealed evidence of better tumor inhibition without weight loss or tissue damage relative to the standard CA-4 (% inhibition = 61.52 and 59.92, respectively). Molecular docking (PDB ID: 1SA0, Discovery Studio 3.5 software) and molecular dynamics (Desmond, Schrödinger software) supported the mode of action mentioned [179].

A set of indoles **225** and pyranoindole **226** has been explored as anticancer agents with tubulin polymerization inhibitory properties. Esterification of 5-hydroxyindoles **224** with the appropriate carboxylic acid (pent-2-ynoic acid, es-2-ynoic acid, or phenylpropionic acid) afforded the corresponding esters **225**. The intramolecular cyclization reaction of **225** under reflux in the presence of PtCl₄ as a catalyst produced the corresponding pyranoindoles **226** (Scheme 46). Some of the synthesized agents showed considerable antiproliferation properties (MTT method), of which **225** with R = H and R¹ = Ph relative to vinblastine against the HeLa cell line (IC₅₀ = 3.6 and 6.7 × 10⁻² μM, respectively) showed tubulin

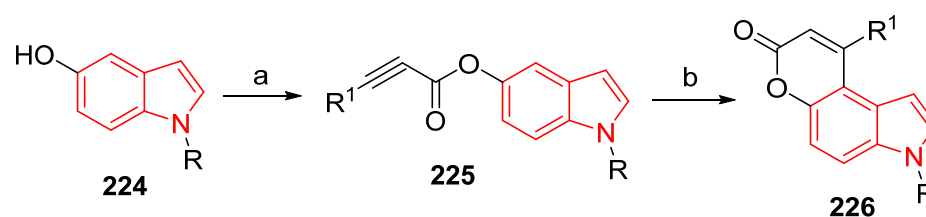
polymerization inhibition (Supplementary Figure S44). In silico/docking studies (PDB ID: 5J2T, Autodock v 4.2.2. software) explained the mode of action [180].



$R^1 = \text{H, Br, OMe}$; $R^2 = \text{H, 4-F, 4-Cl, 4-Br, 4-OMe, 3,4,5-(OMe)}_3, 3,4\text{-(OMe)}_2$; $R^3 = \text{H, 6-Cl, 2-Cl, 6-Me, 6-OMe}$; $X = \text{C, N}$; $Y = \text{C, N}$

(a) $\text{N}_2\text{H}_4 \cdot \text{H}_2\text{O}$, EtOH, reflux, 2 h; (b) substituted nicotinic acid or isonicotinic acid, EDC.HCl, HOBT, acetonitrile/dichloromethane, r.t., 24 h

Scheme 45. Synthetic route towards nicotinoyl pyrazolines bearing *N*-methyl indolyl heterocycle **223**.



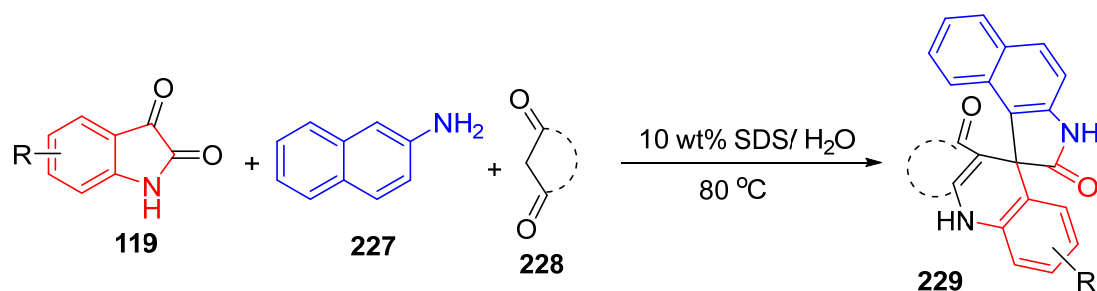
$R = \text{H, Me}$; $R^1 = \text{Et, C}_3\text{H}_7, \text{Ph}$

(a) carboxylic acid, DCC, DMAP, $\text{CH}_2\text{Cl}_2/\text{DMF}$ (10:1), r.t., 4 h;
(b) PtCl_4 , 1,4-dioxane/1,2-dichloroethane (1:1), reflux, 5 h

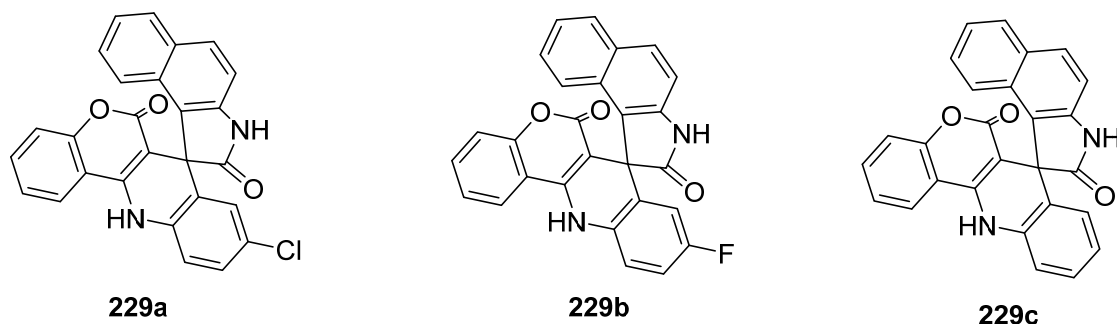
Scheme 46. Synthetic route towards indoles **225** and pyranoindoles **226**.

3.9. Ovarian Cancer

A set of 1*H*-benzo[*e*]indole-2(3*H*)-one spirocyclic derivatives **229** was designed as pyroptosis inducers and synthesized through greenish technique in a one-pot reaction of isatins **119**, 2-naphthylamine **227**, and 1,3-dicarbonyl compounds (including barbituric acid, 1,3-dimethylbarbituric acid, thiobarbituric acid, 1,3-cyclohexanone, 5,5-dimethyl-1,3-cyclohexanone, and 2,4-dimethylbenzopyranone) **228** utilizing free-catalyst conditions and using water as a solvent containing SDS (sodium dodecyl sulfate and cationic surfactant, 10 w%) at 80 °C. X-ray studies have evidenced the structure of **229** (Scheme 47). Antiproliferative properties (MTT assay) were determined against ovarian cancer cell lines (CP70 and AGS). Some of the synthesized agents (Figure 22) revealed considerable antiproliferation properties against the tested cell lines relative to the standard references (5-fluorouracil and oxaliplatin, $\text{IC}_{50} = 55.90 \pm 0.08$ and 4.01 ± 0.67 ; 35.81 ± 0.77 and 1.76 ± 0.68 μM against CP70 and AGS cell lines, respectively). The most promising agent, **229a**, was subjected to further pharmacological studies, observing its ability to hinder the formation of colonies, migration, and invasion of ovarian carcinoma cells. Upregulation of the expression of GSDME-N (pyroptosis-related proteins) in ovarian cancer cells tested (CP70 and A2780) was also evidenced by Western blotting studies. A reduction in ovarian cancer volume and weight was noticed through in vivo studies (mouse xenograft model) [181].



Scheme 47. Synthetic route towards spiroindoles 229.



$IC_{50} = 2.71 \pm 0.61, 1.21 \pm 0.23 \mu M$
against CP70 and AGS cell
lines, respectively

$IC_{50} = 3.76 \pm 0.72, 2.35 \pm 0.59 \mu M$
against CP70 and AGS cell
lines, respectively

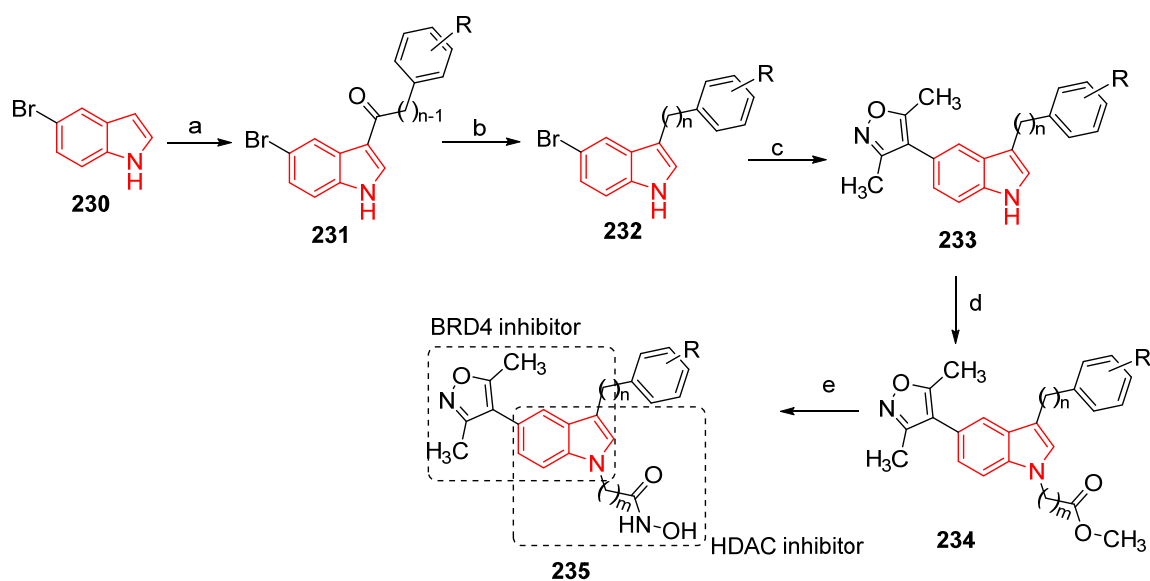
$IC_{50} = 8.79 \pm 1.64, 7.44 \pm 2.30 \mu M$
against CP70 and AGS cell
lines, respectively

Figure 22. Antiproliferation properties of the promising spiroindoles 229a–c against ovarian cancer cell lines.

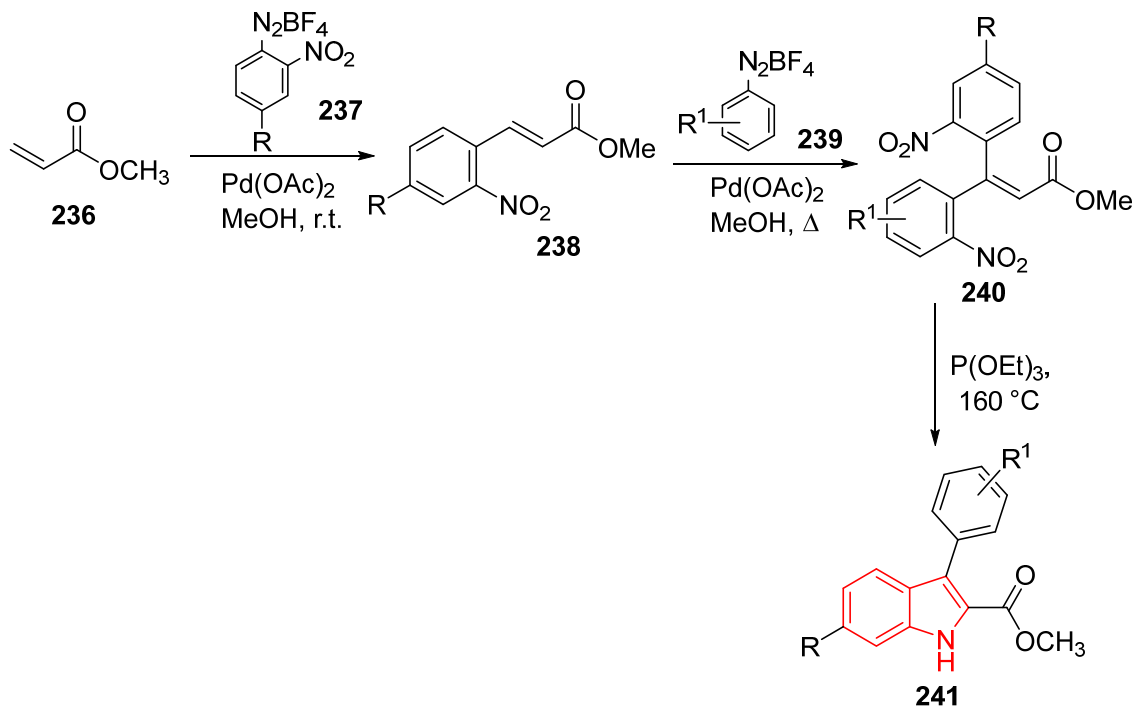
3.10. Leukemia

A set of indole-isoxazole conjugates as histone deacetylases (HDACs)/BRD4 (bromodomain-containing protein) dual inhibitors was designed and synthesized as promising anti-cancer agents. The targeted conjugates 235 were obtained through the acylation reaction of 5-bromoindole 230, giving the intermediates 231, which, via the hydrogenation reaction ($LiAlH_4$, THF), afforded the corresponding indolyl derivatives 232. Coupling 232 with 3,5-dimethylisoxazole-4-boronic acid and pinacol ester, followed by alkylation, produced 234. Ammonolysis of 234 (NH_2OH , NaOH, and MeOH/ H_2O) afforded the targeted hydroxamic conjugates 235 (Scheme 48). Moderate antiproliferation properties of the targeted conjugates 235 against the THP-1 (leukemia) cell line with promising inhibition of HDAC and BRD4 were exhibited (Supplementary Figure S45). The most promising agent 235 discovered is that with $n = 1$, $m = 6$, and $R = 4-F$ ($IC_{50} = 5$ nM against HDAC3 and the % inhibition of BRD4 = 88% at 10 μM). The downregulation of the c-Myc protein and the upregulation of acetylated histone H3 (Ac-H3) are in accordance with the tumor growth inhibitory effect [182].

3,6-Disubstituted-2-carboxyindoles 241 were reported as anti-leukemic agents. The targeted agents 241 were synthesized through Heck-Matsuda arylation of methyl acrylate 236 with arenediazonium salts 237 in the presence of palladium acetate as a catalyst, producing cinnamates 238. The Heck-Matsuda reaction with a 2 mol equivalent of arenediazonium salt 239 under the same catalytic reaction conditions afforded β,β -diarylacrylates 240. Cadogan-Sundberg reductive cyclization of 240, promoted by $P(OEt)_3$, furnished the final targets 241 (Scheme 49). The cytotoxic properties of 241 (MTT assay) against CEM, RS4, and 11 (leukemia) cancer cell lines were studied (Supplementary Figure S46). Indolyl analog 241 with $R = OMe$ and $R^1 = CF_3$ displayed the most promising properties ($IC_{50} = 0.20$ and $0.30 \mu M$, respectively), with tubulin polymerization inhibition targeting/arresting the G2/M phase in addition to DNA damage and apoptosis induction. In vivo studies (xenograft mouse, i.p. 10 mg/kg \times 5 per week) evidenced overall animal survival [183].



Scheme 48. Synthetic route towards indole-isoxazole conjugates 235.



Scheme 49. Synthetic route towards 2-carbomethoxy-3-arylindoles 241.

4. Conclusions

In conclusion, the indole scaffold has emerged as a promising foundation for developing potential anticancer agents, providing numerous opportunities for future research and therapeutic applications. Indole derivatives exhibit diverse chemical structures and versatile pharmacological activities, making them attractive drug discovery and development candidates. The indole scaffold possesses several inherent properties, contributing to its potential as an anticancer agent. It demonstrates favorable drug-like characteristics such as good oral bioavailability, metabolic stability, and cell permeability. Furthermore, indole derivatives have displayed various mechanisms of action, including inhibition of cell proliferation, induction of apoptosis, and interference with key signaling pathways involved in cancer development and progression. A significant advantage of the indole scaffold is its structural flexibility, which allows for extensive modifications and optimization of drug-like properties. Researchers can explore different synthetic strategies to introduce functional groups, alter substitution patterns, and fine-tune the physicochemical properties of indole-based compounds. This enables the design of highly potent and selective anticancer agents with improved efficacy and reduced toxicity. Additionally, the indole scaffold shows promise in targeting specific molecular targets crucial for cancer cell survival and proliferation, such as enzymes like kinases, histone deacetylases, and topoisomerases. Indole-based compounds have demonstrated potent anticancer activity in preclinical studies by selectively inhibiting these targets. Furthermore, aside from their direct anticancer effects, indole derivatives have the potential to modulate multidrug resistance in cancer cells, a common challenge in cancer treatment, by inhibiting efflux pumps and enhancing the intracellular accumulation of chemotherapeutic agents, thus overcoming resistance and sensitizing cancer cells to treatment.

Indole-based compounds are poised to play a significant role in anticancer research in the future. Continual advancements in synthetic chemistry, computational modeling, and high-throughput screening techniques are expected to uncover new indole derivatives with improved potency, selectivity, and pharmacokinetic properties. Moreover, breakthroughs in personalized medicine and identifying specific biomarkers linked to the response to indole-based compounds will facilitate targeted therapy and enhance patient outcomes.

Supplementary Materials: The following supporting information can be downloaded at: <https://www.mdpi.com/article/10.3390/ph17070922/s1>, Figure S1–S46: Exhibited the chemical structure, biological properties and mode of action of the mentioned compounds.

Funding: This work was supported financially by the National Research Centre, Egypt, project ID: 13060103.

Acknowledgments: We thank the College of Science and Mathematics and the Department of Chemistry and Biochemistry at Augusta University for their support.

Conflicts of Interest: The authors declare that they have no known competing financial interests or personal relationships that could have appeared to influence the work reported in this paper.

Abbreviations

5-LOX	5-Lipoxygenase
AAZ	Acetazolamide
ACD	Accidental cell death
BAX	Bcl-2-associated X protein
Bcl-2	B-cell lymphoma 2
BRD	Bromodomain-containing protein
BTG1	B cell translocation gene 1
CA-4	Combretastatin A-4
cdc-2	Cyclin-dependent kinase 1

Cell-CuI NPs	Cellulose-supported CuI nanoparticles
COX	Cyclooxygenase
CPT	Camptothecin
DDR	Discoidin domain receptors
DIPEA	<i>N,N</i> -Diisopropylethylamine
DME	Dimethoxyethane
EDC	<i>N</i> -Ethyl- <i>N</i> -(3-dimethylaminopropyl)carbodiimide
EGF	Epidermal growth factor
ER- α	Estrogen receptor- α
FGFR	Fibroblast growth factor receptor
hCA	Human carbonic anhydrases
HDAC	Histone deacetylase
HDACs	Histone deacetylases
HFIP	Hexafluoroisopropanol
HFIP	Hexafluoroisopropanol
HIV	Human immunodeficiency virus
HOBt	Hydroxybenzotriazole
HPV	Human papillomavirus
IBX	Iodoxybenzoic acid
MTT	3-(4,5-Dimethylthiazol-2-yl)-2,5-diphenyl-tetrazolium bromide
NMPA	National Medical Products Administration
NSAID	Non-steroidal anti-inflammatory drug
NSCLC	Non-small cell lung cancer
PARP-1	Poly(ADP-ribose) polymerase-1
PD-1	Phosphodiesterase 1
PDGFR	Platelet-derived growth factor receptor
p-Erk	Phosphorylated extracellular signal-regulate kinase
RCD	Regulated cell death
ROS	Reactive oxygen species
ROS	Reactive oxygen species
SARS-CoV-2	Severe acute respiratory syndrome coronavirus-2
SDS	Sodium dodecyl sulfate
SRB	Sulforhodamine B
TEBA	Benzyltriethylammonium chloride
Tf ₂ NH	Bis(trifluoromethane sulfonimide)
TK	tyrosine kinase
VEGFR	Vascular endothelial growth factor receptor

References

1. Siegel, R.L.; Miller, K.D.; Wagle, N.S.; Jemal, A. Cancer statistics, 2023. *CA Cancer J. Clin.* **2023**, *73*, 17–48. [CrossRef] [PubMed]
2. Aboshouk, D.R.; Youssef, M.A.; Bekheit, M.S.; Hamed, A.R.; Girgis, A.S. Antineoplastic indole-containing compounds with potential VEGFR inhibitory properties. *RSC Adv.* **2024**, *14*, 5690–5728. [CrossRef] [PubMed]
3. International Agency for Research on Cancer, Cancer Tomorrow. Available online: <https://gco.iarc.fr/tomorrow/en/dataviz/isotype> (accessed on 30 May 2024).
4. Rahib, L.; Wehner, M.R.; Matrisian, L.M.; Nead, K.T. Estimated projection of US cancer incidence and death to 2040. *JAMA Netw. Open* **2021**, *4*, e214708. [CrossRef] [PubMed]
5. Bray, F.; Laversanne, M.; Weiderpass, E.; Soerjomataram, I. The ever-increasing importance of cancer as a leading cause of premature death worldwide. *Cancer* **2021**, *127*, 3029–3030. [CrossRef] [PubMed]
6. Kelley, K.D.; Aronowitz, P. *Cancer. Med. Clin. N. Am.* **2022**, *106*, 411–422. [CrossRef] [PubMed]
7. Vasani, N.; Baselga, J.; Hyman, D.M. A view on drug resistance in cancer. *Nature* **2019**, *575*, 299–309. [CrossRef] [PubMed]
8. Emran, T.B.; Shahriar, A.; Mahmud, A.R.; Rahman, T.; Abir, M.H.; Siddiquee, M.F.-R.; Ahmed, H.; Rahman, N.; Nainu, F.; Wahyudin, E.; et al. Multidrug resistance in cancer: Understanding molecular mechanisms, immunoprevention and therapeutic approaches. *Front. Oncol.* **2022**, *12*, 891652. [CrossRef] [PubMed]
9. Dias, M.P.; Moser, S.C.; Ganesan, S.; Jonkers, J. Understanding and overcoming resistance to PARP inhibitors in cancer therapy. *Nat. Rev. Clin. Oncol.* **2021**, *18*, 773–791. [CrossRef] [PubMed]
10. Cesur-Ergün, B.; Demir-Dora, D. Gene therapy in cancer. *J. Genet. Med.* **2023**, *25*, e3550. [CrossRef]
11. Shimu, A.S.; Wei, H.-X.; Li, Q.; Zheng, X.; Li, B. The new progress in cancer immunotherapy. *Clin. Exp. Med.* **2023**, *23*, 553–567. [CrossRef]

12. Jiang, W.; Liang, M.; Lei, Q.; Li, G.; Wu, S. The current status of photodynamic therapy in cancer treatment. *Cancers* **2023**, *15*, 585. [[CrossRef](#)] [[PubMed](#)]
13. Song, J.; Zhang, B.; Li, M.; Zhang, J. The current scenario of naturally occurring indole alkaloids with anticancer potential. *Fitoterapia* **2023**, *165*, 105430. [[CrossRef](#)] [[PubMed](#)]
14. Islam, F.; Dehbia, Z.; Zehravi, M.; Das, R.; Sivakumar, M.; Krishnan, K.; Billah, A.A.M.; Bose, B.; Ghosh, A.; Paul, S.; et al. Indole alkaloids from marine resources: Understandings from therapeutic point of view to treat cancers. *Chem. Biol. Interact.* **2023**, *383*, 110682. [[CrossRef](#)] [[PubMed](#)]
15. Panda, S.S.; Girgis, A.S.; Aziz, M.N.; Bekheit, M.S. Spirooxindole: A versatile biologically active heterocyclic scaffold. *Molecules* **2023**, *28*, 618. [[CrossRef](#)] [[PubMed](#)]
16. Ghosh, A.K.; Raghavaiah, J.; Shahabi, D.; Yadav, M.; Anson, B.J.; Lendy, E.K.; Hattori, S.I.; Higashi-Kuwata, N.; Mitsuya, H.; Mesecar, A.D. Indole chloropyridinyl ester-derived SARS-CoV-2 3CLpro inhibitors: Enzyme inhibition, antiviral efficacy, structure-activity relationship, and X-ray structural studies. *J. Med. Chem.* **2021**, *64*, 14702–14714. [[CrossRef](#)]
17. Girgis, A.S.; Panda, S.S.; Kariuki, B.M.; Bekheit, M.S.; Barghash, R.F.; Aboshouk, D.R. Indole-based compounds as potential drug candidates for SARS-CoV-2. *Molecules* **2023**, *28*, 6603. [[CrossRef](#)] [[PubMed](#)]
18. Bekheit, M.S.; Panda, S.S.; Kariuki, B.M.; Mahmoud, S.H.; Mostafa, A.; Girgis, A.S. Spiroindole-containing compounds bearing phosphonate group of potential Mpro-SARS-CoV-2 inhibitory properties. *Eur. J. Med. Chem.* **2023**, *258*, 115563. [[CrossRef](#)] [[PubMed](#)]
19. Wyman, K.A.; Girgis, A.S.; Surapaneni, P.S.; Moore, J.M.; Abo Shama, N.M.; Mahmoud, S.H.; Mostafa, A.; Barghash, R.F.; Juan, Z.; Dobarra, R.D.; et al. Synthesis of potential antiviral agents for SARS-CoV-2 using molecular hybridization approach. *Molecules* **2022**, *27*, 5923. [[CrossRef](#)] [[PubMed](#)]
20. Fawazy, N.G.; Panda, S.S.; Mostafa, A.; Kariuki, B.M.; Bekheit, M.S.; Moatasim, Y.; Kutkat, O.; Fayad, W.; El-Manawaty, M.A.; Soliman, A.A.F.; et al. Development of spiro-3-indolin-2-one containing compounds of antiproliferative and anti-SARS-CoV-2 properties. *Sci. Rep.* **2022**, *12*, 13880. [[CrossRef](#)]
21. Girgis, A.S.; Panda, S.S.; Srouf, A.M.; Abdelnaser, A.; Nasr, S.; Moatasim, Y.; Kutkat, O.; El Taweel, A.; Kandeil, A.; Mostafa, A.; et al. 3-Alkenyl-2-oxindoles: Synthesis, antiproliferative and antiviral properties against SARS-CoV-2. *Bioorg. Chem.* **2021**, *114*, 105131. [[CrossRef](#)]
22. Bekheit, M.S.; Panda, S.S.; Girgis, A.S. Potential RNA-dependent RNA polymerase inhibitors as prospective drug candidates for SARS-CoV-2. *Eur. J. Med. Chem.* **2023**, *252*, 115292. [[CrossRef](#)] [[PubMed](#)]
23. Chauhan, M.; Saxena, A.; Saha, B. An insight in anti-malarial potential of indole scaffold: A review. *Eur. J. Med. Chem.* **2021**, *218*, 113400. [[CrossRef](#)] [[PubMed](#)]
24. Li, J.-Y.; Sun, X.-F.; Li, J.-J.; Yu, F.; Zhang, Y.; Huang, X.-J.; Jiang, F.-X. The antimalarial activity of indole alkaloids and hybrids. *Arch. Pharm.* **2020**, *353*, e2000131. [[CrossRef](#)] [[PubMed](#)]
25. Qin, H.-L.; Liu, J.; Fang, W.-Y.; Ravindar, L.; Rakesh, K.P. Indole-based derivatives as potential antibacterial activity against methicillin-resistance *Staphylococcus aureus* (MRSA). *Eur. J. Med. Chem.* **2020**, *194*, 112245. [[CrossRef](#)] [[PubMed](#)]
26. Meng, T.; Hou, Y.; Shang, C.; Zhang, J.; Zhang, B. Recent advances in indole dimers and hybrids with antibacterial activity against methicillin-resistant *Staphylococcus aureus*. *Arch. Pharm.* **2020**, *354*, e2000266. [[CrossRef](#)] [[PubMed](#)]
27. Bokhtia, R.M.; Panda, S.S.; Girgis, A.S.; Samir, N.; Said, M.F.; Abdelnaser, A.; Nasr, S.; Bekheit, M.S.; Dawood, A.S.; Sharma, H.; et al. New NSAID conjugates as potent and selective COX-2 inhibitors: Synthesis, molecular modeling and biological investigation. *Molecules* **2023**, *28*, 1945. [[CrossRef](#)] [[PubMed](#)]
28. Song, L.-L.; Mu, Y.-L.; Zhang, H.-C.; Wu, G.-Y.; Sun, J.-Y. A new indole alkaloid with anti-inflammatory from the branches of *Nauclea officinalis*. *Nat. Prod. Res.* **2020**, *34*, 2283–2288. [[CrossRef](#)] [[PubMed](#)]
29. Jiang, L.; Pu, H.; Qin, X.; Liu, J.; Wen, Z.; Huang, Y.; Xiang, J.; Xiang, Y.; Ju, J.; Duan, Y.; et al. Syn-2,3-diols and anti-inflammatory indole derivatives from *Streptomyces* sp. CB09001. *Nat. Prod. Res.* **2021**, *35*, 144–151. [[CrossRef](#)] [[PubMed](#)]
30. Tivorbex FDA Approval History. Available online: <https://www.drugs.com/history/tivorbex.html> (accessed on 30 May 2024).
31. Delavirdine. Available online: <https://www.drugs.com/search.php?searchterm=Delavirdine> (accessed on 30 May 2024).
32. Ateviridine. Available online: <https://go.drugbank.com/drugs/DB12264> (accessed on 30 May 2024).
33. Sertindole FDA Approval History. Available online: <https://www.drugs.com/history/serdolect.html> (accessed on 30 May 2024).
34. Maxalt. Available online: <https://www.thepharmaletter.com/article/merck-s-maxalt-approved-in-usa> (accessed on 30 May 2024).
35. Ondansetron FDA Approval History. Available online: <https://www.drugs.com/history/zuplenz.html> (accessed on 30 May 2024).
36. Arbidol. Available online: <https://go.drugbank.com/drugs/DB13609> (accessed on 30 May 2024).
37. Sumatriptan. Available online: <https://www.drugs.com/search.php?searchterm=Sumatriptan> (accessed on 30 May 2024).
38. Ropinirole. Available online: <https://www.drugs.com/search.php?searchterm=Ropinirole> (accessed on 30 May 2024).
39. Tadalafil. Available online: <https://www.drugs.com/search.php?searchterm=Tadalafil> (accessed on 30 May 2024).
40. Zolmitriptan. Available online: <https://www.drugs.com/mtm/zolmitriptan.html> (accessed on 30 May 2024).
41. Pindolol. Available online: https://www.accessdata.fda.gov/drugsatfda_docs/label/2007/018285s034bl.pdf (accessed on 30 May 2024).
42. Tang, D.; Kang, R.; Berghe, T.V.; Vandennebeele, P.; Kroemer, G. The molecular machinery of regulated cell death. *Cell Res.* **2019**, *29*, 347–364. [[CrossRef](#)] [[PubMed](#)]

43. Tong, X.; Tang, R.; Xiao, M.; Xu, J.; Wang, W.; Zhang, B.; Liu, J.; Yu, X.; Shi, S. Targeting cell death pathways for cancer therapy: Recent developments in necroptosis, pyroptosis, ferroptosis, and cuproptosis research. *J. Hematol. Oncol.* **2022**, *15*, 174. [[CrossRef](#)]
44. Peng, F.; Liao, M.; Qin, R.; Zhu, S.; Peng, C.; Fu, L.; Chen, Y.; Han, B. Regulated cell death (RCD) in cancer: Key pathways and targeted therapies. *Signal Transduct. Target. Ther.* **2022**, *7*, 286. [[CrossRef](#)]
45. Qin, R.; You, F.M.; Zhao, Q.; Xie, X.; Peng, C.; Zhan, G.; Han, B. Naturally derived indole alkaloids targeting regulated cell death (RCD) for cancer therapy: From molecular mechanisms to potential therapeutic targets. *J. Hematol. Oncol.* **2022**, *15*, 133. [[CrossRef](#)] [[PubMed](#)]
46. Dadashpour, S.; Emami, S. Indole in the target-based design of anticancer agents: A versatile scaffold with diverse mechanisms. *Eur. J. Med. Chem.* **2018**, *150*, 9–29. [[CrossRef](#)]
47. Mondal, D.; Amin, S.A.; Moinul, M.; Das, K.; Jha, T.; Gayen, S. How the structural properties of the indole derivatives are important in kinase targeted drug design?: A case study on tyrosine kinase inhibitors. *Bioorg. Med. Chem.* **2022**, *53*, 116534. [[CrossRef](#)] [[PubMed](#)]
48. Jiang, B.-E.; Hu, J.; Liu, H.; Liu, Z.; Wen, Y.; Liu, M.; Zhang, H.K.; Pang, X.; Yu, L.-F. Design, synthesis, and biological evaluation of indole-based hydroxamic acid derivatives as histone deacetylase inhibitors. *Eur. J. Med. Chem.* **2022**, *227*, 113893. [[CrossRef](#)]
49. Jia, Y.; Wen, X.; Gong, Y.; Wang, X. Current scenario of indole derivatives with potential anti-drug-resistant cancer activity. *Eur. J. Med. Chem.* **2020**, *200*, 112359. [[CrossRef](#)]
50. Sunitinib. Available online: <https://go.drugbank.com/drugs/DB01268> (accessed on 30 May 2024).
51. Sunitinib FDA approved history. Available online: <https://www.drugs.com/history/sutent.html> (accessed on 30 May 2024).
52. Nintedanib. Available online: <https://go.drugbank.com/drugs/DB09079> (accessed on 30 May 2024).
53. Nintedanib FDA Approved History. Available online: <https://www.drugs.com/history/ofev.html> (accessed on 30 May 2024).
54. Jamadar, A.; Suma, S.M.; Mathew, S.; Fields, T.A.; Wallace, D.P.; Calvet, J.P.; Rao, R. The tyrosine-kinase inhibitor Nintedanib ameliorates autosomal-dominant polycystic kidney disease. *Cell Death Dis.* **2021**, *12*, 947. [[CrossRef](#)] [[PubMed](#)]
55. Hilberg, F.; Tontsch-Grunt, U.; Baum, A.; Le, A.T.; Doebele, R.C.; Lieb, S.; Gianni, D.; Voss, T.; Garin-Chesa, P.; Haslinger, C.; et al. Triple angiokinase inhibitor Nintedanib directly inhibits tumor cell growth and induces tumor shrinkage via blocking oncogenic receptor tyrosine kinases. *J. Pharmacol. Exp. Ther.* **2018**, *364*, 494–503. [[CrossRef](#)]
56. Riesco-Martinez, M.C.; Torre, A.S.; García-Carbonero, R. Safety and efficacy of nintedanib for the treatment of metastatic colorectal cancer. *Expert Opin. Investig. Drugs* **2017**, *26*, 1295–1305. [[CrossRef](#)]
57. Kurzrock, R.; Stewart, D.J. Exploring the benefit/risk associated with antiangiogenic agents for the treatment of non-small cell lung cancer patients. *Clin. Cancer Res.* **2017**, *23*, 1137–1148. [[CrossRef](#)]
58. Anlotinib. Available online: <https://go.drugbank.com/drugs/DB11363> (accessed on 30 May 2024).
59. Li, S. Anlotinib: A novel targeted drug for bone and soft tissue sarcoma. *Front. Oncol.* **2021**, *11*, 664853. [[CrossRef](#)] [[PubMed](#)]
60. Shen, G.; Zheng, F.; Ren, D.; Du, F.; Dong, Q.; Wang, Z.; Zhao, F.; Ahmad, R.; Zhao, J. Anlotinib: A novel multi-targeting tyrosine kinase inhibitor in clinical development. *J. Hematol. Oncol.* **2018**, *11*, 120. [[CrossRef](#)] [[PubMed](#)]
61. Syed, Y.Y. Anlotinib: First global approval. *Drugs* **2018**, *78*, 1057–1062. [[CrossRef](#)]
62. Panobinostat. Available online: <https://go.drugbank.com/drugs/DB06603> (accessed on 30 May 2024).
63. Osimertinib. Available online: <https://go.drugbank.com/drugs/DB09330> (accessed on 30 May 2024).
64. Anlotinib. Available online: <https://go.drugbank.com/drugs/DB11885> (accessed on 30 May 2024).
65. Girgis, A.S.; D'Arcy, P.; Aboshouk, D.R.; Bekheit, M.S. Synthesis and bio-properties of 4-piperidone containing compounds as curcumin mimics. *RSC Adv.* **2022**, *12*, 31102–31123. [[CrossRef](#)] [[PubMed](#)]
66. Newman, D.J. Drug discovery from natural sources. *Curr. Pharmacol. Rep.* **2023**, *9*, 67–89. [[CrossRef](#)]
67. Xu, Z.; Eichler, B.; Klausner, E.A.; Duffy-Matzner, J.; Zheng, W. Lead/drug discovery from natural resources. *Molecules* **2022**, *28*, 8280. [[CrossRef](#)] [[PubMed](#)]
68. Atanasov, A.G.; Zotchev, S.B.; Dirsch, V.M.; Supuran, C.T. Natural products in drug discovery: Advances and opportunities. *Nat. Rev. Drug Discov.* **2021**, *20*, 200–216. [[CrossRef](#)] [[PubMed](#)]
69. Hui, Z.; Wen, H.; Zhu, J.; Deng, H.; Jiang, X.; Ye, X.-Y.; Wang, L.; Xie, T.; Bai, R. Discovery of plant-derived anti-tumor natural products: Potential leads for anti-tumor drug discovery. *Bioorg. Chem.* **2024**, *142*, 106957. [[CrossRef](#)] [[PubMed](#)]
70. Thanikachalam, P.V.; Maurya, R.K.; Garg, V.; Monga, V. An Insight into the medicinal perspective of synthetic analogs of indole: A review. *Eur. J. Med. Chem.* **2019**, *180*, 562–612. [[CrossRef](#)] [[PubMed](#)]
71. Vinblastine. Available online: <https://www.drugs.com/mtm/vinblastine.html> (accessed on 30 May 2024).
72. Vinblastine. Available online: <https://go.drugbank.com/drugs/DB00570> (accessed on 30 May 2024).
73. Vincristine. Available online: <https://www.drugs.com/mtm/vincristine.html> (accessed on 30 May 2024).
74. Vincristine. Available online: <https://go.drugbank.com/drugs/DB00541> (accessed on 30 May 2024).
75. Gao, G.; Li, J.; Cao, Y.; Li, X.; Qian, Y.; Wang, X.; Li, M.; Qiu, Y.; Wu, T.; Wang, L.; et al. Design, synthesis, and biological evaluation of novel 4,4'-bipyridine derivatives acting as CDK9-Cyclin T1 protein-protein interaction inhibitors against triple-negative breast cancer. *Eur. J. Med. Chem.* **2023**, *261*, 115858. [[CrossRef](#)]
76. Liu, X.; Luo, B.; Wu, X.; Tang, Z. Cuproptosis and cuproptosis-related genes: Emerging potential therapeutic targets in breast cancer. *Biochim. Biophys. Acta Rev. Cancer* **2023**, *1878*, 189013. [[CrossRef](#)] [[PubMed](#)]

77. El-Gazzar, M.G.M.; Ghorab, M.M.; Amin, M.A.; Korany, M.; Khedr, M.A.; El-Gazzar, M.G.; Sakr, T.M. Computational, in vitro and radiation-based in vivo studies on acetamide quinazolinone derivatives as new proposed purine nucleoside phosphorylase inhibitors for breast cancer. *Eur. J. Med. Chem.* **2023**, *248*, 115087. [CrossRef] [PubMed]
78. Ding, Y.; He, J.; Huang, J.; Yu, T.; Shi, X.; Zhang, T.; Yan, G.; Chen, S.; Peng, C. Harmine induces anticancer activity in breast cancer cells via targeting TAZ. *Int. J. Oncol.* **2019**, *54*, 1995–2004. [CrossRef] [PubMed]
79. Wang, W.; Zhou, Z.; Zhou, X.; Chen, L.; Bie, S.; Jing, Z. Mukonal exerts anticancer effects on the human breast cancer cells by inducing autophagy and apoptosis and inhibits the tumor growth in vivo. *AMB Express* **2020**, *10*, 148. [CrossRef] [PubMed]
80. Duan, F.F.; Liu, L.; Gao, Y.; Peng, X.G.; Meng, X.G.; Ruan, H.L. [11]-Chaetoglobosins from *Pseudeurotium bakeri* induce G2/M cell cycle arrest and apoptosis in human cancer cells. *J. Nat. Prod.* **2021**, *84*, 1904–1914. [CrossRef] [PubMed]
81. Schabath, M.B.; Cote, M.L. Cancer progress and priorities: Lung cancer. *Cancer Epidemiol. Biomarkers Prev.* **2019**, *28*, 1563–1579. [CrossRef]
82. Lung Cancer. Available online: https://www.who.int/news-room/fact-sheets/detail/lung-cancer?gad_source=1&gclid=CjwKCAjwte-vBhBFEiwAQsv_xS3Y12SJADHBJ5AKzeEL9AjY_Srlq1SmesZHPK_QBFTOyhHBItTTixoC7XMQAvD_BwE (accessed on 30 May 2024).
83. Siegel, R.L.; Giaquinto, A.N.; Jemal, A. Cancer statistics, 2024. *CA Cancer J. Clin.* **2024**, *74*, 12–49. [CrossRef] [PubMed]
84. Lim, H.M.; Park, S.-H.; Nam, M.J. Induction of apoptosis in indole-3-carbinol-treated lung cancer H1299 cells via ROS level elevation. *Hum. Exp. Toxicol.* **2021**, *40*, 812–825. [CrossRef] [PubMed]
85. Chen, J.; Guo, Q.; Zhang, J.; Yin, Z.; Song, W.; He, B.; Zhang, Y.; Zhang, W.J.; Chen, L. Chaetoglobosin G inhibits proliferation, autophagy and cell cycle of lung cancer cells through EGFR/MEK/ERK signaling pathway. *Pharmazie* **2020**, *75*, 642–645. [PubMed]
86. Al-Rashed, S.; Baker, A.; Ahmad, S.S.; Syed, A.; Bahkali, A.H.; Elgorban, A.M.; Khan, M.S. Vincamine, a safe natural alkaloid, represents a novel anticancer agent. *Bioorg. Chem.* **2021**, *107*, 104626. [CrossRef]
87. Key Statistics about Stomach Cancer. Available online: <https://www.cancer.net/cancer-types/stomach-cancer/statistics> (accessed on 30 May 2024).
88. Stomach Cancer. Available online: <https://www.cancer.org.au/cancer-information/types-of-cancer/stomach-cancer> (accessed on 30 May 2024).
89. Wang, G.; Liu, G.; Ye, Y.; Fu, Y.; Zhang, X. Bufothionine exerts anti-cancer activities in gastric cancer through Pim3. *Life Sci.* **2019**, *232*, 116615. [CrossRef] [PubMed]
90. Ye, Y.; Li, X.; Feng, G.; Ma, Y.; Ye, F.; Shen, H.; Sun, K.; Lu, R.; Miao, S. 3,3'-Diindolylmethane induces ferroptosis by BAP1-IP3R axis in BGC-823 gastric cancer cells. *Anticancer Drugs* **2022**, *33*, 362–370. [CrossRef] [PubMed]
91. Siegel, R.L.; Wagle, N.S.; Cercek, A.; Smith, R.A.; Jemal, A. Colorectal cancer statistics, 2023. *CA Cancer J. Clin.* **2023**, *73*, 233–254. [CrossRef] [PubMed]
92. Wang, K.; Song, W.; Shen, Y.; Wang, H.; Fan, Z. LncRNA *KLK8* modulates stem cell characteristics in colon cancer. *Pathol. Res. Pract.* **2021**, *224*, 153437. [CrossRef] [PubMed]
93. Srour, A.M.; Panda, S.S.; Mostafa, A.; Fayad, W.; El-Manawaty, M.A.; Soliman, A.A.F.; Moatasim, Y.; El Taweel, A.; Abdelhameed, M.F.; Bekheit, M.S.; et al. Synthesis of aspirin-curcumin mimic conjugates of potential antitumor and anti-SARS-CoV-2 properties. *Bioorg. Chem.* **2021**, *117*, 105466. [CrossRef] [PubMed]
94. Haraldsdottir, S.; Einarsdottir, H.M.; Smaradottir, A.; Gunnlaugsson, A.; Halfdanarson, T.R. Colorectal cancer—Review. *Laeknabla-did* **2014**, *100*, 75–82. [PubMed]
95. Ren, H.; Zhao, J.; Fan, D.; Wang, Z.; Zhao, T.; Li, Y.; Zhao, Y.; Adelson, D.; Hao, H. Alkaloids from *nux vomica* suppresses colon cancer cell growth through Wnt/ β -catenin signaling pathway. *Phytother. Res.* **2019**, *33*, 1570–1578. [CrossRef] [PubMed]
96. Li, J.-M.; Huang, Y.-C.; Kuo, Y.-H.; Cheng, C.-C.; Kuan, F.-C.; Chang, S.-F.; Lee, Y.-R.; Chin, C.-C.; Shi, C.-S. Flavopereirine suppresses the growth of colorectal cancer cells through P53 signaling dependence. *Cancers* **2019**, *11*, 1034. [CrossRef] [PubMed]
97. Pancreatic Cancer Statistics. Available online: <https://www.wcrf.org/cancer-trends/pancreatic-cancer-statistics> (accessed on 30 May 2024).
98. Pancreatic Cancer-Patient Version. Available online: <https://www.cancer.gov/types/pancreatic> (accessed on 30 May 2024).
99. Malsy, M.; Bitzinger, D.; Graf, B.; Bundscherer, A. Staurosporine induces apoptosis in pancreatic carcinoma cells PaTu 8988t and Panc-1 via the intrinsic signaling pathway. *Eur. J. Med. Res.* **2019**, *24*, 5. [CrossRef] [PubMed]
100. Tabassum, F.; Hasan, C.M.; Masud, M.M.; Jamshidi, S.; Rahman, K.M.; Ahsan, M. Indole alkaloids from the leaves of *Ravenia spectabilis* engl. with activity against pancreatic cancer cell line. *Phytochemistry* **2021**, *186*, 112744. [CrossRef]
101. Key Statistics about Liver Cancer. Available online: <https://www.cancer.net/cancer-types/liver-cancer/statistics> (accessed on 30 May 2024).
102. Girgis, A.S.; Panda, S.S.; Ahmed Farag, I.S.; El-Shabiny, A.M.; Moustafa, A.M.; Ismail, N.S.M.; Pillai, G.G.; Panda, C.S.; Hall, C.D.; Katritzky, A.R. Synthesis, and QSAR analysis of anti-oncological active spiro-alkaloids. *Org. Biomol. Chem.* **2015**, *13*, 1741–1753. [CrossRef] [PubMed]
103. Hou, Z.-L.; Han, F.-Y.; Lou, L.-L.; Zhao, W.-Y.; Huang, X.X.; Yao, G.-D.; Song, S.-J. The nature compound dehydrocrenatidine exerts potent antihepatocellular carcinoma by destroying mitochondrial complexes in vitro and in vivo. *Phytother. Res.* **2022**, *36*, 1353–1371. [CrossRef] [PubMed]

104. Guo, X.-X.; Li, X.-P.; Zhou, P.; Li, D.-Y.; Lyu, X.-T.; Chen, Y.; Lyu, Y.-W.; Tian, K.; Yuan, D.-Z.; Ran, J.-H.; et al. Evodiamine induces apoptosis in SMMC-7721 and HepG2 cells by suppressing NOD1 signal pathway. *Int. J. Mol. Sci.* **2018**, *19*, 3419. [CrossRef] [PubMed]
105. Cervical Cancer. Available online: <https://www.awarenessdepot.com/allcancers-cervicalcancer.html> (accessed on 30 May 2024).
106. Types of Cervical Cancer. Available online: <http://www.cancer.gov/cancertopics/types/cervical> (accessed on 30 May 2024).
107. What Is Cervical Cancer. Available online: <https://www.cancer.gov/types/cervical> (accessed on 30 May 2024).
108. Guo, C.; Meng, Q.; Liu, J.; Wu, J.; Jia, H.; Liu, D.; Gu, Y.; Liu, J.; Huang, J.; Fan, A.; et al. Sclerotiamides C-H, notoamides from a marine gorgonian-derived fungus with cytotoxic activities. *J. Nat. Prod.* **2022**, *85*, 1067–1078. [CrossRef] [PubMed]
109. Mao, J.-Q.; Zheng, Y.-Y.; Wang, C.-Y.; Liu, Y.; Yao, G.-S. Sclerotioloids A–C: Three new alkaloids from the marine-derived fungus *Aspergillus sclerotiorum* ST0501. *Mar. Drugs* **2023**, *21*, 219. [CrossRef] [PubMed]
110. Ai, Y.; He, H.; Chen, P.; Yan, B.; Zhang, W.; Ding, Z.; Li, D.; Chen, J.; Ma, Y.; Cao, Y.; et al. An alkaloid initiates phosphodiesterase 3A-schlafen 12 dependent apoptosis without affecting the phosphodiesterase activity. *Nat. Commun.* **2020**, *11*, 3236. [CrossRef] [PubMed]
111. Chen, Y.; Li, L.; Jiang, L.-R.; Tan, J.-Y.; Guo, L.-N.; Wang, X.-L.; Dong, W.; Wang, W.-B.; Sun, J.-K.; Song, B. Alkaloids constituents from the roots of *Phragmites australis* (Cav.), Trin. Ex Steud. with their cytotoxic activities. *Nat. Prod. Res.* **2022**, *36*, 1454–1459. [CrossRef] [PubMed]
112. Ovarian Cancer Statistics. Available online: <https://www.wcrf.org/cancer-trends/ovarian-cancer-statistics/> (accessed on 30 May 2024).
113. Jeong, M.; Kim, H.M.; Ahn, J.-H.; Lee, K.-T.; Jang, D.S.; Choi, J.-H. 9-Hydroxycanthin-6-one isolated from stem bark of *Ailanthus altissima* induces ovarian cancer cell apoptosis and inhibits the activation of tumor-associated macrophages. *Chem. Biol. Interact.* **2018**, *280*, 99–108. [CrossRef] [PubMed]
114. Cancer Stat Facts: Leukemia. Available online: <https://seer.cancer.gov/statfacts/html/leuks.html> (accessed on 30 May 2023).
115. Leukemia-Patient Version. Available online: <https://www.cancer.gov/types/leukemia> (accessed on 30 May 2023).
116. Types of Leukemia. Available online: <https://www.cancercenter.com/cancer-types/leukemia/types> (accessed on 30 May 2023).
117. Cancer Stat Facts: Leukemia. Available online: <https://www.cancer.gov/about-cancer/treatment/drugs/leukemia> (accessed on 30 May 2023).
118. Spirin, P.; Shyrokov, E.; Lebedev, T.; Vagapova, E.; Smirnova, P.; Kantemirov, A.; Dyshlovoy, S.A.; Von Amsberg, G.; Zhidkov, M.; Prassolov, V. Cytotoxic marine alkaloid 3,10-dibromofascaplysin induces apoptosis and synergizes with cytarabine resulting in leukemia cell death. *Mar. Drugs* **2021**, *19*, 489. [CrossRef]
119. Alhuthali, H.M.; Bradshaw, T.D.; Lim, K.H.; Kam, T.-S.; Seedhouse, C.H. The natural alkaloid Jerantinine B has activity in acute myeloid leukemia cells through a mechanism involving c-Jun. *BMC Cancer* **2020**, *20*, 629. [CrossRef]
120. Wang, Y.-P.; Pan, F.; Wang, Y.-D.; Khan, A.; Liu, Y.-P.; Yang, M.-L.; Cao, J.-X.; Zhao, T.-R.; Cheng, G.-G. Anti-leukemic effect and molecular mechanism of 11-methoxytabersonine from *Melodinus cochinchinensis* via network pharmacology, ROS-mediated mitochondrial dysfunction and PI3K/Akt signaling pathway. *Bioorg. Chem.* **2022**, *120*, 105607. [CrossRef] [PubMed]
121. Salucci, S.; Burattini, S.; Buontempo, F.; Orsini, E.; Furiassi, L.; Mari, M.; Lucarini, S.; Martelli, A.M.; Falcieri, E. Marine bisindole alkaloid: A potential apoptotic inducer in human cancer cells. *Eur. J. Histochem.* **2018**, *62*, 2881. [CrossRef] [PubMed]
122. Youssef, M.A.; Panda, S.S.; Aboshouk, D.R.; Said, M.F.; El Taweel, A.; GabAllah, M.; Fayad, W.; Soliman, A.A.F.; Mostafa, A.; Fawzy, N.G.; et al. Novel curcumin mimics: Design, synthesis, biological properties and computational studies of piperidone-piperazine conjugates. *ChemistrySelect* **2022**, *7*, e202201406. [CrossRef]
123. Panda, S.S.; Girgis, A.S.; Thomas, S.J.; Capito, J.E.; George, R.F.; Salman, A.; El-Manawaty, M.A.; Samir, A. Synthesis, pharmacological profile and 2D-QSAR studies of curcumin-amino acid conjugates as potential drug candidates. *Eur. J. Med. Chem.* **2020**, *196*, 112293. [CrossRef] [PubMed]
124. Nofal, Z.M.; Srour, A.M.; El-Eraky, W.I.; Saleh, D.O.; Girgis, A.S. Rational design, synthesis and QSAR study of vasorelaxant active 3-pyridinecarbonitriles incorporating 1H-benzimidazol-2-yl function. *Eur. J. Med. Chem.* **2013**, *63*, 14–21. [CrossRef] [PubMed]
125. Girgis, A.S.; Kalmouch, A.; Ellithy, M. Synthesis of novel vasodilatory active nicotinate esters with amino acid function. *Bioorg. Med. Chem.* **2006**, *14*, 8488–8494. [CrossRef] [PubMed]
126. Girgis, A.S.; Panda, S.S.; Srour, A.M.; Farag, H.; Ismail, N.S.M.; Elgendy, M.; Abdel-Aziz, A.K.; Katritzky, A.R. Rational design, synthesis and molecular modeling studies of novel anti-oncological alkaloids against melanoma. *Org. Biomol. Chem.* **2015**, *13*, 6619–6633. [CrossRef] [PubMed]
127. Galal, S.A.; Abdelsamie, A.S.; Shouman, S.A.; Attia, Y.M.; Ali, H.I.; Tabll, A.; El-Shenawy, R.; El Abd, Y.S.; Ali, M.M.; Mahmoud, A.E.; et al. Part I: Design, synthesis and biological evaluation of novel pyrazole-benzimidazole conjugates as checkpoint kinase 2 (Chk2) inhibitors with studying their activities alone and in combination with genotoxic drugs. *Eur. J. Med. Chem.* **2017**, *134*, 392–405. [CrossRef] [PubMed]
128. Yu, Y.; Yu, Q.; Liu, S.; Wu, C.; Zhang, X. Insight into the binding mode of HIF-2 agonists through molecular dynamic simulations and biological validation. *Eur. J. Med. Chem.* **2021**, *211*, 112999. [CrossRef] [PubMed]
129. Peerzada, M.N.; Khan, P.; Ahmad, K.; Hassan, M.I.; Azam, A. Synthesis, characterization and biological evaluation of tertiary sulfonamide derivatives of pyridyl-indole based heteroaryl chalcone as potential carbonic anhydrase IX inhibitors and anticancer agents. *Eur. J. Med. Chem.* **2018**, *155*, 13–23. [CrossRef]

130. Guo, Y.-L.; Yu, J.-W.; Cao, Y.; Cheng, K.-X.; Dong-Zhi, S.-N.-M.; Zhang, Y.-F.; Ren, Q.-J.; Yin, Y.; Li, C.-L. Design, synthesis, and biological evaluation of harmine derivatives as topoisomerase I inhibitors for cancer treatment. *Eur. J. Med. Chem.* **2024**, *265*, 116061. [[CrossRef](#)] [[PubMed](#)]
131. Singla, R.; Gupta, K.B.; Upadhyay, S.; Dhiman, M.; Jaitak, V. Design, synthesis and biological evaluation of novel indole-benzimidazole hybrids targeting estrogen receptor alpha (ER- α). *Eur. J. Med. Chem.* **2018**, *146*, 206–219. [[CrossRef](#)] [[PubMed](#)]
132. Kazan, F.; Yagci, Z.B.; Bai, R.; Ozkirimli, E.; Hamel, E.; Ozkirimli, S. Synthesis and biological evaluation of indole-2-carbohydrazides and thiazolidinyl-indole-2-carboxamides as potent tubulin polymerization inhibitors. *Comput. Biol. Chem.* **2019**, *80*, 512–523. [[CrossRef](#)] [[PubMed](#)]
133. Gaur, A.; Peerzada, M.N.; Khan, N.S.; Ali, I.; Azam, A. Synthesis and anticancer evaluation of novel indole based arylsulfonylhydrazides against human breast cancer cells. *ACS Omega* **2022**, *7*, 42036–42043. [[CrossRef](#)] [[PubMed](#)]
134. Wang, Y.-T.; Huang, X.; Cai, X.-C.; Kang, X.-X.; Zhu, H.-L. Synthesis, biological evaluation and molecular docking of thiazole hydrazone derivatives grafted with indole as novel tubulin polymerization inhibitors. *J. Mol. Struct.* **2024**, *1301*, 137343. [[CrossRef](#)]
135. Boraie, A.T.A.; Singh, P.K.; Sechi, M.; Satta, S. Discovery of novel functionalized 1,2,4-triazoles as PARP-1 inhibitors in breast cancer: Design, synthesis and antitumor activity evaluation. *Eur. J. Med. Chem.* **2019**, *182*, 111621. [[CrossRef](#)] [[PubMed](#)]
136. Chen, P.; Zhuang, Y.-X.; Diao, P.-C.; Yang, F.; Wu, S.-Y.; Lv, L.; You, W.-W.; Zhao, P.-L. Synthesis, biological evaluation, and molecular docking investigation of 3-amidoindoles as potent tubulin polymerization inhibitors. *Eur. J. Med. Chem.* **2019**, *162*, 525–533. [[CrossRef](#)] [[PubMed](#)]
137. La Regina, G.; Bai, R.; Coluccia, A.; Naccarato, V.; Famigliani, V.; Nalli, M.; Masci, D.; Verrico, A.; Rovella, P.; Mazzoccoli, C.; et al. New 6- and 7-heterocycl-1H-indole derivatives as potent tubulin assembly and cancer cell growth inhibitors. *Eur. J. Med. Chem.* **2018**, *152*, 283–297. [[CrossRef](#)] [[PubMed](#)]
138. Ren, W.; Deng, Y.; Ward, J.D.; Vairin, R.; Bai, R.; Wanniarachchi, H.I.; Hamal, K.B.; Tankoano, P.E.; Tamminga, C.S.; Bueno, L.M.A.; et al. Synthesis and biological evaluation of structurally diverse 6-aryl-3-aryl-indole analogues as inhibitors of tubulin polymerization. *Eur. J. Med. Chem.* **2024**, *263*, 115794. [[CrossRef](#)]
139. Vekariya, R.H.; Aubé, J. Hexafluoro-2-propanol-promoted intermolecular Friedel-Crafts acylation reaction. *Org. Lett.* **2016**, *18*, 3534–3537. [[CrossRef](#)]
140. Ghanim, A.M.; Girgis, A.S.; Kariuki, B.M.; Samir, N.; Said, M.F.; Abdelnaser, A.; Nasr, S.; Bekheit, M.S.; Abdelhameed, M.F.; Almalki, A.J.; et al. Design and synthesis of ibuprofen-quinoline conjugates as potential anti-inflammatory and analgesic drug candidates. *Bioorg. Chem.* **2022**, *119*, 105557. [[CrossRef](#)] [[PubMed](#)]
141. Seliem, I.A.; Girgis, A.S.; Moatasim, Y.; Kandeil, A.; Mostafa, A.; Ali, M.A.; Bekheit, M.S.; Panda, S.S. New pyrazine conjugates: Synthesis, computational studies, and antiviral properties against SARS-CoV-2. *ChemMedChem* **2021**, *16*, 3418–3427. [[CrossRef](#)] [[PubMed](#)]
142. Seliem, I.A.; Panda, S.S.; Girgis, A.S.; Moatasim, Y.; Kandeil, A.; Mostafa, A.; Ali, M.A.; Nossier, E.S.; Rasslan, F.; Srouf, A.M.; et al. New quinoline-triazole conjugates: Synthesis, and antiviral properties against SARS-CoV-2. *Bioorg. Chem.* **2021**, *114*, 105117. [[CrossRef](#)] [[PubMed](#)]
143. Tiwari, A.D.; Panda, S.S.; Girgis, A.S.; Sahu, S.; George, R.F.; Srouf, A.M.; La Starza, B.; Asiri, A.M.; Hall, C.D.; Katritzky, A.R. Microwave assisted synthesis and QSAR study of novel NSAID acetaminophen conjugates with amino acid linkers. *Org. Biomol. Chem.* **2014**, *12*, 7238–7249. [[CrossRef](#)] [[PubMed](#)]
144. Mishriky, N.; Asaad, F.M.; Ibrahim, Y.A.; Girgis, A.S. New 2-pyrazolines of anticipated molluscicidal activity. *Pharmazie* **1996**, *51*, 544–548. [[PubMed](#)]
145. Shareef, M.A.; Ganapathi, T.; Khan, I.; Rani, S.; Rajanna, A.; Akbar, S.; Kumar, C.G.; Babu, B.N. New indolyl-arylamino propenone conjugates: Synthesis, cytotoxicity and apoptotic inducing studies. *ChemistrySelect* **2020**, *5*, 2063–2069. [[CrossRef](#)]
146. Naaz, F.; Ahmad, F.; Lone, B.A.; Pokharel, Y.R.; Fuloria, N.K.; Fuloria, S.; Ravichandran, M.; Pattabhiraman, L.; Shafi, S.; Yar, M.S. Design and synthesis of newer 1,3,4-oxadiazole and 1,2,4-triazole based Toposentin analogues as anti-proliferative agent targeting tubulin. *Bioorg. Chem.* **2020**, *95*, 103519. [[CrossRef](#)] [[PubMed](#)]
147. Jain, R.; Gahlyan, P.; Dwivedi, S.; Konwar, R.; Kumar, S.; Bhandari, M.; Arora, R.; Kakkar, R.; Kumar, R.; Prasad, A.K. Design, synthesis and evaluation of 1H-1,2,3-triazol-4-yl-methyl tethered 3-pyrrolylisatins as potent anti-breast cancer agents. *ChemistrySelect* **2018**, *3*, 5263–5268. [[CrossRef](#)]
148. Chavan, P.V.; Desai, U.V.; Wadgaonkar, P.P.; Tapase, S.R.; Kodam, K.M.; Choudhari, A.; Sarkar, D. Click chemistry based multicomponent approach in the synthesis of spirochromenocarbazole tethered 1,2,3-triazoles as potential anticancer agents. *Bioorg. Chem.* **2019**, *85*, 475–486. [[CrossRef](#)]
149. Sharma, B.; Singh, A.; Gu, L.; Saha, S.T.; Singh-Pillay, A.; Cele, N.; Singh, P.; Kaur, M.; Kumar, V. Diastereoselective approach to rationally design tetrahydro- β -carboline-isatin conjugates as potential SERMs against breast cancer. *RSC Adv.* **2019**, *9*, 9809–9819. [[CrossRef](#)]
150. Kumar, S.; Gu, L.; Palma, G.; Kaur, M.; Singh-Pillay, A.; Singh, P.; Kumar, V. Design, synthesis, anti-proliferative evaluation and docking studies of 1H-1,2,3-triazole tethered Ospemifene-isatin conjugates as selective estrogen receptor modulators. *New J. Chem.* **2018**, *42*, 3703–3713. [[CrossRef](#)]
151. Altowyan, M.S.; Soliman, S.M.; Haukka, M.; Al-Shaalan, N.H.; Alkharboush, A.A.; Barakat, A. Synthesis, characterization, and cytotoxicity of new spirooxindoles engrafted furan structural motif as a potential anticancer agent. *ACS Omega* **2022**, *7*, 35743–35754. [[CrossRef](#)] [[PubMed](#)]

152. Eldehna, W.M.; EL-Naggar, D.H.; Hamed, A.R.; Ibrahim, H.S.; Ghabbour, H.A.; Abdel-Aziz, H.A. One-pot three-component synthesis of novel spirooxindoles with potential cytotoxic activity against triple-negative breast cancer MDA-MB-231 cells. *J. Enzyme Inhib. Med. Chem.* **2018**, *33*, 309–318. [[CrossRef](#)] [[PubMed](#)]
153. Hendy, M.S.; Ali, A.A.; Ahmed, L.; Hossam, R.; Mostafa, A.; Elmazar, M.M.; Naguib, B.H.; Attia, Y.M.; Ahmed, M.S. Structure-based drug design, synthesis, in vitro, and in vivo biological evaluation of indole-based biomimetic analogs targeting estrogen receptor- α inhibition. *Eur. J. Med. Chem.* **2019**, *166*, 281–290. [[CrossRef](#)] [[PubMed](#)]
154. Rhodes, S.; Short, S.; Sharma, S.; Kaur, R.; Jha, M. One-pot mild and efficient synthesis of [1,3]thiazino[3,2-*a*]indol-4-ones and their anti-proliferative activity. *Org. Biomol. Chem.* **2019**, *17*, 3914–3920. [[CrossRef](#)] [[PubMed](#)]
155. Zhao, W.; He, L.; Xiang, T.-L.; Tang, Y.-J. Discover 4 β -NH-(6-aminoindole)-4 desoxy-podophyllotoxin with nanomolar-potency antitumor activity by improving the tubulin binding affinity on the basis of a potential binding site nearby colchicine domain. *Eur. J. Med. Chem.* **2019**, *170*, 73–86. [[CrossRef](#)] [[PubMed](#)]
156. Bakherad, Z.; Safavi, A.; Fassihi, A.; Sadeghi-Aliabadi, H.; Bakherad, M.; Rastegar, H.; Ghasemi, J.B.; Sepehri, S.; Saghaie, L.; Mahdavi, M. Anti-cancer, anti-oxidant and molecular docking studies of thiosemicarbazone indole-based derivatives. *Res. Chem. Intermed.* **2019**, *45*, 2827–2854. [[CrossRef](#)]
157. Das Mukherjee, D.; Kumar, N.M.; Tantak, M.P.; Das, A.; Ganguli, A.; Datta, S.; Kumar, D.; Chakrabarti, G. Development of novel bis(indolyl)-hydrazide-hydrazine derivatives as potent microtubule-targeting cytotoxic agents against A549 lung cancer cells. *Biochemistry* **2016**, *55*, 3020–3035. [[CrossRef](#)] [[PubMed](#)]
158. Manuel-Manresa, P.; Korrodi-Gregório, L.; Hernando, E.; Villanueva, A.; Martínez-García, D.; Rodilla, A.M.; Ramos, R.; Fardilha, M.; Moya, J.; Quesada, R.; et al. Novel indole-based tambjamine-analogues induce apoptotic lung cancer cell death through p38 mitogen-activated protein kinase activation. *Mol. Cancer Ther.* **2017**, *16*, 1224–1235. [[CrossRef](#)]
159. Martínez-García, D.; Pérez-Hernández, M.; Korrodi-Gregório, L.; Quesada, R.; Ramos, R.; Baixeras, N.; Pérez-Tomás, R.; Soto-Cerrato, V. The natural-based antitumor compound T21 decreases survivin levels through potent STAT3 inhibition in lung cancer models. *Biomolecules* **2019**, *9*, 361. [[CrossRef](#)]
160. Nguyen, T.D.; Le, T.M.D. Development of a novel indirubin derivative with enhanced anticancer properties: Synthesis, in vitro, and in vivo evaluation. *Chem. Pap.* **2024**, *78*, 2469–2478. [[CrossRef](#)]
161. Lu, F.L.; Chen, B.B.; Wang, C.H.; Zhuang, C.L.; Miao, Z.Y.; Zhang, X.D.; Wu, Y.L. Design, synthesis, and biological evaluation of novel trimethoxyindole derivatives derived from natural products. *Monatsh. Chem.* **2019**, *150*, 1545–1552. [[CrossRef](#)]
162. Liu, S.; Li, X.; Chen, C.; Lin, X.; Zuo, W.; Peng, C.; Jiang, Q.; Huang, W.; He, G. Design, synthesis, and biological evaluation of novel discoidin domain receptor inhibitors for the treatment of lung adenocarcinoma and pulmonary fibrosis. *Eur. J. Med. Chem.* **2024**, *265*, 116100. [[CrossRef](#)]
163. He, P.; Du, L.; Dai, Q.; Li, G.; Yu, B.; Chang, L. Design, synthesis and biological evaluation of structurally new 4-indolyl quinazoline derivatives as highly potent, selective and orally bioavailable EGFR inhibitors. *Bioorg. Chem.* **2024**, *142*, 106970. [[CrossRef](#)] [[PubMed](#)]
164. Yang, W.; Peng, H.; He, M.; Peng, Z.; Wang, G. Novel tubulin polymerization inhibitors based on the hybridization of coumarin and indole ring: Design, synthesis and bioactivities evaluation. *J. Mol. Struct.* **2024**, *1305*, 137761. [[CrossRef](#)]
165. Song, Y.; Feng, S.; Feng, J.; Dong, S.; Yang, K.; Liu, Z.; Qiao, X. Synthesis and biological evaluation of novel pyrazoline derivatives containing indole skeleton as anti-cancer agents targeting topoisomerase II. *Eur. J. Med. Chem.* **2020**, *200*, 112459. [[CrossRef](#)]
166. Song, M.; Wang, S.; Wang, Z.; Fu, Z.; Zhou, S.; Cheng, H.; Liang, Z.; Deng, X. Synthesis, antimicrobial and cytotoxic activities, and molecular docking studies of N-arylsulfonylindoles containing an aminoguanidine, a semicarbazide, and a thiosemicarbazide moiety. *Eur. J. Med. Chem.* **2019**, *166*, 108–118. [[CrossRef](#)] [[PubMed](#)]
167. Al-Wabli, R.I.; Almomen, A.A.; Almutairi, M.S.; Keeton, A.B.; Piazza, G.A.; Attia, M.I. New isatin-indole conjugates: Synthesis, characterization, and a plausible mechanism of their in vitro antiproliferative activity. *Drug Des. Devel. Ther.* **2020**, *14*, 483. [[CrossRef](#)] [[PubMed](#)]
168. Demir-Yazıcı, K.; Trawally, M.; Bua, S.; Öztürk-Civelek, D.; Akdemir, A.; Supuran, C.T.; Güzel-Akdemir, Ö. Novel 2-(hydrazinocarbonyl)-3-phenyl-1H-indole-5-sulfonamide based thiosemicarbazides as potent and selective inhibitors of tumor-associated human carbonic anhydrase IX and XII: Synthesis, cytotoxicity, and molecular modelling studies. *Bioorg. Chem.* **2024**, *144*, 107096. [[CrossRef](#)]
169. Sigalapalli, D.K.; Pooladanda, V.; Singh, P.; Kadagathur, M.; Guggilapu, S.D.; Uppu, J.L.; Tangellamudi, N.D.; Gangireddy, P.K.; Godugu, C.; Bathini, N.B. Discovery of certain benzyl/phenethyl thiazolidinone-indole hybrids as potential anti-proliferative agents: Synthesis, molecular modeling and tubulin polymerization inhibition study. *Bioorg. Chem.* **2019**, *92*, 103188. [[CrossRef](#)]
170. Barakat, A.; Islam, M.S.; Ghawas, H.M.; Al-Majid, A.M.; El-Senduny, F.F.; Badria, F.A.; Elshaier, Y.A.; Ghabbour, H.A. Substituted spirooxindole derivatives as potent anticancer agents through inhibition of phosphodiesterase 1. *RSC Adv.* **2018**, *8*, 14335–14346. [[CrossRef](#)] [[PubMed](#)]
171. Islam, M.S.; Ghawas, H.M.; El-Senduny, F.F.; Al-Majid, A.M.; Elshaier, Y.A.M.M.; Badria, F.A.; Barakat, A. Synthesis of new thiazolo-pyrrolidine-(spirooxindole) tethered to 3-acylindole as anticancer agents. *Bioorg. Chem.* **2019**, *82*, 423–430. [[CrossRef](#)] [[PubMed](#)]
172. Qin, X.; Cui, X. Methyl-indole inhibits pancreatic cancer cell viability by down-regulating ZFX expression. *3 Biotech.* **2020**, *10*, 187. [[CrossRef](#)] [[PubMed](#)]

173. Cascioferro, S.; Petri, G.L.; Parrino, B.; El Hassouni, B.; Carbone, D.; Arizza, V.; Perricone, U.; Padova, A.; Funel, N.; Peters, G.J.; et al. 3-(6-Phenylimidazo[2,1-*b*][1,3,4]thiadiazol-2-yl)-1*H*-indole derivatives as new anticancer agents in the treatment of pancreatic ductal adenocarcinoma. *Molecules* **2020**, *25*, 329. [[CrossRef](#)] [[PubMed](#)]
174. El-Sharief, A.M.S.; Ammar, Y.A.; Belal, A.; El-Sharief, M.A.M.S.; Mohamed, Y.A.; Mehany, A.B.M.; Ali, G.A.M.E.; Ragab, A. Design, synthesis, molecular docking and biological activity evaluation of some novel indole derivatives as potent anticancer active agents and apoptosis inducers. *Bioorg. Chem.* **2019**, *85*, 399–412. [[CrossRef](#)]
175. Li, Z.; Luo, M.; Cai, B.; Rashid, H.-U.; Huang, M.; Jiang, J.; Wang, L.; Wu, L. Design, synthesis, biological evaluation and structure-activity relationship of sophoridine derivatives bearing pyrrole or indole scaffold as potential antitumor agents. *Eur. J. Med. Chem.* **2018**, *157*, 665–682. [[CrossRef](#)] [[PubMed](#)]
176. Wu, L.; Liu, Y.; Li, Y. Synthesis of spirooxindole-O-naphthoquinone-tetrazolo[1,5-*a*]pyrimidine hybrids as potential anticancer agents. *Molecules* **2018**, *23*, 2330. [[CrossRef](#)] [[PubMed](#)]
177. Naaz, F.; Pallavi, M.C.P.; Shafi, S.; Mulakayala, N.; Yar, M.S.; Kumar, H.M.S. 1,2,3-Triazole tethered indole-3-glyoxamide derivatives as multiple inhibitors of 5-LOX, COX-2 & tubulin: Their anti-proliferative & anti-inflammatory activity. *Bioorg. Chem.* **2018**, *81*, 1–20.
178. Khan, I.; Garikapati, K.R.; Shaik, A.B.; Makani, V.K.K.; Rahim, A.; Shareef, M.A.; Reddy, V.G.; Pal-Bhadra, M.; Kamal, A.; Kumar, C.G. Design, synthesis and biological evaluation of 1,4-dihydro indeno[1,2-*c*]pyrazole linked oxindole analogues as potential anticancer agents targeting tubulin and inducing p53 dependent apoptosis. *Eur. J. Med. Chem.* **2018**, *114*, 104–115. [[CrossRef](#)]
179. Chen, K.; Zhang, Y.-L.; Fan, J.; Ma, X.; Qin, Y.-J.; Zhu, H.-L. Novel nicotinoyl pyrazoline derivatives bearing N-methyl indole moiety as antitumor agents: Design, synthesis and evaluation. *Eur. J. Med. Chem.* **2018**, *156*, 722–737. [[CrossRef](#)]
180. Iacopetta, D.; Catalano, A.; Ceramella, J.; Barbarossa, A.; Carocci, A.; Fazio, A.; La Torre, C.; Caruso, A.; Ponassi, M.; Rosano, C.; et al. Synthesis, anticancer and antioxidant properties of new indole and pyranoindole derivatives. *Bioorg. Chem.* **2020**, *105*, 104440. [[CrossRef](#)] [[PubMed](#)]
181. Wu, J.; Liu, X.; Zhang, J.; Yao, J.; Cui, X.; Tang, Y.; Xi, Z.; Han, M.; Tian, H.; Chen, Y.; et al. Green synthesis and anti-tumor efficacy via inducing pyroptosis of novel 1*H*-benzo[*e*]indole-2(3*H*)-one spirocyclic derivatives. *Bioorg. Chem.* **2024**, *142*, 106930. [[CrossRef](#)] [[PubMed](#)]
182. Cheng, G.; Wang, Z.; Yang, J.; Bao, Y.; Xu, Q.; Zhao, L.; Liu, D. Design, synthesis and biological evaluation of novel indole derivatives as potential HDAC/BRD4 dual inhibitors and anti-leukemia agents. *Bioorg. Chem.* **2019**, *84*, 410–417. [[CrossRef](#)] [[PubMed](#)]
183. Cury, N.M.; Capitão, R.M.; de Almeida, R.d.C.B.; Artico, L.L.; Corrêa, J.R.; Dos Santos, E.F.S.; Yunes, J.A.; Correia, C.R.D. Synthesis and evaluation of 2-carboxy indole derivatives as potent and selective anti-leukemic agents. *Eur. J. Med. Chem.* **2019**, *181*, 111570. [[CrossRef](#)]

Disclaimer/Publisher's Note: The statements, opinions and data contained in all publications are solely those of the individual author(s) and contributor(s) and not of MDPI and/or the editor(s). MDPI and/or the editor(s) disclaim responsibility for any injury to people or property resulting from any ideas, methods, instructions or products referred to in the content.